NEUTRON OPTICS

D. J. HUGHES

INTERSCIENCE TRACTS ON PHYSICS AND ASTRONOMY

number 1

INTERSCIENCE TRACTS ON PHYSICS AND ASTRONOMY

Edited by R. E. MARSHAK
University of Rochester

NEUTRON OPTICS

D. J. HUGHES
Brookhaven National Laboratories, Upton, Long Island, New York

INTERSCIENCE PUBLISHERS, INC. NEW YORK
Interscience Publishers Ltd., London **1954**

Library of Congress Catalog Card Number 53-10758

INTERSCIENCE PUBLISHERS, INC.
250 Fifth Avenue, New York 1, N. Y.

For Great Britain and Ireland:
INTERSCIENCE PUBLISHERS, LTD.
88/90 Chancery Lane, London W. C. 2, England

PRINTED IN THE UNITED STATES OF AMERICA

PREFACE

In this volume we shall be interested in the basic physical principles as well as the applications of neutron optics, a field of research made possible in the last ten years by the high neutron fluxes available in chain-reacting piles. Much of the research in neutron optics in this period has dealt with the fundamental processes involved in neutron scattering and their relationship to familiar optical principles. The experimental investigation of neutron optics in itself is of value because it leads the way to fruitful applications to the structure of matter and to measurement of fundamental nuclear constants. An examination of the interactions that are important in neutron optics is highly instructive for it illustrates well the complementary particle and wave characteristics of neutrons and provides a comparison of the optics of neutrons and electromagnetic waves. In the discussion of principles the detailed theory of nuclear interactions will be avoided, as will the theory of solid state in connection with the applications of neutron optics. A sufficient amount of nuclear and collision theory will be included, however, so that the applications to the important phenomena of neutron optics will be well understood. Of solid state theory only enough detail will be given to explain the significance of the results of neutron optics in the fields of crystal and magnetic structure.

The first chapter is devoted to a discussion of the fundamentals of neutron scattering, a comparison of the optics of neutrons to electromagnetic waves, and the manner in which neutron scattering determines refraction, reflection, and diffraction. A brief survey of experimental methods is given in Chapter 2, although it is not our purpose to discuss detailed experimental techniques but rather to give the general features of the methods and their potentialities. The rest of the volume covers the appli-

cations of neutron optics; to nuclear interactions (Chapter 3), to analysis of structure (Chapter 4), and to magnetic properties (Chapter 5). In these discussions the material is arranged according to the particular phenomenon under study, such as the neutron-proton interaction, location of hydrogen atoms, paramagnetism, etc., rather than according to the particular techniques involved. In this way it is possible to put the major emphasis on the results obtained from neutron optics, as well as to examine the manner in which various techniques are applied to the same end.

It is a pleasure to acknowledge the help of George Cox in the preparation of the illustrations and of Adele Kentoffio in the typing of the various drafts of the manuscript.

CONTENTS

CHAPTER 1

Principles of Neutron Optics

In the study of neutron optics we are concerned with cooperative phenomena involving many atoms — the interference effects of scattered neutron waves and the typical optical effects that result. Inasmuch as neutrons possess well-defined wavelengths, one might expect that all the well-studied optical results could be applied directly to neutron optics. In a general way this procedure is legitimate, for neutrons are refracted and reflected at boundaries and diffracted in crystals in accordance with simple optical relationships. Passing beyond such obvious similarities, however, we find many differences that complicate the simple neutron-light analogy but at the same time make the optical properties of neutrons powerful research tools. Some of the differences are manifested immediately, as the scattering of neutrons by magnetic fields; others, such as the effects of the large momentum change at scattering in temperature diffuse scattering (related to the large neutron mass), are more subtle. Although our procedure will consist of the adoption of the well-known optical results whenever applicable, we shall be cognizant at all times of the important differences.

1.1 Optics of Neutrons and Electromagnetic Waves

In their interaction with matter, neutrons of "high" energy, i.e., in the Mev region, resemble particles more closely than waves. A neutron of energy 10 Mev, for example, has a de Broglie wavelength of 0.9×10^{-12} cm, of the same order of magnitude as nuclear dimensions, but smaller by a factor of 10^4 than interatomic spacings. It is true that some interference

effects are observed for these short wavelength neutrons on the scale of nuclear dimensions. These effects constitute the "shadow scattering," which is quite similar to diffraction from a small obstacle and is of angular range λ/a, where λ is the wavelength and a is the nuclear radius. For most of the scattering properties of fast neutrons, however, the particle characteristics predominate. Thus in the theory of "slowing down," or moderation of neutrons, they are considered correctly as point particles colliding, usually elastically, with the nuclei encountered.

As the neutrons are slowed down by nuclear collisions, their wavelength increases and the optical properties become easier to observe. Finally they reach thermal equilibrium with the moderating material, in which state energy gains are as frequent as energy losses. The wavelength of these "thermal neutrons" is of the order of several angstrom units, and in this energy region the wave properties of neutrons predominate over their particle characteristics. It is extremely fortunate that the wavelength region (several angstrom units) that is most interesting for neutron optical effects corresponds to just that energy region in which copious intensities of neutrons are available. As a result of the thermal equilibrium that obtains between neutrons and matter at room temperature, the highest available neutron densities occur at thermal energy in moderating materials. It is because of the extremely high thermal neutron fluxes available in chain-reacting piles that neutron optics has become an important field of physics in the decade during which chain-reacting piles have been available. The experiments of neutron optics are particularly analogous to those performed with x-rays, because not only are the wavelengths about the same but the index of refraction of most materials for neutrons has about the same numerical value as for x-rays.

Just as the experimental methods are similar to those of optics, so we might expect the explanation of the phenomena of neutron optics to proceed by analogy with the familiar optical

principles, including a discussion of those respects wherein neutron behavior differs from electromagnetic optics. This is the usual procedure and one that we also shall follow for the most part in this chapter. In some cases however, for example polarization of neutrons (Sec. 5.5), the analogy becomes far fetched because the phenomenon involved for neutrons is a fundamentally different process from the apparently analogous optical effect. In still other phases of the discussion the approach by analogy is not profitable because the neutron interaction is of a simpler nature and a completely fresh procedure, not involving the analogy to light, is superior. For example, given the basic constants of neutron optics, such as the index of refraction and the coherent and incoherent scattering amplitudes, the application of these quantities to the observed phenomena is closely similar to that of light or x-rays. However, in the evaluation of these basic quantities the quantum mechanical approach, unencumbered by analogy to a more complex situation, certainly seems better.

The differences between, and the similarities of, neutrons and light can be illustrated by a brief examination of refraction. In the usual classical treatment, light is considered as an electromagnetic wave that excites the particles of the medium it traverses, which in turn send out secondary scattered waves. In a material such as glass the absorption is negligible (far from the region of anamolous dispersion), and the scattering is coherent, that is, there are no random phase shifts involved. Because of the coherence in phase, the amplitudes of the scattered waves are added and the sum is squared to obtain the intensity. The scattering amplitudes add to zero in all but the forward direction, and in this direction the addition of the scattered to the incident wave results in a phase shift of the resultant wave. This phase shift represents a change in the velocity of the wave (the phase velocity as we will shortly see), and the ratio of the velocity outside the medium to that inside is of course the index of refraction.

The velocity ratio that gives the index of refraction n can

be obtained directly from Maxwell's equations for the electromagnetic wave in the medium as:

$$v_0/v_i = n = \sqrt{K} \tag{1-1}$$

where v_0 and v_i are the wave (phase) velocities outside and inside the medium, and K is the dielectric constant of the material (assumed to be a nonconductor). This simple result that the index is given by the square root of the dielectric constant certainly does not hold in the frequency range of ordinary light, but it is correct in the limit of long wavelength radio waves. The failure of the law for higher frequencies (optical wavelengths) is interpreted classically as the failure of the oscillating dipoles to follow the impressed frequencies. We shall examine in more detail the derivation of the index for light in connection with the neutron index in Sec. 1.3.

The refraction of light waves of index given by Eq. (1-1) is illustrated in Fig. 1-1, which shows a plane wave entering a medium of index greater than unity. Here we see the usual construction in which the secondary waves add to form a wave front whose normal (the "ray") is bent toward the perpendicular to the surface in the medium. The refraction results from the decreased velocity of the waves in the medium and it follows that

$$\frac{\sin i}{\sin r} = \left(\frac{v_0}{v_i}\right)_{\text{wave}} = n, \tag{1-2}$$

the usual wave interpretation of Snell's law of refraction.

We can consider the refraction of a material particle as it enters a medium in a completely classical manner and obtain a law of refraction analogous to that of the wave of Fig. 1-1. For a particle of velocity v_0 entering a medium, shown in Fig. 1-2, the refraction will be toward the perpendicular to the surface if the particle's velocity inside the material, v_i, is greater, that is, if the potential is less, than outside. This "refraction" is seen to follow from elementary mechanics. As the particle enters the medium, the component of its velocity

parallel to the surface is of course unchanged while that normal to the surface is increased by an amount given by the potential

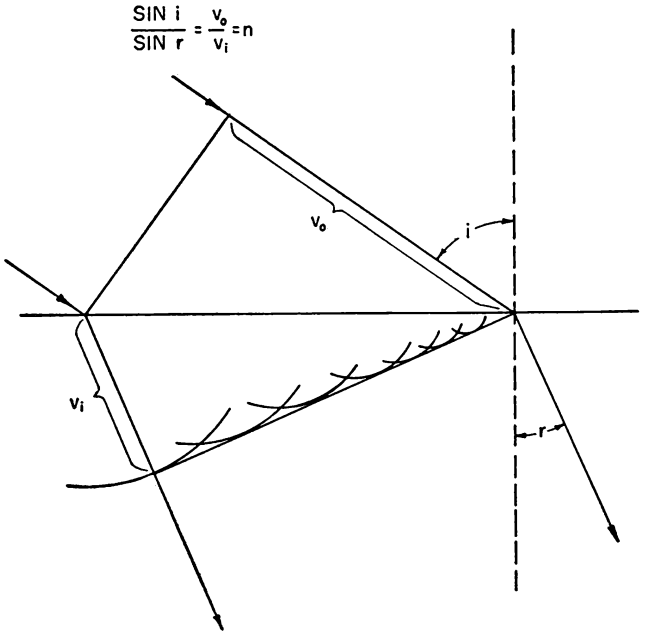

FIG. 1-1. Refraction of light waves entering a medium of index greater than unity.

change. As shown in Fig. 1-2, we thus obtain directly the law of refraction for a classical particle

$$\frac{\sin i}{\sin r} = \left(\frac{v_i}{v_0}\right)_{\text{particle}} = n, \tag{1-3}$$

which differs from Eq. (1-2) in that the velocity ratio is reversed.

Snell's law follows from both the classical wave or particle picture with the important difference, however, that the wave must move more slowly inside a medium with n greater than unity, while the particle has a larger velocity inside the medium.

This difference between the two approaches with regard to velocity is no contradiction for the velocities concerned are not the same. The association of the de Broglie wavelength with

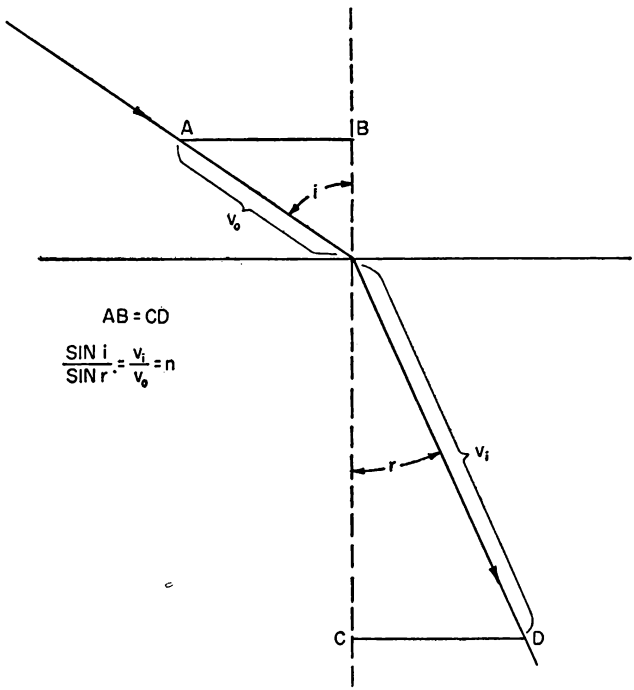

FIG. 1-2. Refraction of a material particle entering a medium in which its velocity increases.

the particle makes the two approaches completely equivalent. The velocity in Fig. 1-1 is of course the phase velocity while that of 1-2 is the group velocity, thus illustrating the well-known fact that these velocities vary inversely as the index of refraction changes. As shown in Fig. 1-1, the wavelength decreases on entry into the medium hence the phase velocity ($= \nu\lambda$, with ν the frequency) does likewise, and this decrease in wavelength

must mean an inversely proportionate increase in group velocity by de Broglie's relation, $v_g = h/m\lambda$.

It is customary to use the wave picture for refraction of light and to refer to the phase velocity, whereas the group velocity (the observable particle velocity) is used in connection with neutrons. The refraction of neutrons could in a completely equivalent manner be considered as a refraction of waves, with wavelengths given by de Broglie's equation

$$\lambda = \frac{h}{mv_g}, \tag{1-4}$$

and frequency given by the usual equation

$$E = h\nu, \tag{1-5}$$

where E is the total energy (strictly speaking, including the rest energy of the particle). The index of refraction is then given either in terms of the particle or the phase velocity,

$$n = \left(\frac{v_i}{v_0}\right)_{\text{particle}} = \left(\frac{v_0}{v_i}\right)_{\text{phase}}. \tag{1-6}$$

Because of the indefiniteness of the energy, for example the arbitrary inclusion of the rest energy, the assignment of a definite frequency and phase velocity to the neutron is not useful. It is customary and much more meaningful to use the group velocity and wavelength in the discussion of refraction. It is thus seen that the refraction of light and of neutrons can be considered as fundamentally the same process, the difference between them lying mainly in the appropriateness of a particular treatment for actual calculations.[1]

1.2 Coherence Effects in Neutron Scattering

It is a well-known fact that scattered waves of any type can add coherently or incoherently. Coherent scattering is

[1] An interesting nonmathematical discussion of the wave-particle aspects of matter may be found in W. Heitler, *Elementary Wave Mechanics* (Oxford, 1944) Chs. 1 and 2.

related to constancy of phase relations of the waves scattered by different centers, and incoherence to irregular or random phase relations. An important property of these types of scattering is that the amplitudes of coherently scattered waves add directly while intensities, or amplitudes squared, add for incoherent scattering. These simple facts are familiar from elementary optics but a closer examination of coherence reveals many complications, particularly in the case of neutron scattering.

In most of the usual phenomena of optics little difficulty is encountered involving the question of coherence. As a matter of fact, many optics texts discuss coherence only in connection with the light sources used in interference experiments. Thus coherent sources for an interference experiment may be formed by dividing the light from a single source, as by a partially reflecting mirror in the Michelson interferometer. The two beams of light in this arrangement obviously have constant phase differences whereas two physically independent light sources would have random phase differences. No interference effects of course are observed with the independent sources, and it is explained that these are illustrations of incoherent sources. Even for a single source, however, random phases may occur when light is transmitted through a medium and to some extent scattered diffusely from the particles (charges) of the medium, with resultant incoherent scattering.

In the transmission of light through glass, the scattering is almost completely coherent and all the light is found in the refracted beam, there being little diffuse scattering. The practical absence of incoherence is related to the fact that, on an optical wavelength scale, glass is a medium of *uniform* scattering power, hence exhibiting no random variation of scattered amplitude. As we shall see, the diffuse scattering is a measure of the incoherent contribution in scattering, whereas the scattering that gives rise to a refracted beam is proportional to the coherent scattering.

Incoherent scattering of light is more important in the

case of refraction in a gas. The scattering of the individual molecules of the gas give rise to a wave that travels according to geometrical optics, being refracted in the gas in accordance with an index of refraction dependent on the *average* scattering power of the gas. As the average scattering power varies with the density of the gas, which in turn exhibits random fluctuations from point to point, the scattering power will have a component that also varies at random. This variable component gives rise to a component of the scattering that exhibits random phase relations, is distributed diffusely, and is proportional to the square of the deviations of the individual scattering amplitudes.[2] Fluctuation scattering of light does occur to a small extent in solids, where it is proportional to the compressibility; for liquids near the critical point, however, it becomes appreciable (critical opalescence).

The coherence and incoherence of neutron scattering is much more complicated than light because the incoherent scattering is generally larger in magnitude and arises from a number of causes that do not exist for light scattering. The neutron refraction resembles best the index of refraction of light in a gas and, as for that case, the average coherent amplitude determines the index of refraction whereas the variation in amplitude contributes to the incoherent scattering. There are several causes for the variation of neutron scattering amplitude from atom to atom; because of the somewhat complicated nature of the variation it is necessary to look at the scattering from a single center before considering the superposition of the scattered waves.

In the quantum mechanical treatment of scattering, the incident neutron is considered a plane wave of indefinite extent. Incidentally, according to the Heisenberg uncertainty relationship, this consideration implies that the momentum of the neutron is accurately known but that its position is completely

[2] This incoherent fluctuation scattering is the Rayleigh scattering; it is thoroughly treated from a classical viewpoint in M. Born, *Optik* (Edwards, 1943), pp. 371–390.

unknown. The incident plane wave plus the scattered wave originating at the nucleus (taken as the center of coordinates) is given by the equation[3]

$$\psi = e^{i\mathbf{k}\cdot\mathbf{r}} + \frac{e^{ikr}}{r} f(\theta), \tag{1-7}$$

where ψ is the neutron wave function and $\mathbf{k}$ its propagation vector ($= 1/\lambda\!\!\!^{-} = mv/\hbar$). As shown by Eq. (1-7), the amplitude of the scattered wave is in general a function of the distance r from the scattering center and the angle of scattering θ. The scattering is usually divided into components corresponding to various *partial waves*, each of which refers to a definite angular momentum of the neutron, classically to a single impact parameter, considering the neutron as a point particle. Each scattered partial wave has a particular angular distribution and shift in phase relative to the incident wave.

Because of the short range of nuclear forces the interaction of low-energy neutrons is zero for angular momenta larger than zero (corresponding to impact parameters $\lambda\!\!\!^{-}$ or larger). The scattering with angular momentum zero, called s scattering, results in an isotropic wave with a phase shift δ. The wave equation for s scattering, which corresponds to all scattering in the field of neutron optics, is

$$\psi = e^{i\mathbf{k}\cdot\mathbf{r}} + \frac{e^{ikr}}{2ikr}(e^{2i\delta} - 1), \tag{1-8}$$

which for $\delta \ll 1$, becomes simply

$$\psi = e^{i\mathbf{k}\cdot\mathbf{r}} + \frac{\delta e^{ikr}}{kr}. \tag{1-9}$$

The phase shift is not necessarily a real number and is so only

[3] The complete expressions describing the scattering of neutrons, from which are obtained the simple ones appropriate to neutron optics given in this chapter, may be found in the texts: N. F. Mott and H. S. W. Massey, *The Theory of Atomic Collisions*, 2nd ed. (Oxford, 1949); L. I. Schiff, *Quantum Mechanics* (McGraw-Hill, 1949).

if no absorption accompanies the scattering. In general, the phase shift can be divided into a real and imaginary part:

$$\delta = \delta_r + i\delta_i \tag{1-10}$$

with both δ_r and δ_i real numbers.

The absolute value of the amplitude of the scattered wave, δ/k, gives the outward flux from the nucleus, in other words the scattering cross section, as

$$\sigma_s = \frac{4\pi}{k^2}(\delta_r^2 + \delta_i^2). \tag{1-11}$$

The net loss of flux is the absorption cross section

$$\sigma_a = \frac{4\pi}{k^2}\delta_i(1 - 2\delta_i), \tag{1-12}$$

and the sum of σ_a and σ_s gives the total cross section,

$$\sigma_t = \frac{4\pi}{k^2}(\delta_r^2 + \delta_i - \delta_i^2). \tag{1-13}$$

In the last three equations, the simplifying assumption is made that the δ's are small compared to unity. We shall also neglect the absorption at present because for most substances used in neutron optics it is sufficiently small so that it has only a negligible effect on the optical phenomena. The scattering cross section is then simply

$$\sigma_s = 4\pi\frac{\delta_r^2}{k^2} = 4\pi a^2 \tag{1-14}$$

where δ_r/k, the *distance* the wave is shifted by the potential, is the amplitude of the scattered wave a. The evaluation of the phase shift is fortunately much simpler than for the phase shifts of ordinary optics, for the shift is close to 180° for most substances and to 0° for a few others. We are here using the convention that the usual phase shift of 180°, corresponding to scattering by an impenetrable sphere, represents a positive amplitude.

The phase shifts can easily be evaluated for the case of scattering by a definite potential shape, the method that is usually applied to the scattering of neutrons by protons. This method reveals the manner in which the phase shifts change with neutron wavelength, becoming large when the neutron wavelength bears a simple relation to the size of the potential well. For more complex nuclei the Breit-Wigner dispersion treatment[4] is usually used, in which the scattering is arbitrarily divided into two parts; first, the potential scattering in which the neutron scatters from the nucleus much as for the case of a potential and, second, the scattering in which the neutron enters the nucleus and is re-emitted without change of energy. The Breit-Wigner formula for the case of scattering that is applicable for heavy nuclei and hence of most interest to us, follows:

$$\sigma_s = \frac{4\pi}{k^2}\left|\frac{\Gamma_n/2}{E - E_0 + \frac{i}{2}\Gamma} + e^{ikR}\sin kR\right|^2 \qquad (1\text{-}15)$$

In this equation the first term in the phase shift expression has a typical resonance structure, becoming very large when the neutron energy E becomes equal to the resonance energy, E_0. The quantities Γ and Γ_n are the total width and the neutron width of the resonance level, where $\Gamma = \Gamma_n + \Gamma_\gamma$, with Γ_γ the radiation width. Eq. (1–15) applies to scattering from a zero-spin nucleus of radius R; the added complication of spin dependent scattering will be considered shortly.

The manner in which the resonance phase shift combines coherently with the potential phase shift (the second term) can best be shown diagrammatically. Both amplitudes, or phase shifts times k^{-1}, lie on circles in the complex plane, Fig. 1-3, that for the potential scattering having a diameter of k^{-1}, while the resonance amplitude circle has a diameter of k^{-1}

[4] A good description of the basis of the dispersion formula is given by H. Feshbach, D. C. Peaslee, and V. F. Weisskopf, *Phys. Rev.* **71**, 145 (1947); a complete discussion is given in J. M. Blatt and V. F. Weisskopf, *Theoretical Nuclear Physics* (Wiley, 1952).

Γ_n/Γ. The vector sum of the two amplitudes reaches a minimum (actually zero if the circles are of equal size, i.e., if $\Gamma_\gamma = 0$) at an energy several times Γ below E_0; at this point the inter-

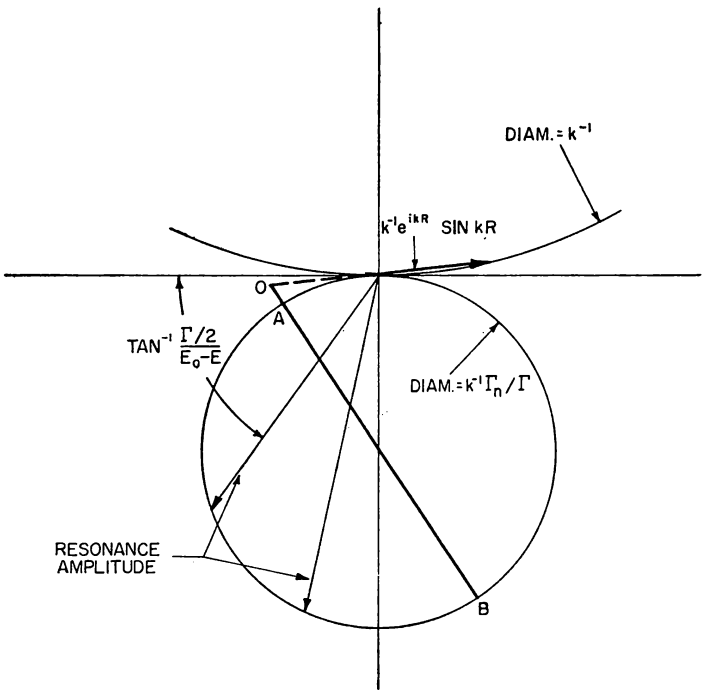

FIG. 1-3. The coherent superposition of the resonance and potential amplitudes in scattering near a resonance. As the net amplitude is given by a vector drawn from point O to the lower circle, the minimum amplitude is represented by OA and the maximum by OB.

ference of potential and resonance scattering is almost complete. In the resonance region the phase shift is far from 0° or 180°, hence it is not correct to refer to a "positive" or "negative" amplitude. However, when the resonance amplitudes are of the order of R (the potential amplitude) the phase shift is close to 0° or 180° and most materials have positive amplitudes, with

the exception of a few, H, Li, Mn, and Ti, for example. We shall consider the actual values of the amplitudes in connection with the discussion of their measurement in Sec. 3.1 and 3.2.

The cross section calculated from Eq. (1-15) will have the form given in Fig. 1-4, which is drawn for a typical case of

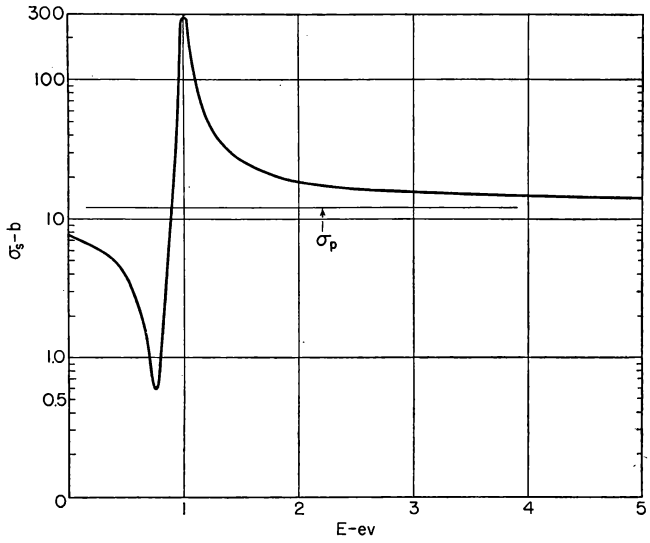

FIG. 1-4. Scattering cross section calculated from Eq. (1-15) illustrating the dip below the resonance resulting from interference between resonance and potential scattering. The constants assumed for the resonance are $\Gamma_n = 10^{-3}$ ev and $\Gamma_\gamma = 0.1$ ev, with the nucleus of spin zero and $R = 10^{-12}$ cm.

$\Gamma_n = 10^{-3}$ ev, $\Gamma_\gamma = 0.1$ ev, $E_0 = 1$ ev, $R = 10^{-12}$ cm. It is seen that the cross section dips below the resonance to an exceedingly low value, in fact (for $\Gamma_n \ll \Gamma$) the ratio of the minimum to the potential cross section is the same as the ratio of the latter to the maximum cross section (this fact may be demonstrated easily from the geometry of Fig. 1-3, assuming that point O is on the real axis, i.e., that $\Gamma_n \ll \Gamma$).

In Eq. (1-15) and Fig. 1-4 the assumption is made that

the target nucleus has zero spin. Even for scattering from a single nucleus the question of coherence and incoherence enters if the nucleus has a nonzero spin. This incoherence arises because the scattering amplitude for the two possible spins of the compound nucleus will be different if a resonance is nearby. As the compound nucleus formed by addition of the neutron to the target nucleus, of spin i, can have spin $i + \frac{1}{2}$ or $i - \frac{1}{2}$, the cross section resonance, having a definite spin, will correspond to only one of the spin states, the cross section for the other (the "nonresonant spin state") consisting of the potential scattering only. Because the distribution of the two spin states, $i \pm \frac{1}{2}$, is random the scattering amplitude will also vary at random. As a result, part of the scattering will not be able to interfere with the incident wave and will thus be incoherent.

Here we are considering incoherence even for a single nucleus in terms of the ability of the scattered wave to interfere with the incident wave. Actually the quantum mechanical definition of coherence is more rigorous and according to it the scattering is incoherent only if the quantum state of the scatterer is changed in the process of scattering.[5] For the spin dependent scattering, now under discussion, the spin of the nucleus can be changed in the process of scattering and this change in quantum state (which is accompanied by a change in the spin of the neutron) is the cause of the lack of interference. If we define the scattering amplitude for the compound nucleus spin of $i + \frac{1}{2}$ as a_+ and for $i - \frac{1}{2}$ as a_-, the coherent scattering amplitude, which is the average amplitude, is given by

$$a_{\text{coh}} = \frac{i+1}{2i+1} a_+ + \frac{i}{2i+1} a_- , \qquad (1\text{-}16)$$

[5] See the discussion of G. Breit, *Rev. Mod. Phys.* **5**, 91 (1933), pp. 106–117. Random amplitude variation can occur even with no change in quantum state, of course, as for the isotope scattering we shall discuss shortly. Although the resulting diffuse scattering is not incoherent in the quantum mechanical sense, we shall follow the almost universal custom and speak of isotopic incoherent scattering.

where the amplitudes are weighted according to the relative probability of their occurrence.

The total scattering amplitude is just the square root of the sum of the intensity ($\sigma = 4\pi a_t^2$) or,

$$a_t = \left(\frac{i+1}{2i+1}\, a_+^2 + \frac{i}{2i+1}\, a_-^2\right)^{1/2}. \tag{1-17}$$

The incoherent scattering amplitude, which is given by $(a_t^2 - a_{\text{coh}}^2)^{1/2}$, is thus seen to be proportional to the amplitude difference,

$$a_{\text{inc}} = \frac{\sqrt{i(i+1)}}{2i+1}\,(a_+ - a_-). \tag{1-18}$$

For each type of amplitude there is a corresponding cross section, given by 4π times the amplitude squared. The scattering amplitude rather than the cross section, however, is of more direct use in neutron optics.

When the scattering from many nuclei is considered, there are several types of incoherence present, some of which do, and others do not, occur for light and x-rays. One type of incoherence that does occur for x-rays, for instance, is the well-known temperature diffuse scattering resulting from the fact that the atoms are not locked rigidly at lattice points in crystals. This scattering, which incidentally does not change the index of refraction because it is zero in the forward direction, will be treated briefly in Sec. 1.4 (the Debye-Waller factor). A type of incoherent scattering occurring for neutrons but not for x-rays is the isotope scattering, which results from the fact that an element possessing isotopes will exhibit some incoherent scattering if the amplitudes of the isotopes differ. The formulas for the isotopic incoherence follow directly by analogy with the spin dependent scattering, that is, the coherent amplitude for an element of two isotopes is given by the weighted average,

$$a_{\text{coh}} = c_1 a_1 + c_2 a_2, \tag{1-19}$$

where c_1 and c_2 ($c_1 + c_2 = 1$) are the abundances of the isotopes of amplitudes a_1 and a_2. The total amplitude will thus be

(from $\sigma_t = 4\pi a_t^2$),

$$a_t = (c_1 a_1^2 + c_2 a_2^2)^{1/2}, \tag{1-20}$$

and the incoherent, again calculated from the intensity difference, is

$$a_{\text{inc}} = (c_1 c_2)^{\frac{1}{2}}(a_1 - a_2). \tag{1-21}$$

The cross sections corresponding to each of the amplitudes will of course be given by 4π times the amplitudes squared.

Although the formulas for isotope incoherent scattering are closely analogous to those for spin dependent scattering, there is an important difference in the actual process taking place. As we have seen in the spin dependent incoherence there is an actual change in the quantum state of the scatterer as well as of the neutron; as a result this incoherence can be considered strict incoherence. For the isotopic scattering, on the other hand, there is no change in the quantum state of the scatterer, and the incoherence is merely the result of the mixture of isotopes. Strictly speaking, the isotopic incoherence is not incoherence at all but merely a type of interference containing a component of diffuse scattering. It is true that the intensity of this diffuse component varies as the square of the amplitude variation and hence resembles strict incoherence, but quantum mechanically there is no change of state, hence no incoherence.

As yet we have not mentioned the magnetic scattering that occurs because of the interaction of the magnetic moment of the neutron with the atomic magnetic fields. This magnetic scattering complicates the coherence relations even more because the magnetic scattering may be coherent or incoherent. For the moment we shall not consider the magnetic scattering in the interest of clarity but shall take up its effects in Sec. 5.1. It is clear, however, that the questions of coherence require great care in the consideration of the phenomena of neutron optics.

1.3 Index of Refraction

As we have already indicated in Sec. 1.1, the geometrical optics of neutrons (refraction and reflection) is closely similar

to light, once the index of refraction is given. In actuality, the geometrical optics is much simpler in the case of neutrons because the phase changes at reflection do not exhibit the complexity of light, which involves the separate phase relations of the electric and magnetic vectors. The derivation of the index of refraction for neutrons is quantum mechanical in nature and does not bear an obvious resemblance to the usual classical definitions of the index for light. For this reason it is instructive to compare the basic phenomena underlying the indices in the two cases.

In the usual derivation of the index for light, involving the classical dispersion theory, light is considered as an electromagnetic wave in a medium in which Maxwell's equations hold. When the classical wave equation in a vacuum is compared to that in a nonconductor such as glass, of dielectric constant K, it is found[6] that the velocity of the wave (this is the phase velocity as we have seen) in the medum is just $1/\sqrt{K}$ of the vacuum velocity. As a result the index (see Sec. 1.1) is given by

$$n^2 = K. \tag{1-22}$$

As K is simply related to the electron susceptibility κ,

$$K = 1 + 4\pi\kappa, \tag{1-23}$$

the index can be derived from a consideration of the electronic structure of the medium, i.e., from the classical electron theory.

It is assumed that bound charges (electrons) are located in the medium, held by elastic forces, and subject to a periodic field G of frequency $2\pi\omega$. Under these conditions a dipole moment will be induced by a unit field G per electron given by

$$\text{Dipole moment} = \frac{e^2/m}{\omega_0^2 - \omega^2} \tag{1-24}$$

[6] See for example, G. Joos, *Theoretical Physics* (Stechert, 1934), Ch. 25; J. C. Slater and N. H. Frank, *Electromagnetism* (McGraw-Hill, 1947) Ch. 9.

where ω_0 is the natural frequency of the bound electron. The suspectibility κ is the induced polarization per unit field strength, hence for N atoms, each containing f electrons, per cm^3, we have

$$\kappa = \frac{Nfe^2/m}{\omega_0^2 - \omega^2}, \tag{1-25}$$

and the index will be

$$n^2 = 1 + 4\pi\kappa = 1 + \frac{4\pi Nfe^2/m}{\omega_0^2 - \omega^2}. \tag{1-26}$$

The susceptibility as used above is defined in terms of the external field G whereas for a dense material the effective field at a particular electron is modified by the field of all the other dipoles produced by the external field G. Correction of the field for the effect of the other dipoles in a dense system changes the formula for the index slightly, and results in the well-known equation

$$\frac{n^2 - 1}{n^2 + 1} = \frac{4\pi Nfe^2/m}{3(\omega_0^2 - \omega^2)}. \tag{1-27}$$

Whereas the dispersion equation just derived gives the quantitative behavior of optical dispersion reasonably well at frequencies far from ω_0, it is of course not accurate near ω_0, for it would indicate an infinite index of refraction. Inclusion of absorption, however, which is high at a natural frequency, gives an index in closer correspondence to the actual behavior. The quantum mechanical treatment of dispersion gives results that are in close analogy with the classical equations, especially near resonances. We have already seen that the theory of the scattering of neutrons from complicated nuclei results in the Breit-Wigner dispersion formula, Eq. (1-15), which resembles closely the optical dispersion formula.

The derivation of the index of refraction for neutrons is in many respects simpler than that for light. While it can be considered either from the standpoint of wave or classical particle mechanics, we shall use the former. The wave equation

satisfied by the neutron is

$$\nabla^2\psi + \frac{2m}{\hbar^2} E\,\psi = 0, \tag{1-28}$$

outside the medium and

$$\nabla^2\psi + \frac{2m}{\hbar^2} (E - V)\,\psi = 0, \tag{1-29}$$

inside. The wave number outside the medium, k_0, is given by

$$k_0^2 = \frac{2mE}{\hbar^2}, \tag{1-30}$$

and that inside by

$$k^2 = \frac{2m(E - V)}{\hbar^2}. \tag{1-31}$$

The index of refraction, as seen in Sec. 1.1, is just

$$n = \frac{k}{k_0}. \tag{1-32}$$

In the equations just considered, both the wave and the particle picture are combined, for the particle energy E and the wave number k appear together. We can think of the index as the ratio of the wave number inside the medium to that outside, in other words, the ratio of the phase velocity; however, because the wave number is proportional to the particle velocity (the group velocity), this equation can also be thought of as giving the ratio of the particle velocity.

Although there are several methods for calculating the ratio of the wave number inside the medium to that outside, one that is especially instructive is based on a consideration of the phase shift that occurs at the individual nucleus. If the neutron energy is far from a nuclear resonance, the usual neutron-optical case, the scattering cross section is given in term of the amplitude by Eq. (1-14) as

$$\sigma_s = 4\pi a^2 = 4\pi R^2, \tag{1-33}$$

where the scattering amplitude a is equal to the nuclear radius (the distance the wave is shifted) and the scattering is the so-called hard sphere scattering, corresponding to an infinite repulsive potential. We are considering here the scattering from an individual nucleus neglecting the interference effects of Bragg scattering; our results hold therefore for non-Bragg directions.

The scattering amplitude can be easily related to the actual

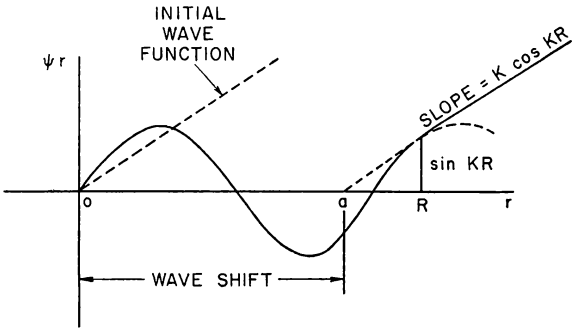

FIG. 1-5. The relationship between the shift of the wave function, or scattering amplitude, and the potential well of depth $U(K = (2mU)^{1/2}\hbar^{-1})$ and range R.

potential well producing the scattering, as we shall now show. The scattering amplitude, hence the potential, when averaged throughout the medium will be just the quantity V in the wave equation needed to evaluate the neutron index inside the medium. The relationship between phase shift and potential can be obtained from Fig. 1-5, which shows the initial wave function and the shift caused by the potential. The function ψr has the form $\sin Kr$ inside the nucleus, where $K[= (2mU)^{1/2}\hbar^{-1}$, with U the depth of the nuclear potential well] is the wave number[7] corresponding to the energy of the neutron inside the nucleus (of the order of 20 Mev so K is about 10^{13}). Outside the

[7] Not to be confused with the K of Eq. (1-22).

nucleus, the wavelength is so long that ψr is linear as shown in Fig. 1-5. In this figure it is clear that the distance the wave is shifted, or the amplitude a, is given by

$$a = R - \frac{\tan KR}{K}. \tag{1-34}$$

This relation follows from the value of ψr ($\sin KR$) and the slope ($K \cos KR$) at $r = R$. If $\tan KR$ is expanded and K replaced by $(2mU)^{1/2}\hbar^{-1}$, this equation can be simplified with the result that the scattering amplitude is expressed in terms of the depth of the nuclear potential well U as

$$a = \frac{2}{3}\frac{mUR^3}{\hbar^2}. \tag{1-35}$$

The potential U of course extends throughout a volume $\frac{4}{3}\pi R^3$ per nucleus and if smoothed out through the medium will represent an average potential of

$$\begin{aligned} \bar{V} &= U \times \frac{4\pi R^3}{3} \Big/ \frac{1}{N} \\ &= \frac{Na2\pi\hbar^2}{m} \end{aligned} \tag{1-36}$$

because the volume occupied per nucleus is just $1/N$, where N is the number of nuclei per cubic centimeter. Substitution of this value for $\bar{V}$ into Eq. (1-31) gives

$$\begin{aligned} k^2/k_0^2 = n^2 &= 1 - \bar{V}/E \\ &= 1 - \frac{Na4\pi\hbar^2}{m^2v^2} \end{aligned} \tag{1-37}$$

or

$$n^2 - 1 = -\frac{\lambda^2 Na}{\pi}. \tag{1-38}$$

Following the procedure described earlier for the refraction of light, we could now make a correction for the fact that the

effective field at each nucleus is not simply the external field but is the latter modified slightly by the scattering from other particles. However, for all the phenomena of neutron optics this correction factor differs from unity by only a negligible amount.[8]

This simple derivation of the neutron index involves only the motion of a particle in a potential and as such is close to the classical particle picture, the behavior of the wave function

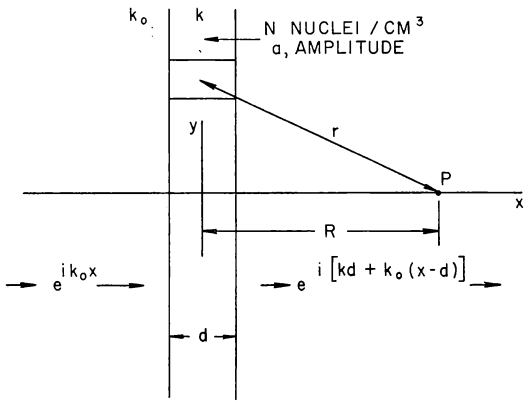

FIG. 1-6. The method used to derive the index of refraction by adding scattering amplitudes from a thin slab of material.

being used, however, in order to relate the scattering potential to the neutron cross section. A more consistently wavelike picture can be used to obtain the index of refraction and this method, which in fact is the customary one, is illustrated in Fig. 1-6. Here the scattered waves from a thin slab of material are added at the point P and the resulting phase shift at P represents a change in the phase velocity of the wave in the thin slab. This change in phase velocity is then used to obtain the

[8] The various coherent and incoherent effects of multiple scattering of neutrons are reviewed by M. Lax, *Rev. Mod. Phys.* **23**, 287 (1951), and L. L. Foldy, *Phys. Rev.* **67**, 107 (1945); the effective field in particular is discussed by Lax in *Phys. Rev.* **85**, 621 (1952).

index of refraction in accordance with the wave picture of Fig. 1-1. From Fig. 1-6, the phase shift at P is given in terms of the propagation vectors k_0 and k as

$$(k - k_0)\, d = k_0(n - 1)\, d, \tag{1-39}$$

where d is the slab thickness. The shift also follows from the addition of the scattered amplitudes as

$$-2\pi aNd \int_0^\infty \frac{1}{r}\, e^{ik_0(r-R)} y dy = -2\pi aNd \int_R^\infty e^{ik_0(r-R)} dr. \tag{1-40}$$

The integral is evaluated as $1/k_0$ and the expressions (1-39) and (1-40) for the phase shift are combined to give

$$n = 1 - \frac{2\pi aN}{k_0^2} = 1 - \frac{\lambda^2 Na}{2\pi}, \tag{1-41}$$

the same result as Eq. (1-38). We shall devote little space to this alternative derivation of the expression for the index of refraction because the treatment of the index in terms of the average potential in the medium will be more useful to us later.

In the considerations of this section, we have omitted the incoherent scattering arising from the types of random scattering discussed in the previous section. This incoherent scattering will have only an extremely small effect on the value of the index, but will produce a diffuse background of incoherently scattered neutrons with the result that the coherent transmitted wave will decrease exponentially in the medium. The decrease in intensity caused by diffuse scattering resembles very closely the decrease in intensity resulting from neutron absorption by the nuclei of the medium.

Although the absorption has been thus far neglected in the present section, it can easily be taken into account, however, by inclusion of complex values for the phase shift. The real part of the phase shift, as we saw in Sec. 1.2, gives the coherent scattering and the imaginary part the absorption. The complete expression for the index including absorption is as follows:[9]

[9] M. L. Goldberger and F. Seitz, *Phys. Rev.* **71**, 294 (1947).

$$n^2 - 1 = \frac{4\pi N}{k_0^2}\left[\pm\left(\frac{\sigma_s}{4\pi} - \frac{k_0^2\sigma_a^2}{16\pi^2}\right)^{1/2} + \frac{ik_0\sigma_a}{4\pi}\right], \qquad (1\text{-}42)$$

an expression that of course reduces to the one already derived as the absorption becomes negligible. Considering practical cases the effect of absorption on the index is almost always negligible. Even for as strong an absorber as cadmium, for instance, with absorption cross section 3000 barns (at thermal, $\lambda = 2A$) and scattering cross section 5 barns, the effect of absorption on the index is only about 0.5%. The effect of absorption in reducing the intensity of a beam is of course important in neutron-optical experiments, but it is clear that the effect on phenomena determined by the index of refraction can be neglected.

The effects of refraction in neutron optics are extremely small because the index is so close to unity. For the case of beryllium for example, for which the coherent scattering is 7.5 barns and the incoherent scattering zero, the index of refraction given by Eq. (1-38) differs from unity by only 6×10^{-6}. This index is so close to unity that the deviation of a neutron beam at a medium will be at most of the order of several minutes of arc. The effects thus will resemble the refraction of x-rays, for which the index is also extremely close to unity, rather than of light. The largest angular deviations are of course observed at the critical angle; for this case the incident angle is $\sin^{-1} n$, where the angle is measured relative to the normal to the surface. If we call θ_c the critical angle measured relative to the surface itself, it follows immediately that the critical angle is given by the equation

$$\theta_c = \lambda\sqrt{\frac{Na_{\text{coh}}}{\pi}}, \qquad (1\text{-}43)$$

the fundamental relationship used in the determination of coherent scattering amplitudes by means of mirror reflection.

As we shall see in Ch. 2, the measurement of the critical angle for neutrons of a particular wavelength is used as a measurement of the coherent scattering amplitude because this

method gives the largest observable refraction effects. The critical angle for beryllium, for example, for a neutron wavelength of 2 A (the wavelength for thermal neutrons) will be 12 minutes and proportionately larger if longer wavelength neutrons are used. Absorption tends to make the critical angle a gradual transition but, as for the index of refraction, the effect for practically all materials is negligible.

1.4 Diffraction

With regard to refraction and reflection of neutrons, we have seen that the analogy with the corresponding optical phenomena is often useful as an aid to understanding the behavior of neutrons. In certain respects the analogy is not at all instructive because the greater simplicity of the neutron behavior makes the direct approach more valuable. In the diffraction of neutrons from crystal, however, the analogy to electromagnetic waves holds extremely well, and practically all the standard diffraction treatment may be applied directly to neutrons.

The most useful analogy for neutrons in optical diffraction is supplied by x-rays because of the similarity in wavelength. While there are some differences in detail between the diffraction of neutrons and x-rays, as we shall see, they are relatively unimportant compared to the large number of respects in which their behavior is identical. In analyzing the diffraction of neutrons by crystals, the coherent neutron scattering amplitudes are used in all the standard formulas of x-ray diffraction. The sources of incoherence are more numerous for neutrons than for x-rays (neither isotopic nor spin dependent incoherence occurs for x-rays), but the incoherently scattered neutrons have no direct effect on the diffraction pattern, merely decreasing the intensity in the diffraction peaks and adding a diffuse background. The complete dynamical theory of x-ray diffraction[10] is not at all simple but fortunately all the results can be

[10] This may be found in W. H. Zachariasen *X-Ray Diffraction in Crystals* (Wiley, 1947).

taken over for use with neutrons. In the adaptation to neutron diffraction with its simpler wave function, it is necessary to consider only the electromagnetic wave polarized perpendicular to the plane of incidence, and the nuclear scattering amplitude replaces the complex polarizability of the medium.[11] The similarity of results is enhanced by the fact that the amplitudes are of the same order of magnitude as the polarizabilities. Concerning *absorption* of the radiation passing through the crystal, however, there is a great difference for this effect is much greater for x-rays in most materials.

The main interest in neutron diffraction at the present time is with regard to its practical use in analysis of crystals rather than in the study of the process itself. The reason for the small interest in the latter activity arises simply from the close similarity between neutron and x-ray diffraction. As far as the practical use of neutron diffraction is concerned, only a few simple results of diffraction theory are involved in the present state of the technique.[12] The principle result of course is the Bragg equation, which gives the neutron wavelength that will be diffracted when incident on a set of lattice planes (h, k, l) at an angle θ,

$$n\lambda = 2d \sin \theta, \tag{1-44}$$

where n is the order of the reflection. In this equation, d is the spacing of the planes denoted by the Miller indices h, k, l, and for a cubic unit cell of side a_0, d is given in terms of the indices as

$$d = \frac{a_0}{(h^2 + k^2 + l^2)^{1/2}}. \tag{1-45}$$

The Bragg equation relates the angles at which reflections

[11] M. L. Goldberger and F. Seitz, *Phys. Rev.* **71**, 294 (1947).

[12] Extensive treatments of diffraction theory specifically applied to neutron diffraction patterns are given by O. Halpern, M. Hamermesh, and M. H. Johnson, *Phys. Rev.* **59**, 981 (1941) and M. L. Goldberger and F. Seitz, *loc. cit.*

are found to the lattice spacings present in the crystal. In order to determine crystal structure from observed reflections, however, it is necessary to consider the neutron *intensity* in the different reflections as well as their location in angle. The intensity of a particular reflection, arising as it does from the coherent addition of amplitudes, is proportional to the square of the net amplitude of the wave function scattered from a particular set of lattice planes. The net amplitude will be a definite function of the number and positions of the atoms in the planes because the waves scattered by the atoms will have definite phase differences at the neutron detector. The amplitude per unit cell of the crystal for a particular reflection is given in terms of the coherent amplitudes of the individual atoms by the *structure factor* of the unit cell,

$$F_{hkl} = \sum_j a_j e^{2\pi i(hx_j+ky_j+lz_j)}, \tag{1-46}$$

where the summation is over the j atoms of the unit cell, located at the coordinates x_j, y_j, z_j, in units of the unit cell dimensions. We shall discuss the structure factor for several specific crystals in later chapters; it is derived and applied to various crystal forms in standard x-ray texts.[13]

The coherent amplitudes a_j in the structure factor are less than the coherent bound amplitudes that we have considered earlier. As the atoms in a crystal are in constant motion, exhibiting the Debye spectrum of lattice vibrations, these motions introduce variations in phase, which decrease the intensity of the Bragg reflections and produce diffuse scattering. The decrease in the effective coherent amplitudes can be calculated in a completely classical manner[14] in terms of the randomness of location introduced by the temperature vibrations. This decrease is given by the Debye-Waller factor, which must be applied to the coherent bound amplitude to obtain a_j:

[13] For example, C. S. Barrett, *Structure of Metals* (McGraw-Hill, 1943).

[14] As is done by W. H. Zachariasen, *loc. cit.*, for example.

$$a_j = a_{\text{bound}} e^{-D(\sin\theta/\lambda)^2}. \tag{1-47}$$

The constant D is a function of the temperature of the scatterer and the frequency spectrum of its lattice vibrations.[15] Whereas a classical calculation gives the reduction in coherent scattering correctly, the correct quantum mechanical treatment reveals that the incoherent scattering produced is inelastic, involving appreciable energy exchanges with the lattice. We shall consider the details of the inelastically scattering later, Sec. 4.4; fortunately they are not needed in the evaluation of the Debye-Waller factor, which can be taken over directly from x-ray theory.

The structure factor of Eq. (1-46) differs from the x-ray structure factor in one important respect — a respect that simplifies the neutron structure factor greatly. Because the scattering of slow neutrons is s scattering, the angular distribution is isotropic and the amplitude in Eq. (1-46) for each atom is a constant, independent of scattering angle. In the case of x-ray scattering, the atomic form factor, which appears in place of the constant nuclear amplitude, is a function of angle because the electrons that give rise to x-ray scattering are distributed over distances of the same order of magnitude as the x-ray wavelength, hence appreciable phase differences are introduced. In addition, the x-ray scattering from an individual electron is not isotropic and an angular variation arises from this cause as well. The atomic form factor enters Eq. (1-46) for neutron scattering only for a few substances, to be considered in Ch. 5, for which there is appreciable scattering of neutrons by electrons, that is, the magnetic materials.

Another difference between x-ray and neutron diffraction arises from the fact that the absorption of neutrons is usually much smaller than it is for x-rays. As a result, diffraction of neutrons can be studied either by observation of the scattered neutrons, as is done for x-rays, or of the neutrons removed from

[15] O. Halpern, M. Hamermesh, and M. H. Johnson, *loc. cit.* Values for specific materials are given by F. C. Blake, *Rev. Mod. Phys.* **5**, 169 (1933).

a beam by Bragg scattering, that is, by "transmission" measurements (Sec. 2.5). Whatever the arrangement, however, the crystal structure is always determined from the crystal structure factor, which in turn is proportional to the measured scattered intensity. As the structure factor we are considering here is the same, except for the absence of the atomic structure factor, as for x-rays, the analysis of crystal structure by means of these factors follows exactly the same procedure as is used in x-ray diffraction techniques.

In considering the intensity scattered from a crystal, the depth of penetration of the neutrons into the single crystal grains must be taken into account. In this respect, the results of the dynamical theory of x-rays are applicable, which show that the neutrons incident at the Bragg angle penetrate to the order of 10^{-4} cm before a $1/e$ decrease occurs.[16] Concerning the *reflectivity* of a crystal, the same x-ray theory can also be applied with the result that the reflectivity is found to be complete for an angular range of about one second of arc at the Bragg angle for a single neutron wavelength. This figure applies to an ideal crystal and is increased to several minutes for a real crystal because of the angular variation of the crystal planes introduced by mosaic structure. The effect of mosaic structure on the reflectivity has an important bearing on the design of monochromating crystals used to select narrow wavelength bands of neutrons for diffraction work (Sec. 2.2).

[16] M. L. Goldberger and F. Seitz, *loc. cit.*

CHAPTER 2

Experimental Methods in Neutron Optics

In the previous chapter it was found that some of the principles of neutron optics could be obtained most simply by analogy with the optics of light or x-rays. An independent development, containing no reference to electromagnetic waves, was preferable for other phases, however. We shall now see that in some cases the experimental techniques used in neutron optics are also taken over practically directly from standard optical and x-ray methods. As an example of this transfer of techniques, we may cite neutron diffraction from powders, for which the experimental methods are almost identical with those normally used for x-rays. For some phenomena, however, the neutron methods have been developed independently, for instance the reflection of neutrons from mirrors, which although of some use in x-rays, had not been developed quantitatively to any extent.

There are many differences in detail, of course, between the use of neutrons and of x-rays, differences arising from the nature of the available radiation sources and the collimation and intensities available. Neutron and x-ray sources differ with regard to physical shape, intensity, and wavelength distribution, and corresponding differences in technique result. These differences in source characteristics, although important in the attainment of actual results, have no effect on the basic principles involved. We shall not consider the techniques in detail for our object is rather to make clear the principles of the methods in use, the applicability of these methods, the accuracy available, and the range of phenomena that can be covered.

2.1 Neutron Sources

Relative to their use in neutron optics, the important properties of neutron source are high intensity, narrow range of of wavelengths (i.e., nearly monoenergetic neutrons), and low intensities of other interfering radiations. The neutron wavelength available in the source must of course be in the correct range for the phenomena to be investigated; for example, in neutron diffraction the wavelength should be of the order of interatomic distances, otherwise the spatial order of the atoms could not be determined accurately from the observed structure factors. Fortunately the highest intensities of neutrons that are available have wavelengths (a few angstrom units) in just the desired range for diffraction from crystals.

Beams of highest intensity are obtained from neutrons in thermal equilibrium with matter at room temperature; the velocity of these neutrons exhibit the Maxwell distribution familiar from kinetic theory:

$$n(v)\,dv = \frac{4n}{v_0^3\sqrt{\pi}}\, v^2 e^{-v^2/v_0^2}\,dv. \tag{2-1}$$

This equation, illustrated in Fig. 2-1, gives the density of neutrons per unit volume, $n(v)$, as a function of velocity, where n is the total number per unit volume. The velocity v_0 is the "most probable velocity," corresponding to a kinetic energy of kT (0.025 ev); numerically it is 2200 m per sec at room temperature (293° K). The wavelength of the neutrons of most probable velocity is 1.8 A, of just the order of magnitude required for crystal diffraction experiments. The neutron *flux* is obtained by multiplying the density by the velocity; this quantity gives the number of neutrons crossing a unit area per second in a neutron beam.[1] Neutrons of the wavelength required for a particular experiment must be selected from the

[1] The manner in which the fast neutrons are slowed down to thermal, or "moderated," as well as various properties of the Maxwell distribution of slow neutrons, is discussed by the author in *Pile Neutron Research* (Addison-Wesley, 1953), especially Chs. 1, 2, and 3.

distribution of Fig. 2-1, which drops off rapidly both above and below v_0. Attempts to shift v_0 by varying the temperature of the neutron source have not been fruitful, mainly because of the difficulty of changing the temperature of a sizable section of a chain-reacting pile.

Before the advent of chain-reacting piles neutron experiments had been performed with a variety of sources in conjunc-

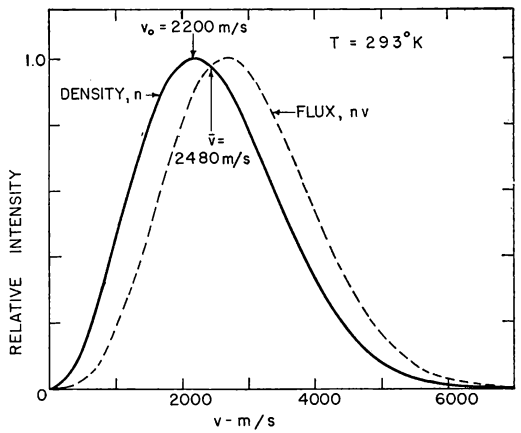

FIG. 2-1. The distribution of neutrons in equilibrium with a moderator at room temperature (T = 293° K); the neutron density and flux are given as functions of velocity.

tion with a material in which the neutrons were thermalized (paraffin or graphite). However, all these sources give such low intensities that accurate neutron optical experiments can hardly be performed. A 1-curie Ra- α-Be source, for example, has a neutron emission rate of about 10^7 fast neutrons per second and if this source is placed in a moderating medium, graphite, for example, the maximum thermal flux (nv) will be of the order of 10^4 sec^{-1} cm^{-2}. A particle accelerator such as a cyclotron, Van de Graaff, or transformer-rectifier accelerator can produce higher intensities of fast neutrons but only of the order of 10 to 100 times that obtained from a Ra- α-Be source.

The fluxes quoted refer to those found *within* the moderating material, of course, and if neutron beams are obtained from any of these arrangements the intensity will be reduced greatly by geometrical factors with a resulting beam flux that is extremely small. The only experiments that can be performed with such weak sources are transmission measurements which, although they show some neutron interference effects, cannot be used for most neutron optics experiments.

The intensities of thermal neutrons available with chain-reacting piles are so large compared with the sources just mentioned that experiments can be performed that are completely out of the question with the non-pile sources. The extensive development of neutron optics as a field of research was a direct result of the advent of chain-reacting piles in 1942 and practically all the experimental results that we shall discuss were obtained with pile neutrons. Pile neutrons constitute a radiation source differing in essential respects from optical and x-ray sources. The pile, for example, emits neutrons more or less uniformly from a large area; hence the geometrical relationships differ from those for x-ray sources, which are of small size.

The actual neutron flux available in a pile neutron beam is calculated directly from the geometry of the hole that is opened into the pile to form the beam. For example, let us assume that a hole (Fig. 2-2) of 10 cm by 10 cm cross section is opened into the pile to a point where the flux is 5×10^{12}. The flux in the beam formed by this hole will be given by the number of neutrons crossing a 1 cm^2 area at the point of interest in the beam, which distance will be of the order of 5 m. The beam flux will then be[2]

$$\frac{5 \times 10^{12} \times 10^2}{4\pi(500)^2} = 1.6 \times 10^8 \text{ neutrons cm}^{-2} \text{ sec}^{-1}. \quad (2\text{-}2)$$

[2] The pile flux chosen for this example is the value at the center of the Brookhaven pile for full power (25 megawatts). The flux at the Argonne and Oak Ridge piles is of the same order of magnitude and that at Chalk River, Canada, about tenfold higher.

The collimation (angular divergence of neutrons in the beam) in this particular case will be of the order of 10/500 or about 1°.

The angular resolution needed for crystal diffraction is higher than that just calculated by an order of magnitude, and for mirror experiments even greater collimation is necessary. Higher resolution is obtained by installation of diaphragms to limit the angular divergence of the beam, with an attendant reduction in intensity. Thin sheets of cadmium suffice to stop

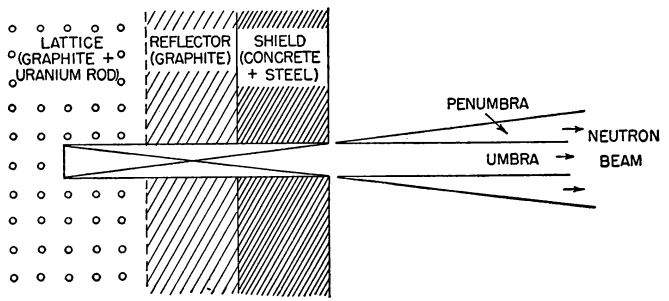

FIG. 2-2. Geometrical relationships involved in the formation of a neutron beam in an experimental hole at a pile. The intensity is constant in the umbra and decreases to zero at the outer edge of the penumbra.

the thermal neutrons, but it is necessary also to reduce the fast neutrons that are always present as a background. As fast neutrons are much more penetrating than thermals, collimators usually consist of large blocks of material. In actual practice, combinations of materials, for example plastic, iron, and lead, are used in order to stop the various types of radiation that are present. The intensities in pile beams are so high that it is of utmost importance to limit the stray radiation, not only from the standpoint of interference with the experiments but to eliminate the possibility of harm to the experimenters. The techniques for the formation of beams have been developed sufficiently well so that neutron fluxes of the

order of 10^7 thermal neutrons are available in beams sufficiently well-collimated for diffraction experiments, while somewhat lower intensities with correspondingly higher collimation are used for neutron mirror research.[3]

2.2 Production of Monoenergetic Neutrons

Once a copious flux of well-collimated thermal neutrons is available it is then necessary in almost all cases to select monoenergetic neutrons in order to perform neutron optical experiments. Whereas in some work the entire Maxwell distribution has been used, at the present time there are very few experiments that are still performed with the wide energy spread represented by the Maxwellian. There are several methods available for selecting monoenergetic neutrons, or more precisely, neutrons whose velocities (hence energies and wavelengths) lie within a narrow band. Some of these methods perform only a crude "monochromatization" but allow high intensity, whereas others give almost monoenergetic beams but of course at a correspondingly high loss in intensity.

One of the first methods used for isolation of discrete energy groups involves the use of neutron filters; for special applications filters are still of great value, as we shall see later. The type of filter that concerns us here is based on the fact that in a polycrystalline material no Bragg reflection occurs for which the wavelength is longer than twice the largest lattice spacing. This result is obtained directly from Eq. (1-44) with $n = 1$ and d taken as its maximum value, d_m, given by the smallest sum in the denominator of Eq. (1-45). In principle, the latter sum would be unity, for the (100) planes, but if the form factor Eq. (1-46) should be zero for the (100) reflection the planes of next smaller spacing, probably the (110) planes would give d_m.[4] For wavelengths longer than this "cutoff wave-

[3] For details of these techniques, see D. J. Hughes, *Pile Neutron Research*, Sec. 9.1, 10.5, 11.1, 2, 3, and 12.4.

[4] This is the case for iron, for example, which has a face-centered unit cell. The largest d is given by $a_0/\sqrt{2} = 2.86\text{A}/\sqrt{2} = 2.02$ A hence the longest reflected wavelength is 4.04 A.

length" no Bragg scattering occurs and the only remaining processes that remove neutrons from a beam are incoherent scattering and neutron reactions (usually neutron capture).

For certain materials the capture and incoherent scattering are extremely low, and these materials are therefore suitable for neutron filters. The materials that have been used most extensively are graphite, beryllium, and beryllium oxide, with cutoff wavelengths 6.7, 4.0, and 4.5 A. The neutrons of wavelength beyond the cutoff are transmitted through a block of filter material, Fig. 2-3, with practically no loss in intensity whereas the shorter wavelength neutrons are removed by Bragg

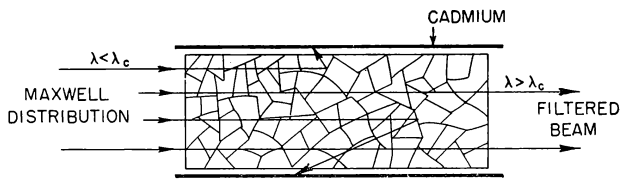

FIG. 2-3. The manner in which a polycrystalline material acts as a neutron filter. Neutrons of $\lambda < \lambda_c$ (the cutoff wavelength) are Bragg scattered and captured in cadmium while wavelengths greater than cutoffs penetrate the filter.

scattering. Although the resultant beam is not monoenergetic, it has an exceedingly sharp cutoff wavelength, which for some purposes, particularly mirror reflection, is as useful as a monoenergetic beam. Figure 2-4 shows the energy distribution of thermal neutrons after filtration through a graphite block 10 cm in length.

Direct methods of neutron velocity selection by measurement of time of flight, which had been used with cyclotron neutrons and even with Ra-Be sources, are now extensively used with pile neutrons. The velocity selection consists of the production of a burst of neutrons by some method and the measurement of the time of arrival of the neutrons at a detector several meters away. The timing is performed by sorting the counts that are produced in the neutron detector into various

channels according to arrival time, and in this way many velocities are recorded at the same time.

Whereas the techniques of timing are the same whether the neutrons are produced by the cyclotron or the pile, the burst production methods are necessarily different. The neutron

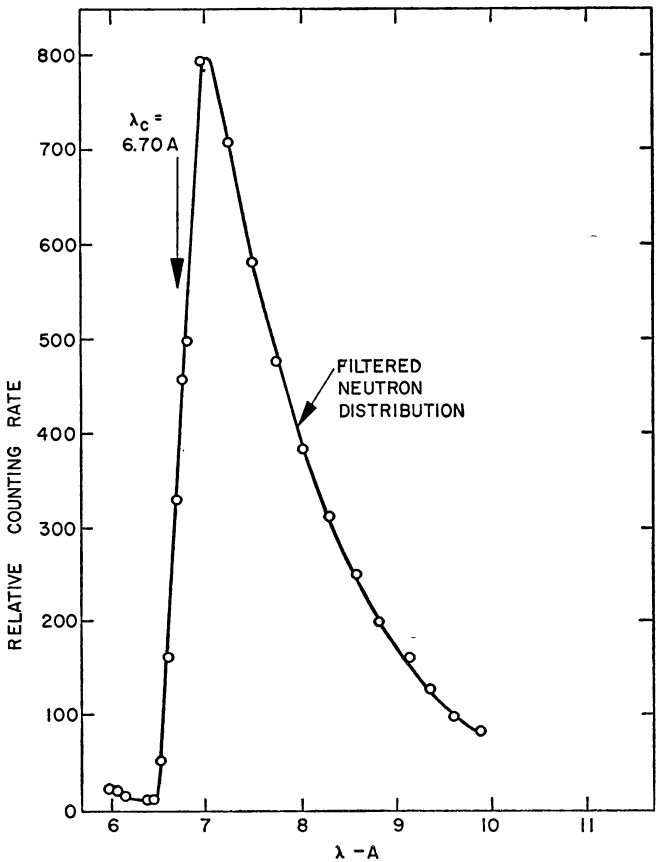

FIG. 2-4. Wavelength distribution of neutrons after passage through a graphite filter of the type illustrated in Fig. 2-3. The distribution would show an abrupt drop at λ_c were it not for the finite resolution of the detecting instrument, the Brookhaven slow chopper.

source can be modulated with the cyclotron, for example by pulsing the arc source of the cyclotron, whereas the pile neutrons must be interrupted mechanically by some type of shutter placed in the beam. Although the mechanical shutter, the so-called pile chopper, reduces the beam intensity greatly because of its low duty cycle, it has many applications arising from the fact that neutrons of a wide wavelength range can be utilized, from the thermal region out to wavelengths as long as 25 A.[5] The velocity selectors do not produce true monoenergetic neutrons, as do the crystal monochromators to be considered next, for all velocities are still present in the pulsed beam that strikes the detector. Any practical difference between velocity "selection" and true "monochromatization," as far as neutron optics is concerned, is negligible, however.

The principal method of monochromatization in use for pile neutrons is of course Bragg reflection at a single crystal. This method fits naturally into diffraction work because the angular resolution desired for investigation of crystals with the monochromatic beam is of the same order as that used for the monochromating crystal. The crystal monochromator is also used for energies other than thermal, but its use for higher energies, where interference effects are negligible, does not interest us here. For wavelengths longer than thermal, the monochromatic beam is contaminated with neutrons of shorter wavelength, reflecting with values of n higher than unity. These higher order reflections make the use of the crystal for long wavelengths very difficult. At the most intense part of the Maxwell distribution a crystal can give an intensity of about 10^4 neutrons per second with a resolution in wavelength of about 3%. The wavelength resolution in terms of the collimation of the incident beam, $\Delta\theta$, follows from Eq. (1-44),

$$\frac{\Delta\lambda}{\lambda} = \cot\theta\Delta\theta, \tag{2-3}$$

[5] The wavelength distribution of Fig. 2-4 was measured with the Brookhaven "slow chopper," for example.

thus the $\Delta\lambda/\lambda$ of 3% just mentioned corresponds to a $\Delta\theta$ of 0.5 degree.

The intensity of neutrons reflected by the monochromating crystal is larger for increased mosaic spread of the crystal, Sec. 1.4. As the mosaic spread is usually less than the beam collimation, a few minutes compared with 30 minutes, increase of the former will increase the reflected intensity without affecting the resultant wavelength spread appreciably. A good

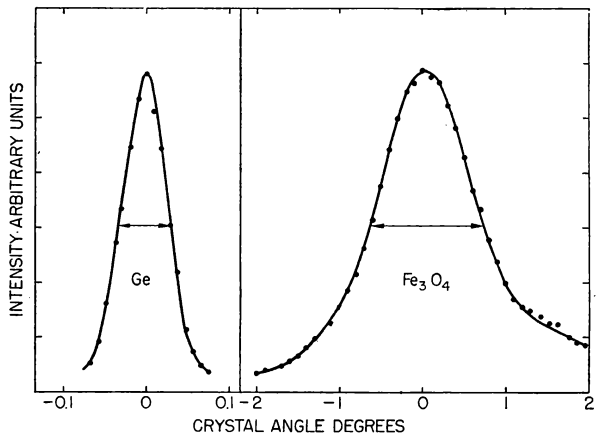

FIG. 2-5. The mosaic spread of germanium and natural magnetite crystals as measured by McReynolds. The spread for germanium is only three minutes, whereas that for magnetite is 1.3 degrees.

crystal monochromator is thus one with a large mosaic spread, and the metal crystals, for example lead, are advantageous for this reason. Some recent investigations of McReynolds[6] show the wide variation in mosaic spread among different crystals; for example (Fig. 2-5) Ge has a spread of only 3′ whereas that for natural magnetite (Fe_3O_4) is 1.3°.

There has been some use of combinations of the devices used described for special applications. For instance, a filter can be used with a crystal monochromator to eliminate the higher

[6] A. W. McReynolds, *Phys. Rev.* **88,** 958 (1952).

order reflections and thus enable use of the crystal for long neutron wavelengths. It is also possible to use mirror reflection, which gives a sharp cutoff similar to that of a neutron filter, in conjunction with crystals for the same purpose. We shall have occasion to refer to various combinations of monochromators applied to specific measurements as we consider later the various results of neutron optics.[7]

2.3 Small Angle Scattering

A group of neutron optical phenomena that illustrates the fundamentals of neutron refraction is made up of various small angle scattering effects. These effects illustrate extremely well the transition from geometrical to physical optics of neutrons, for in some cases geometrical or ray optics predicts the observed scattering, whereas in other cases, for which the particle size is comparable to the neutron wavelength, it is necessary to consider the physical optics of diffraction. Small angle scattering of neutrons was observed by accident in several materials in connection with cross section measurements and later investigated in detail. While they do not have many important applications, these examples of small angle scattering are instructive in the study of optics of neutrons. The experiments were useful, not so much for the direct experimental results, but because they led to development of experimental methods that did have important applications.

The first observation of the small angle scattering of neutrons was made in magnetic materials. It was found[8] that a well-collimated beam of neutrons was spread slightly on passage through unmagnetized iron (about one minute of arc in a 1-cm block), but that no spreading took place with magnetized iron. Comparison of the experimental scattering distribution with a Gaussian, as well as its variation with block

[7] The brief description of neutron monochromatization techniques given in Sec. 2.2 may be supplemented by reference to D. J. Hughes, *op. cit.*, Chs. 6 and 9.

[8] D. J. Hughes, M. T. Burgy, R. B. Heller, and J. R. Wallace, *Phys. Rev.* **75**, 565 (1949).

thickness (as the square root), showed that the scattering was a multiple process that was related to magnetic domain structure. The deviation experienced by a neutron as it passes from one magnetic domain to another can be calculated from the index of refraction for a ferromagnetic material, which we shall consider in Sec. 5.1. For the case of two adjacent domains in which the magnetizations are antiparallel, the relative index will be

$$n^2 = 1 \pm \frac{2\mu B}{E} \tag{2-4}$$

where μ is the neutron moment and B the component of the magnetic induction in the domain boundary. The maximum deviation (twice the critical angle) occurs when a neutron is incident on a domain boundary at the critical angle, which angle follows from Eq. (1-43) and (2-4);

$$\theta_c = \sqrt{\frac{2\mu B}{E}}. \tag{2-5}$$

The average deviation, (less than 1 % of the maximum), which must be calculated for comparison with the observed scattering distribution, is given by a straightforward but lengthy calculation. The result, however, agreed extremely well with the experimental scattering. Whereas the magnetic scattering was not used for any practical applications, the finding that iron is doubly refracting led to the production of highly polarized neutron beams and other valuable applications.

Shortly after the experiments with iron, small angle scattering was also observed[9] for nonmagnetic powders, in connection with transmission cross sections measurements at long wavelength. Again, as for the magnetic scattering, careful measurements as a function of wavelength and geometry showed that the scattering could be interpreted as multiple refraction of the neutrons in the small particles composing the sample. The

[9] By H. H. A. Krueger, D. Meneghetti, G. R. Ringo, and L. Winsberg, *Phys. Rev.* **80**, 507 (1950).

refracting surfaces in this instance are the actual boundaries of the separated particles, unlike the magnetic small angle scattering, where only a magnetic discontinuity exists. For solid materials such as copper and lead the scattering was not observed. Detailed investigations of small angle scattering from powders was later carried out by Weiss[10] in order to check the variation of the average scattering angle with wavelength and particle size. The particle sizes used ranged from the magnitude for which geometrical optics is valid to the small sizes where it is necessary to consider the scattering as diffraction. The refraction treatment is valid when the average deviation calculated from the refraction approach above is larger than the diffraction deviation ($\sim\lambda/a$ where a is the particle size), and vice versa. It was found that the scattering varied in good accord with the theoretical formulations with regard to wavelength, particle size and sample thickness.

Some practical application of the small angle scattering techniques was made by Weiss to the determination of nuclear constants. The small angle scattering was measured for a particular powder sample, then the powder was immersed in a liquid of known index of refraction. The change in the small angle scattering, which of course is determined by the relative index of the material and the liquid, gives the sign of the scattering amplitude of the powdered material. No quantitative results were obtained in this work, because of the average nature of the scattering and the small size of the observed deviations. Although the experiments are instructive, much better results can be obtained for neutron refraction phenomena when investigated by means of mirror reflection.

The small angle scattering of neutrons is actually closely similar to the analogous scattering that has been thoroughly studied with x-rays for the last few years. In connection with the x-ray work there has been extensive theoretical study and the results of these studies are easily applicable to neutrons. Accurate calculation of the small angle scattering is complicated

[10] R. J. Weiss, *Phys. Rev.* **83**, 379 (1951).

by the coherence that exists between waves scattered from the various particles. A review of the theoretical papers developed for x-rays has been given by Vineyard,[11] while calculations specificially applicable to neutrons have been made by Gerjuoy and Halpern.[12] As the experimental methods of small angle neutron scattering have not been used for results that we shall consider later there is no point in purusing them further at this point. The actual research techniques used in the measurements mentioned are reviewed by Hughes,[13] and given in detail in the references quoted in the present section.

2.4 Refraction and Reflection

The methods that are used for measurements of nuclear and atomic properties by means of neutron refraction and reflection are not based on analogous x-ray techniques. Although these phenomena are known for x-rays, they are not used to any appreciable extent to study the interaction of x-rays with matter. The refraction and reflection of neutrons, however, furnish useful tools for the investigation of neutron interactions. One reason for the greater applicability of these phenomena for neutrons than for x-rays is related to the fact that there are more sources of incoherent scattering for neutrons than for x-rays. As we shall see, refraction effects are particularly adaptable for measurement of coherent and incoherent scattering and as a result find more applications for neutrons than for x-rays.

The deviation of a neutron beam that occurs at a single surface could be used for a measurement of the index of refraction but this method would not give accurate results. The angular changes involved would be exceedingly small, and in addition the scattering of neutrons in passing through the material would in most cases decrease the intensity appreciably. For refraction at a surface, the maximum deviation is half the

[11] G. H. Vineyard, *Phys. Rev.*, **85,** 633 (1952).
[12] E. Gerjuoy and O. Halpern, *Phys. Rev.* **76,** 1117 (1949).
[13] D. J. Hughes, *Pile Neutron Research*, Ch. 11.

critical angle for total reflection and this value, which (Sec. 1.3) would be 6 minutes for thermal neutrons in Be for example, would occur only for a grazing incident angle.

The best method for measurement of the index of refraction is observation of the critical angle for total reflection, for

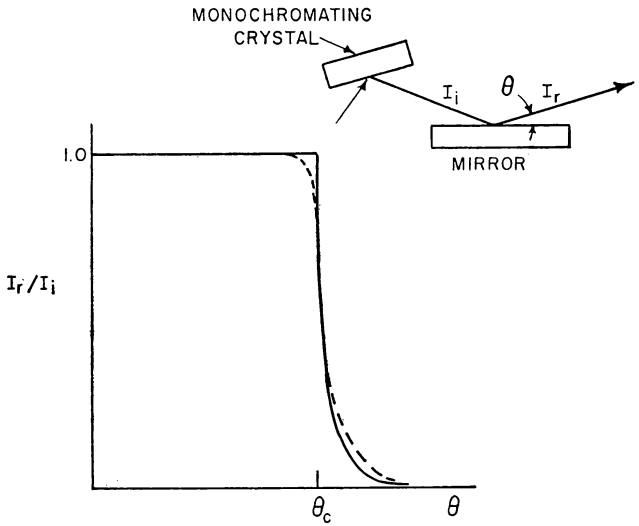

FIG. 2-6. Intensity reflected from a mirror for an incident monochromatic beam. The solid line, which gives the behavior for infinite resolution, is modified (dashed line) by the finite resolution of actual experiments.

the observed effect is then the largest and usually no passage of neutrons through the material is necessary. In the most direct approach, the critical angle would be determined by use of monochromatic neutrons and observation of the angle at which the reflected intensity from a neutron mirror decreases suddenly, Fig. 2-6. As used by Fermi and Marshall,[14] this method involves monochromatization of the incident neutrons by Bragg reflection at a single crystal. The available intensity

[14] E. Fermi and L. Marshall, *Phys. Rev.* **71**, 666 (1947).

is rather small because the angular divergence of the monochromatic beam must be reduced to a few minutes in order to observe the critical angle with any accuracy, and this collimation lowers the resultant beam intensity.

Another method for critical angle measurement, developed by Hughes and Burgy,[15] utilizes a neutron beam filtered through

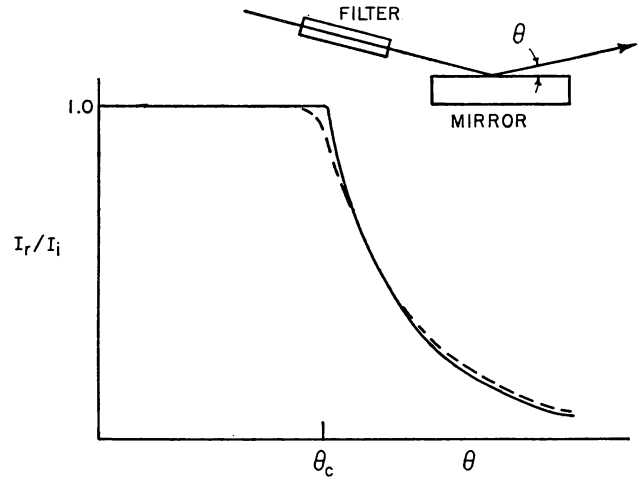

FIG. 2-7. Intensity reflected from a mirror for an incident filtered Maxwell distribution, the effect of finite resolution being shown by the dashed line.

beryllium oxide or graphite. Filters of these materials, as we saw in Sec. 2.2, produce a beam with a sharp cutoff wavelength with very little loss in intensity. The filtered beam is reflected from a mirror, and measurement of the reflected intensity as the incident angle is increased gives the critical angle. The reflected intensity, Fig. 2-7, begins to decrease at the critical angle for the longest incident wavelength (the filter cutoff wavelength). Although the intensity decrease above the critical angle is less rapid than it is for monochromatic neutrons, it is

[15] D. J. Hughes and M. T. Burgy, *Phys. Rev.* **81**, 498 (1951).

possible to fix the critical angle accurately because the shape of the reflectivity curve is a simple function of the Maxwell velocity distribution. In obtaining an accurate value for the critical angle it is necessary to make minor corrections for the finite spread in incident wavelengths and the slight reflectivity that takes place above the critical angle. It is possible with careful work, however, to measure critical angles to the order of 0.5 %.

The principal advantages of the mirror method follows from the direct connection between the critical angle and the coherent scattering amplitude of the mirror material, Eq. (1-43). The amplitude in this equation is the coherent bound amplitude, there being no correction for temperature diffuse scattering (the Debye-Waller factor is unity) because the index of refraction is determined by scattering in the forward direction. In addition, the amplitude is an average over the atoms of the mirror and is independent of the crystalline state. In other words, because the scattering is forward, all form factors are unity. Critical angles can thus be obtained for mirrors made up of mixtures of materials and the result will give the average amplitude of the components directly. This averaging property implies, for example, that an unmagnetized ferromagnetic material will have a single critical angle in which only the nuclear amplitudes enter. The independence of structure that is such an advantage in the determination of coherent amplitudes by mirror reflection implies, of course, that the method finds little application to crystal structure investigation.

A possible source of uncertainty in the determination of coherent amplitudes by mirror reflection is associated with the nature of the surface layer from which the reflection takes place. On first thought, it might appear that thin layers of foreign material on a surface, oxides for example, might vitiate the measurements. However, the depth of penetration of the neutron wave into the mirror at incident angles near critical is surprisingly large. The wave drops off exponentially with distance into the mirror and the depth of penetration for a $1/e$

decrease in intensity, d_e, is given[16] by

$$d_e = \frac{\lambda\!\!\!^{-}}{(\sin^2 \theta_c - \sin^2 \theta)^{1/2}}. \tag{2-6}$$

While it is true, as pointed out by Goldberger and Seitz,[17] that d_e is only about 100 λ at $\sin \theta = 0$, it becomes infinite for incidence precisely at the critical angle. Although the neutrons are incident over a range extending about a minute from the critical angle in actual experiments, the depth of penetration will still be of the order of 10^3 angstroms. The average amplitude that enters the critical angle expression will thus be that for the bulk material and will be unaffected by any surface layers a few atoms thick.

The direct measurement of a coherent amplitude in terms of the critical angle is limited in accuracy by the dependence of the amplitude on the critical angle squared. Balancing techniques can be invoked, however, and accurate coherent amplitudes measured in spite of the sensitivity of the amplitude to the critical angle.[18] The balancing techniques consist of measurement of the critical angle for a combination of materials, in which case one material can be measured relative to the other with great accuracy. The combination can be obtained by mixing materials in a single mirror, for example a liquid mirror, or by reflecting neutrons from the interface formed by a combination of two materials. We shall examine several specific cases later in which this balancing technique has been used to good advantage.

2.5 Diffraction Techniques

Although the diffraction of neutrons from crystals resembles that for x-rays closely, both qualitatively and quantitatively, there are a few differences that give rise to experimental methods for neutrons that are not applicable for x-rays.

[16] M. Born, *Optik* (Edwards, 1943) pp.
[17] M. L. Goldberger and F. Seitz, *Phys. Rev.* **71**, 294 (1947).
[18] D. J. Hughes, *op. cit.*, Ch. 11.

Thus the absorption cross section, which is appreciable for x-rays, is extremely small for neutrons in certain low capture elements, for example Be, C, and O. As a result of this difference, it is possible to study neutron diffraction by observation of the beam transmitted through a sample as well as by the standard x-ray methods of scattered intensity measurement. Another obvious difference in technique arises from the magnetic scattering of neutrons, which necessitates diffraction measurements as a function of state of magnetization of various samples. In all the diffraction work, however, as for x-rays, the main concern is the relationship between the coherent scattering amplitudes and the intensity in the Bragg reflected peaks. The intensities can be used to measure the coherent scattering amplitudes, or, if the latter are known, for a determination of the structure of the material.

The measurement of diffraction effects by transmission is useful only for those materials in which the capture cross section is quite low, but for these materials it has certain advantages arising from the fact that a wide range of neutron velocities may be used. Crystal diffraction is practicable only for the most intense part of the Maxwell distribution, but transmission measurements, possible with much smaller intensities, can be used in the less intense region of the velocity distribution.

We shall examine briefly the transmission of neutrons in a polycyrstalline material as a function of wave length because it illustrates several of the fundamental principles of all diffraction measurements. For wavelengths longer than twice the largest lattice spacing of the crystal lattice, the transmission cross section will be extremely small for a low capture material because no Bragg reflections are possible. As the wavelength is decreased, the cross section will suddenly increase as the wavelength passes the value $2d_m$ (Sec. 2.2). For wavelengths just shorter than $2d_m$ only the set of lattice planes of spacing $2d_m$ is active and the cross section is proportional to λ^2, as shown in Fig. 2-8. As the wavelength decreases further, additional discontinuities occur in the cross section as each set of lattice

planes is passed. Precisely at the cutoff for each wavelength, neutrons scatter only from those crystal grains in the material for which the lattice planes are perpendicular to the neutron motion, whereas for shorter wavelengths those crystal grains for which the neutrons are incident at the angle given by the Bragg equation produce reflections.

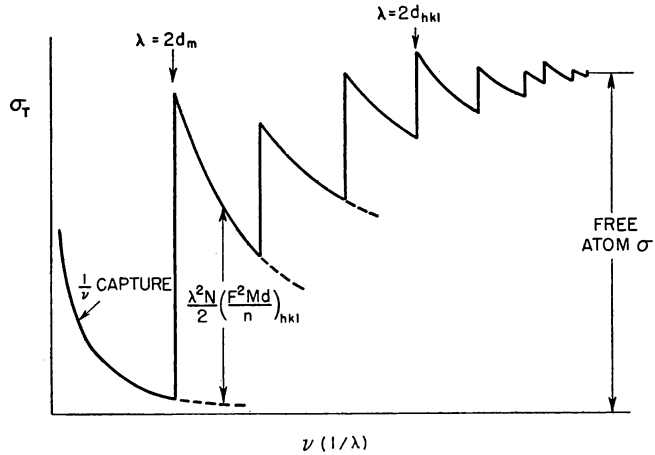

FIG. 2-8. The total cross section of a polycrystalline material as a function of neutron velocity, illustrating $1/v$ capture and the contributions of various sets of lattice planes to the total cross section.

The scattering averaged over the randomly oriented crystal grains can be expressed[19] as a cross section per nucleus,

$$\sigma = \frac{\lambda^2 N}{2} \sum \left(|F|^2 M \frac{d}{n} \right)_{h,k,l}. \tag{2-7}$$

where the summation is over the lattice planes effective at the particular wavelength (i.e., those for which $2d/n < \lambda$). The structure factor F (which contains the Debye-Waller factor)

[19] O. Halpern, M. Hamermesh, and M. H. Johnson, *Phys. Rev.* **59**, 981 (1941); E. Fermi, W. Sturm, and R. Sachs, *Phys. Rev.* **71**, 589 (1947).

and the lattice spacing d have already been discussed (Sec. 1.4), and M is the *multiplicity* or the number of possible orientations of a crystal grain that give the same reflection ($M = 6$ for a simple cube, for example). For short wavelengths so many planes are active that the cross section becomes practically constant.

Only incoherent scattering occurs for wavelengths beyond the cutoff and studies of these nondiffraction effects by neutron transmission are useful in investigation of the various types of incoherent scattering, Sec. 4.4. The "crystal breaks" of Fig. 2-8 can be related to definite lattice reflections and the structure factors measured from the size of the discontinuities. For studies of crystal structure, however, for which neutrons in the wavelength region 1-2 A are appropriate, the structure may be determined much more easily by conventional neutron diffraction studies of the scattered intensity.

The methods used in the study of neutrons scattered from single crystals or powders, rather than those transmitted, are almost exactly the same as those developed extensively for x-rays. Thus the Laue method may be used in which a polycrystalline beam is incident on a single crystal and the structure determined from the observed Laue spots. The available neutron intensities are so low, however, that this method has been of extremely limited value for neutron studies. Techniques analogous to the rotation analysis, utilizing monochromatic neutrons with single crystals, are of definite value however; for example in the early work of Fermi and Marshall,[20] and in more recent studies described in Ch. 4. In this method of analysis, the single crystal is rotated into different orientations in order to produce the Bragg reflections. The powdered crystal or Debye-Scherrer method, however, has been most extensively used in neutron diffraction. Here monochromatic neutrons are scattered from a polycrystalline sample, and each set of reflecting lattice planes produces a conical distribution of scattered neutrons centered about the unscattered beam. Some loss of

[20] E. Fermi and L. Marshall, *Phys. Rev.* **71**, 666 (1947).

intensity relative to single crystal diffraction results because the reflected neutrons for a particular set of planes are distributed in a complete cone around the incident neutron direction.

Much of the development of the powder diffraction approach has been carried out by Shull and Wollan at Oak Ridge.[21]

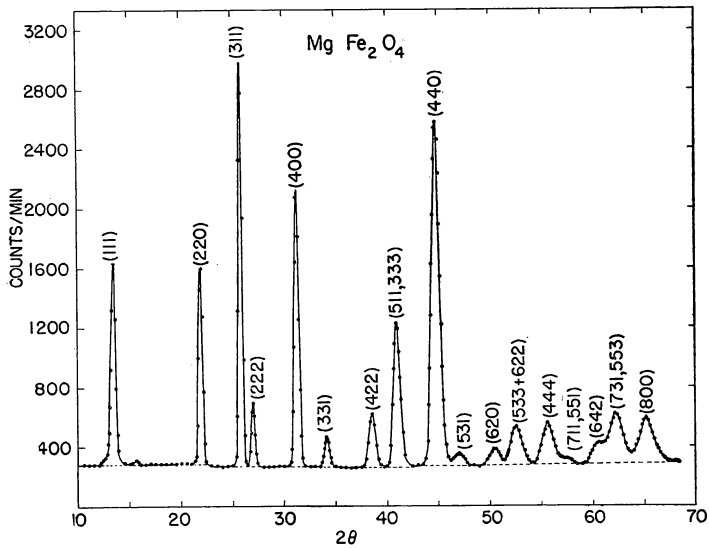

FIG. 2-9. The diffraction pattern of magnesium ferrite obtained with the diffraction apparatus of Corliss and Hastings at Brookhaven Laboratory.

Because the presently available neutron intensities are still somewhat low in diffraction work (of the order of several hundred counts per minute in powder patterns), it is necessary to make extended runs. For this reason, diffraction equipment is designed to operate automatically, the detecting counter and powder sample being moved periodically and counting rates recorded automatically. Some improvements in the standard diffraction equipment have been made recently by Corliss and

[21] E. O. Wollan and C. G. Shull, *Phys. Rev.* **73**, 830 (1948).

Hastings at Brookhaven Laboratory. Their equipment produces intensities of Bragg peaks in some crystals as high as several thousand counts per minute, as shown in the pattern of Fig. 2-9. The intensity is increased in this apparatus by the use of multiple parallel slits, which do not increase the angular spread of neutrons arriving at the crystal but do result in higher intensity, and by a lead monochromating crystal, of large mosaic spread. The crystal rotation, counter arm motion and counting rate recording are carried out by means of automatic controls, the powder patterns being obtained during as much as 72 hr of unattended operation.

The experimental data obtained with the diffraction equipment consist of a series of intensities for different Bragg reflections. These intensities can be related to the structure factors for individual reflections in a manner essentially the same as given by Eq. (2-7). Thus for the experimental arrangement used for Fig. 2-9, the reflected intensity for a reflection relative to the incident intensity for the (h, k, l) set of planes is easily obtained from Eq. (2-7) as,

$$\frac{I_{h,k,l}}{I_0} = \frac{\lambda^2 N^2 l h}{4\pi \sin 2\theta \cos\theta} \left(|F|^2 M \frac{d}{n} \right)_{h,k,l}. \qquad (2\text{-}8)$$

Here the intensity is calculated for a detector of height l at distance h from the sample, and the other factors follow from the geometry of the path length in the sample and the distribution of the scattered neutrons in an entire cone. The use of Eq. (2-8) to obtain the structure factors as well as the methods of analyzing these factors to obtain either the structure of the material or the scattering cross section will follow the same principles as x-ray work, and these details need not concern us. We shall examine later the applications of powder diffraction to particular important cases and shall see the respects in which neutron diffraction does reveal characteristics not sensitive to x-rays.

CHAPTER 3

Measurement of Nuclear Interactions by Means of Neutron Optics

The observed interference effects of neutron optics, diffraction patterns, transmission cross sections, or critical angles, can be interpreted to give various types of data, depending on the information already available for the particular scattering system. For example, should the coherent scattering cross sections of the components of a crystal be accurately known, the observed intensities in a diffraction pattern can be used to determine the constants of the crystal structure factor, i.e., to fix the structure of the crystal itself. The opposite procedure may apply for other crystals, for which the observed intensities from a known structure are used to obtain the coherent scattering cross sections of the constituents. In the present chapter we shall consider this latter procedure, the measurement of coherent cross sections (more precisely, amplitudes) by interference effects. The coherent amplitude measurement must of course precede structural determinations for the amplitudes are necessary for the interpretations of structure. An examination of the methods involved in the amplitude work illustrates clearly the basic principles we have already discussed and will aid in the understanding of the later structure measurements.

In addition to the need for coherent cross sections in diffraction applications, certain coherent cross sections, those of the fundamental particles, are of basic interest for nuclear theory. These latter cross sections usually require results of high accuracy, and we shall consider their measurement in some detail. These measurements illustrate the power of neutron-optical methods, and the results themselves are interesting be-

cause of their application to fundamental nuclear physics theory. Our consideration of the experimental material will be arranged according to the nuclear properties of interest, rather than the experimental methods, for our interest is mainly in the fundamental neutron-optical phenomena involved and the results obtained, rather than the details of experimental techniques. Our method of approach also allows a comparison of the various methods of measurements with regard to a particular coherent cross section at a single point in the discussion.

3.1 Direct Measurement of Coherent Cross Sections

Coherent cross sections may be determined in two general ways; by the direct measurement of interference effects or by inference from the total cross section. The specific applications of these two methods may vary greatly in experimental technique, depending on the specific material involved, but the general principles still apply. We shall see that the direct method is used for most elements but that the indirect method gives high accuracy for several important standards.

The direct determination of the coherent scattering amplitude of an element is simple in principle for it involves merely the measurement of the structure factor, Eq. (1-46), or of a critical angle, Eq. (1-43), quantities that are simple functions of the coherent amplitude. As the coherent cross section for an isolated nucleus (isotropic scattering) is just $4\pi a^2$, we need not at present distinguish between the coherent amplitude and cross section. The amplitude is used in the evaluation of the structure factor and index of refraction, but the conversion to cross section is often convenient. In the case of magnetic scattering, we shall see that the angular distribution is nonisotropic even for an isolated nucleus, hence the "cross section" ($4\pi a^2$) has little meaning.

Considering the diffraction pattern obtained from an element, we see that Eq. (1-46) gives the coherent amplitude in terms of the scattered intensity in a particular peak (h, k, l) relative to the incident intensity. In practice it is exceedingly

difficult to determine the ratio of the scattered to the incident intensity, hence relative measurements are usually made in which the unknown amplitude is determined relative to that of a standard contained in the same crystal compound. The observed intensities for the different diffraction peaks of a compound give algebraic combinations (the structure factors) of the coherent amplitudes of the constituents, that is of the a_j's of Eq. (1-46). Measurements of the structure factors for several different reflections can be combined to give the individual a_j's in terms of that of the standard.

Even though only relative intensities are needed in the method just described there are several interfering effects that make accurate measurements difficult. The observed amplitudes are of course not the true bound amplitudes, but are reduced because of temperature diffuse scattering by an amount given by the Debye-Waller factor, Eq. (1-47). The correction of the observed amplitudes to the completely bound values can be made either by calculations of the Debye-Waller factor or by extrapolation of the observed amplitudes to zero angle, at which the Debye-Waller factor becomes unity. While the calculated Debye-Waller factor is accurate for elements it is highly inaccurate for the case of compounds because of the assumption of a single Debye temperature for a compound. The extrapolation to zero angle, however, can usually be made to an accuracy of a few per cent.

Difficulty is experienced if the material involved has appreciable diffuse scattering, for the observed diffraction peaks will then be observed above a high background and their intensity therefore harder to estimate. An extreme case of diffuse scattering is that of hydrogen, as we shall see in Sec. 3.3 (Fig. 3-2). A similar diffuse background will arise if the sample is large enough so that multiple scattering can occur. Further complications arise if the individual crystal grains in the sample are larger than the penetration distance of the neutrons.* In

* While this distance is only about 10^{-4} cm for a perfect crystal, the presence of mosaic structure means that the individual crystal

this case the neutron wave will not fully illuminate each grain, and this extinction effect will change the relative intensities of different reflections, thus causing errors in the relative amplitudes.

The coherent amplitude of the standard material, to which the relative measurements are referred, is obtained from the total cross section in the manner to be discussed in Sec. 3.2. If it is possible to use such a well-established standard as carbon or oxygen, only a negligible error will arise from the inaccuracy of the standard. Fortunately, it is almost always possible to utilize a compound containing an accurate standard.

Many measurements of coherent scattering by diffraction were made by Wollan and Shull[1] as a necessary preliminary to studies of structure. Their results for the scattering cross section have an accuracy in general of about 5 %, but in a few favorable cases it is of the order of 1 %. In general, the determination of coherent cross sections from diffraction patterns is advisable if there is little incoherent scattering and if the material can be obtained in a well-understood, simple, crystal form. Examples of actual results of neutron diffraction measurements of coherent scattering will be listed in Sec. 3.2.

We now turn to a brief consideration of the other method of direct amplitude measurement, that of mirror reflection. Accurate determination of coherent cross sections by critical reflection have not been made for many materials, largely because each case presents a specific problem in its own right. As we shall see, the method has been used rather for a few problems in which high accuracy is necessary, and for these particular applications the mirror method has given greater accuracy than diffraction. In the neutron mirror technique, the amplitude is determined directly from the critical angle by means of Eq. (1-43), with no corrections analogous to those described for the

grain can be much larger, of the order of 0.1–1.0 mm. (Secs. 1.4 and 4.1).

[1] E. O. Wollan and C. G. Shull, *Phys. Rev.* **73,** 830 (1948); C. G. Shull and E. O. Wollan, *ibid.* **81,** 527 (1951).

diffraction method. The Debye-Waller factor is unity because the index of refraction, hence the critical angle, is determined by the scattering in the forward direction. In addition, the critical angle is completely independent of the structure of the mirror

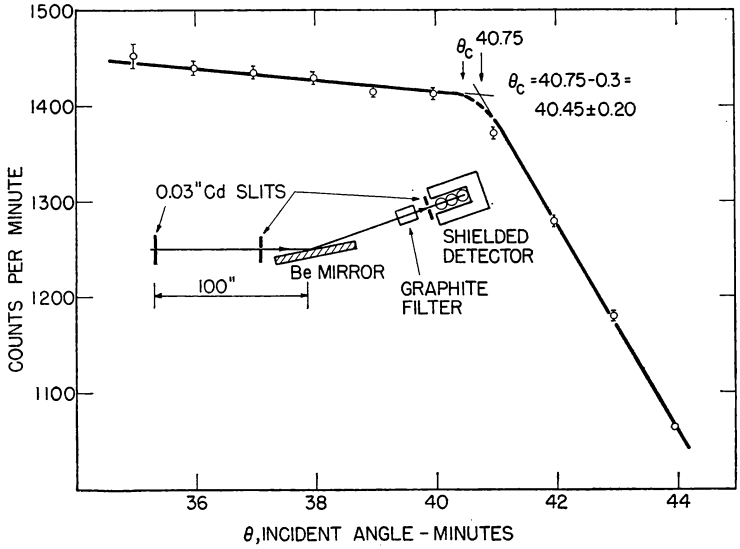

FIG. 3-1. Experimental arrangement and reflectivity curve for the measurement of the critical angle of beryllium by reflection. The dashed curve is the theoretical shape near the critical angle, taking into account the finite reflectivity and resolution. This curve is used to obtain θ_c from the observed "break" by subtraction of 0.3 minute.

material, that is of its crystalline structure. Equation (1-43) gives the coherent amplitude correctly, whether the mirror is liquid, solid or gas, if N is the corresponding density of nuclei.

In spite of these advantages in the principle of the method, in practice the determination based on a simple application of Eq. (1-43) does not have great accuracy. The limitation in accuracy follows from the fourth power dependence of the scattering cross section on the critical angle. A careful application

of the direct mirror method was made by Harvey, Goldberg, and Hughes[2] to beryllium in order to assess the power of the method (Fig. 3-1). High angular resolution of the incident beam ($\frac{1}{4}'$ of arc) and careful intensity measurements made possible an accuracy of $\frac{1}{2}$ % in the critical angle, hence 1 % in the amplitude or 2 % in the coherent cross section. This accuracy is inferior to that obtained by the method to be described in Sec. 3.2, even though Be was particularly adapted to the mirror method because it polishes well and has an unusually large density of nuclei (N).

The coherent cross section of several rare gases was measured by McReynolds;[3] here the mirror method was of advantage, even though the accuracy was only about 10 % for the amplitudes, because these elements would be extremely difficult to measure by neutron diffraction. The mirror method has found its most useful application for a few coherent cross sections, difficult to measure by other methods, that require precision of a few tenths of a per cent. The measurement of these specific cases by mirror methods will be considered in Sec. 3.3 (neutron-proton scattering) and 3.4 (neutron-electron interaction) as well as the other methods used for these important cross sections.

3.2 Determination of Coherent Cross Sections from Free Atom Cross Sections

The second method by which coherent cross sections are obtained is applicable to a few materials only, but is capable of great accuracy in these cases. In this procedure, the coherent cross section is obtained from the total cross section, consisting of capture and scattering. The total cross section, obtained by a transmission measurement, is usually known with great accuracy for it depends on a *relative* flux measurement only. The number of neutrons removed from a beam by a sample of ap-

[2] J. Harvey, M. Goldberg, and D. J. Hughes, *Phys. Rev.* **86,** 604 (1952).

[3] A. W. McReynolds and G. W. Johnson *Phys. Rev.* **82,** 344 (1951).

propriate thickness is measured by insertion of the sample into the beam, and the total cross section follows directly from the ratio of beam intensity with sample to that without, this ratio being the transmission T:

$$T = e^{-N\sigma_T x}. \tag{3-1}$$

In this equation x is the thickness of the sample, containing N nuclei per cubic centimeter. We are not concerned here with the detailed techniques of total cross section measurement (geometrical conditions, correction for background, etc.), which allow an accuracy of about $\frac{1}{2}$ % in the cross section, or $\frac{1}{4}$ % in the amplitude.

If the total cross section is mainly scattering, the effect of capture can be calculated and subtracted to give the scattering cross section with high accuracy. In order to obtain the total cross section that is appropriate for an isolated nucleus, hence that can be readily interpreted, it is necessary to measure the transmission for a neutron energy sufficiently high so that the atom acts independently of its neighbors during the scattering process. Because the energy transferred to a heavy atom by a neutron is small, it might be expected that neutron energies of well over 100 ev would be necessary to reach this "free atom" behavior. However, because of the large number of excitation energies available in the crystal lattice, the recoiling atom acts as if free during the collision although it remains bound in the crystal.[4] This behavior holds even for neutrons of a few volts energy and as a result free atom cross sections can be measured with neutrons in the 1–10 ev range. As neutrons of a few electron volts are much more available than those in the region of several hundred electron volts (for example in pile beams), it is fortunate that free atom cross sections are measurable at the low energies.

For a nucleus possessing no resonances near thermal, it is a simple matter to convert from the free atom cross section

[4] G. Placzek, *Phys. Rev.* **86**, 377 (1952); H. Ekstein, *ibid.* **87**, 31 (1952).

to the coherent bound value used in neutron optics. In the coherent optical effects the entire crystal (or mirror) recoils as a unit, hence the struck atom is of effective infinite mass and the correct cross section is the "bound atom cross section." This cross section is related to the free atom value simply as

$$\sigma_{\text{bound}} = \left(\frac{A+1}{A}\right)^2 \sigma_{\text{free}}, \tag{3-2}$$

where σ_{free} is the scattering cross section obtained from the total cross section by subtraction of absorption, and A is the atomic weight.

While the bound atom cross section has a definite meaning, as expressed by Eq. (3-2), it is fictitious in the sense that it can hardly be observed experimentally. It represents the cross section of a nucleus that is completely bound, yet scatters independently of its neighbors. In general, of course, such independent scattering does not occur; interference effects always intervene and the bound atom cross section does not represent the observed total scattering per atom. Although the bound atom cross section is not directly measured, the amplitude obtained from it by means of the general relationship, $\sigma = 4\pi a^2$, is the correct amplitude to be used in Eqs. (1-17) and (1-20) for the total bound amplitude a_t.

In order to obtain the *coherent* bound amplitude, σ_{coh} from σ_{bcund}, however, it is necessary to subtract incoherent scattering from the bound atom cross section before calculating the coherent amplitude. This subtraction does not occur for a monoisotopic element of zero spin, but, as such elements are almost nonexistent, it is usually an important step in the free atom method for obtaining coherent amplitudes. To recapitulate, in this method capture is subtracted from the total cross section to give the free atom scattering cross section, this latter is converted to the bound atom cross section by means of Eq. (3-2), subtraction of incoherent scattering then gives the coherent bound atom cross section, and finally the amplitude is obtained as $(\sigma_{\text{coh}}/4\pi)^{1/2}$.

The incoherent scattering that must be subtracted from the bound atom cross section was discussed in Sec. 1.2, in fact, in some cases it may be obtained most accurately simply by calculation from the equations given, Eqs. (1-18) and (1-21). For example, the isotope incoherent scattering, which is usually small, can be calculated if the coherent cross sections of the individual isotopes are known even approximately. Thus the effect of the isotope incoherent scattering of iron can be estimated with accuracy even though the scattering cross sections of the individual isotopes have not been measured with great precision.

The incoherent scattering can also be measured by observation of the cross section for neutrons beyond the cutoff wavelength. The discussion of Sec. 2.2 has shown that the scattering in this wavelength region consists of incoherent scattering only. The observed scattering, which thus represents isotopic, spin-dependent and thermal diffuse scattering, can be analyzed to identify the individual components. This work, usually done with the slow neutron chopper, involves analysis of the cross section as a function of sample temperature and wavelength, which enables separation of the individual components of the incoherent scattering. This method of investigation is especially applicable for a sample of low capture, an example being the analysis of beryllium, for which measurements of Palevsky and Smith[5] showed that the incoherent scattering was less than 0.01 barn. These "cold neutron" measurements will be considered again, Sec. 4.4, in connection with crystal lattice vibrations.

The present discussion, together with that of the preceding section, leads to the conclusion that the correct approach for coherent scattering determinations is dictated by the relative magnitude of the various components of scattering. In some cases the best coherent amplitude values have been obtained from crystal diffraction measurements, while in others, particularly those of a few important standards, the highest ac-

[5] H. Palevsky and R. R. Smith, *Phys. Rev.* **86,** 604 (1952).

curacy is attained via the free atom cross sections. Individual examples may best be discussed in connection with the numerical results for all the elements and isotopes that have been measured. In Table 3-1 the measured bound atom and coherent cross sections are listed together with experimental errors. These values are obtained from the Atomic Energy Commission compilation "Neutron Cross Sections," together with its first two supplements.[6] The coherent amplitude is also given, calculated from σ_{coh} with the exception of Th^{232} for which σ_{coh} is identical with σ_b.

The most accurately known coherent cross sections in Table 3-1, obtained by subtraction of measured incoherent scattering from the bound atom values, are those for Be, C, Fe, and Bi. The hydrogen cross section, as we shall see, is based on a precise amplitude comparison with carbon. Although the coherent value quoted for oxygen is the directly measured result, of much less accuracy than σ_b, it can safely be taken as equal to the bound atom value because of the negligible abundance of O^{17} and O^{18}. Inspection of the table shows that for most elements σ_{coh} and σ_b are equal within experimental error, indicating that incoherent scattering is small for most elements. There are a few cases of appreciable isotopic incoherence, however; one of these is nickel, which has about five barns incoherent scattering arising from the exceptionally large coherent cross section of Ni^{58}. The scattering amplitudes for all heavy elements with the single exception of Sm^{152}, are positive; there are six examples of negative amplitudes for the light elements, however. The negative scattering amplitude for most of these cases is explained by a known resonance near thermal energy. By chance, the amplitudes of the two spin states for vanadium are such that the net coherent cross section, obtained from Eq. (1-16), is only 0.03 barn.

[6] AECU-2040 (Office of Technical Services, Dept. of Commerce, Washington, 25, D. C., 1952), supplements available from Technical Information Service, Atomic Energy Commission, Oak Ridge, Tennessee.

Table 3-1. Scattering cross sections of elements and isotopes. Listed are the bound scattering (σ_b), the bound coherent (σ_{coh}) and the amplitude (a_{coh}), calculated from the latter.

Element or isotope	σ_b barns	σ_{coh} barns	a_{coh} 10^{-13} cm
$_1$H	81.4 ± 0.4	1.79 ± 0.02	−3.78
H^2	7.5 ± 0.1	5.4 ± 0.3	6.6
$_2$He	1.3 ± 0.2	1.1 ± 0.2	3.0
$_3$Li	1.2 ± 0.3	0.40 ± 0.03	−1.78
Li^6		6 ± 3	7
Li^7	2.0 ± 0.5	0.80 ± 0.05	−2.52
$_4$Be	7.54 ± 0.07	7.54 ± 0.07	7.74
$_5$B	4.4 ± 0.2		
B^{10}	2.9 ± 0.2		
B^{11}	4.4 ± 0.3		
$_6$C	5.50 ± 0.04	5.49 ± 0.04	6.61
C^{13}	5.5 ± 1.0	4.5 ± 0.6	6.0
$_7$N	11.4 ± 0.5	11.0 ± 0.5	9.4
$_8$O	4.24 ± 0.02	4.2 ± 0.3	5.81
$_9$F	4.0 ± 0.1	3.8 ± 0.3	5.5
$_{10}$Ne	2.9 ± 0.2		
$_{11}$Na	3.6 ± 0.3	1.55 ± 0.05	3.51
$_{12}$Mg	3.7 ± 0.1	3.6 ± 0.1	5.35
$_{13}$Al	1.51 ± 0.03	1.5 ± 0.1	3.5
$_{14}$Si	2.4 ± 0.2	2.0 ± 0.2	4.0
$_{15}$P	3.6 ± 0.3	3.1 ± 0.1	5.0
$_{16}$S	1.2 ± 0.2	1.20 ± 0.08	3.1
$_{17}$Cl	15 ± 3	12.1 ± 0.8	9.8
$_{18}$A	0.9 ± 0.2		
$_{19}$K	2.0 ± 0.2	1.5 ± 0.1	3.5
$_{20}$Ca	3.2 ± 0.3	3.0 ± 0.1	4.9
Ca^{40}	3.1 ± 0.3	3.0 ± 0.1	4.9
Ca^{44}		0.40 ± 0.03	1.78
$_{21}$Sc		13 ± 1	10.1
$_{22}$Ti	4.0 ± 0.4	1.4 ± 0.3	−3.3
$_{23}$V	5.1 ± 0.1	0.032 ± 0.008	−0.51
$_{24}$Cr	4.1 ± 0.3	1.56 ± 0.03	3.52
$_{25}$Mn	2.0 ± 0.1	1.7 ± 0.1	−3.7
$_{26}$Fe	11.80 ± 0.04	11.37 ± 0.05	9.52
Fe^{54}	2.5 ± 0.3	2.20 ± 0.13	4.18
Fe^{56}	12.8 ± 0.2	12.8 ± 0.2	10.1

Table 3-1—Continued

Element or isotope	σ_b barns	σ_{coh} barns	a_{coh} 10^{-13} cm
Fe^{57}	2.0 ± 0.5	0.64 ± 0.04	2.3
$_{27}Co$	6 ± 1	1.00 ± 0.06	2.82
$_{28}Ni$	18.04 ± 0.05	13.2 ± 0.2	10.2
Ni^{58}	24.4 ± 0.5	25.9 ± 0.3	14.4
Ni^{60}	1.0 ± 0.1	1.1 ± 0.1	3.0
Ni^{62}	9 ± 1	9.5 ± 0.4	−8.7
$_{29}Cu$	8.0 ± 0.1	7.0 ± 0.4	7.5
$_{30}Zn$	4.1 ± 0.2	4.3 ± 0.3	5.9
$_{31}Ga$	7.5 ± 0.5		
$_{32}Ge$	8.6 ± 0.5	8.8 ± 0.5	8.4
$_{33}As$	7 ± 1	5.0 ± 0.3	6.3
$_{34}Se$	9 ± 1	10.0 ± 0.6	8.9
$_{35}Br$	6.1 ± 0.2	5.7 ± 0.4	6.7
$_{37}Rb$	5.5 ± 0.5	3.8 ± 0.3	5.5
$_{38}Sr$	12.5 ± 1.0	4.1 ± 0.3	5.7
$_{40}Zr$	7.0 ± 0.5	5.0 ± 0.3	6.3
$_{41}Nb$	6.4 ± 0.3	6.0 ± 0.2	6.9
$_{42}Mo$	6.1 ± 0.2	5.6 ± 0.2	6.7
$_{44}Ru$	6.6 ± 0.5		
$_{45}Rh$		4.5 ± 0.5	6.0
$_{46}Pd$	4.8 ± 0.3	5.0 ± 0.3	6.3
$_{47}Ag$	6.5 ± 0.5	4.6 ± 0.3	6.1
Ag^{107}	10 ± 1	8.7 ± 0.5	8.3
Ag^{109}	6 ± 1	2.3 ± 0.2	4.3
$_{50}Sn$	4.9 ± 0.5	4.6 ± 0.3	6.1
$_{51}Sb$	4.2 ± 0.3	3.7 ± 0.3	5.4
$_{52}Te$	4.5 ± 0.3	4.2 ± 0.3	5.8
$_{53}I$	3.8 ± 0.4	3.4 ± 0.2	5.2
$_{55}Cs$	7 ± 1	3.0 ± 0.2	4.9
$_{56}Ba$	5 ± 1	3.5 ± 0.2	5.3
$_{57}La$	9.3 ± 0.8	8.7 ± 0.4	8.3
$_{58}Ce$	4 ± 1	2.7 ± 0.3	4.6
Ce^{140}	2.8 ± 0.5	2.78 ± 0.10	4.70
Ce^{142}	2.6 ± 0.5	2.6 ± 0.2	4.6
$_{59}Pr$	4 ± 1	2.4 ± 0.2	4.4
$_{60}Nd$	15 ± 5	6.5 ± 0.4	7.2
Nd^{142}		7.5 ± 0.6	7.7
Nd^{144}		1.0 ± 0.2	2.8

Continued

Table 3-1—Concluded

Element or isotope	σ_b barns	σ_{coh} barns	a_{coh} 10^{-13} cm
Nd^{146}		9.5 ± 0.4	8.7
$_{62}Sm^{152}$		2.5 ± 1.0	−4.5
$_{72}Hf$	8 ± 1		
$_{73}Ta$	6 ± 1	6.1 ± 0.4	7.0
$_{74}W$	5.7 ± 0.6	2.74 ± 0.05	4.67
$_{76}Os$	15 ± 2		
$_{78}Pt$	12 ± 1	11.2 ± 0.7	9.5
$_{79}Au$		7.3 ± 0.1	7.62
$_{80}Hg$		22 ± 2	13.2
$_{81}Tl$	10.0 ± 0.5	10 ± 2	9
$_{82}Pb$	11.4 ± 0.1	11.5 ± 0.2	9.6
$_{83}Bi$	9.37 ± 0.03	9.35 ± 0.04	8.63
$_{90}Th$	12.5 ± 0.2		10.0

3.3 Neutron-Proton Scattering

Accurate measurements of the interactions between the neutron and proton are important because of the fundamental nature of the neutron-proton force. In addition, these interactions furnish excellent illustrations of neutron-optical phenomena because of the large amount of spin dependence that is present. It is interesting that properties of the extremely small nuclear force range can be obtained from interference effects of neutrons whose wavelength is about 10^5 times this range. The difference in amplitude for the two possible spin orientations in the scattering collision gives directly the spin dependence of the fundamental neutron-proton force. Whereas these amplitudes have been measured by various slow neutron techniques, involving methods that differ greatly in the actual measurements, they all involve the same neutron-optical properties of coherence and incoherence.

As the spins of the neutron and of the proton are both one-half, the spin of the compound nucleus formed during the scattering is 1 or 0 and the weighting factor, Eq. (1-16), becomes 3 to 1 for the spin 1 (triplet) state relative to the spin 0 (singlet)

state. The coherent and incoherent scattering amplitudes of hydrogen will then be given in terms of Eqs. (1-16) and (1-18) as

$$a_{\text{coh}} = \tfrac{3}{4}\, a_t + \tfrac{1}{4}\, a_s\,, \tag{3-3}$$

$$a_{\text{inc}} = (\tfrac{3}{16})^{1/2}\,(a_t - a_s), \tag{3-4}$$

where we neglect the extremely small effect of the H^2 present in hydrogen. The amplitudes a_t and a_s are the bound atom values, which are related to the total free atom cross section by the reduced mass factor. From Eqs. (1-17) and (3-2) it follows that the free atom cross section gives the following combination of the amplitudes:

$$\begin{aligned}\sigma_{\text{free}} &= \left(\frac{A}{A+1}\right)^2 4\pi \left(\frac{3}{4}\, a_t^2 + \frac{1}{4}\, a_s^2\right) \\ &= \frac{\pi}{4}\,(3a_t^2 + a_s^2)\end{aligned} \tag{3-5}$$

The free atom cross section, combined with either the coherent or incoherent bound amplitude, can thus be used to evaluate the singlet and triplet amplitudes.

The scattering amplitudes for the singlet and triplet interaction are directly related to the depth and range of the potential well for the corresponding neutron-proton interactions in the manner briefly sketched in Sec. 1.3, Eq. (1-35). A more complete potential theory of neutron-proton scattering[7] shows that the triplet amplitude, when combined with the binding energy of the deuteron, gives the range of the neutron-proton potential in the triplet state, the state corresponding to the neutron-proton alignment in the stable deuteron. The triplet amplitude, as expected from the bound nature of the deuteron, is positive while the singlet amplitude is negative, corresponding to a virtual state. The singlet amplitude, when combined with the neutron-proton scattering at an energy of about 1 Mev, gives the range of the neutron-proton force in the singlet state. Whereas the

[7] J. M. Blatt and V. F. Weisskopf, *Theoretical Nuclear Physics* (Wiley, 1952) pp. 48–86.

triplet range can be obtained with an accuracy comparable with that of the triplet amplitude and the deuteron binding energy that are used to obtain it, the singlet range depends in a very sensitive way on the 1 Mev scattering cross section, and is not known with comparable accuracy.

One important use of the neutron-proton ranges is the comparison with the corresponding proton-proton ranges in order to ascertain if nuclear forces depend on the charge of the particles involved. Unfortunately for this comparison there is no *triplet* proton-proton interaction (because of the Pauli exclusion principle) with which to compare the accurate triplet neutron-proton range. As a result, only the singlet neutron-proton range can be compared with the corresponding proton-proton range, which incidentally is known to high accuracy from proton-proton scattering.

Of the methods that have been used to obtain the neutron-proton scattering amplitudes we shall first consider briefly the scattering of neutrons from ortho- and para-hydrogen, the approach first used for this problem. The scattering from gaseous ortho-hydrogen (in which the two proton spins are aligned) and from para-hydrogen (in which they are antiparallel) illustrates well the effects of interference in neutron scattering. In scattering from ortho-hydrogen the amplitude of the molecule will be either twice the singlet amplitude or twice the triplet amplitude, depending on the spin orientation of the neutron relative to that of the nuclei. This simple relationship will hold only if the wavelength is so long that the protons in a molecule are effectively at a point, i.e., that the phase differences introduced by their separation are negligible. For para-hydrogen, again considering extremely long wavelengths, the amplitude for each molecule will be the same, that is, $2(\frac{1}{4}a_s + \frac{3}{4}a_t)$, regardless of the orientation of the neutron relative to the molecule. As the scattering is observed from hydrogen gas the individual molecules scatter independently, and the cross section per molecule is obtained directly from the observed scattering of the entire gas, with no correction for intermolecular interference.

Under the ideal conditions just described, the scattering from para-hydrogen gives the coherent hydrogen amplitude directly as we see by examination of Eq. (3-3). In the actual experiments, however, in which cyclotron velocity-selected neutrons were used, conditions were much more complicated than those assumed. As the wavelength was not extremely long compared to the size of the molecule, molecular interference effects similar to those observed with x-ray gas scattering must be corrected for in the calculations. Inelastic incoherent scattering may also take place, in which the spin of the neutron and of the protons are reversed (interconversion of ortho- and para-hydrogen). Additional inelastic scattering involving excitation of rotations and vibrations of the molecules may also occur. The coherent scattering that is obtained from para-hydrogen is the important quantity in determination of the neutron-proton amplitudes, but its measurement is unfortunately made difficult by the much larger scattering from ortho-hydrogen. As it is difficult to obtain pure para-hydrogen, the measured coherent scattering is likely to be raised by a small ortho impurity.

The early results[8] obtained for the coherent scattering from para-hydrogen led to a singlet range approximately zero, and later results, which gave smaller cross sections for para-hydrogen hence a somewhat larger singlet range, were still not in agreement with the proton-proton singlet range. Thus the Los Alamos measurements[9] of 1947, using moderated cyclotron neutrons and time-of-flight techniques, gave $-3.95 \pm 0.12 \times 10^{-13}$ cm for the bound coherent hydrogen amplitude. This value, although still possessing a somewhat large experimental error, seemed to indicate[10] charge dependence of nuclear forces (unequal neutron-proton and proton-proton ranges).

[8] J. Halpern, I. Estermann, O. C. Simpson, and O. Stern, *Phys. Rev.* **52,** 142 (1937); F. G. Brickwedde, J. R. Dunning, H. J. Hoge, and J. H. Manley, *ibid.* **54,** 266 (1938); L. W. Alvarez and K. S. Pitzer, *ibid.* **58,** 1003 (1940).

[9] R. B. Sutton, T. Hall, E. E. Anderson, H. S. Bridge, J. W. De Wire, L. S. Lavatelli, E. A. Long, T. Synder, and R. W. Williams, *Phys. Rev.* **72,** 1147 (1947).

[10] J. M. Blatt and J. D. Jackson, *Phys. Rev.* **76,** 18 (1949).

The second method that was applied to the neutron-proton scattering amplitudes is based on a coherent hydrogen amplitude measurement by crystal diffraction, which gives the individual amplitudes when combined with the free atom cross section. The measurement of the hydrogen amplitude is quite straightforward in principle, involving nothing more than the method already described for determination of coherent amplitudes by diffraction. However, hydrogen is an extremely difficult element to study by neutron diffraction because the bound coherent cross section constitutes only about 2 barns of a total bound cross section of 80 barns.

Diffraction from hydrogen was studied carefully by Shull *et al.*[11] in connection with an investigation of the diffraction pattern of NaH. In this work the observed structure factors for the hydride gave the coherent amplitude of hydrogen relative to that of sodium, which in turn can be related to a standard scatterer. The standard used by Shull *et al.* for the hydrogen work was carbon; its coherent amplitude was obtained from the free atom cross section as described in Sec. 3.2. An accurate measurement of the structure factor for NaH was hampered greatly by the high intensity of spin dependent diffuse scattering, for it was necessary to estimate the height of the Bragg peaks above this diffuse background to a few per cent in order to obtain the desired accuracy in the coherent hydrogen amplitude. The diffraction pattern observed with NaH appears in Fig. 3-2, from which the interfering effect of the background diffuse scattering is evident. Further difficulty occurred in connection with the correction of the observed intensities for the Debye-Waller factor, because of uncertainty in the Debye spectrum of the lattice vibrations for NaH (for a compound, assumption of a single Debye temperature is inaccurate). Instead of using an uncertain theoretical correction, Shull *et al.* analyzed the observed variation of intensity with angle to obtain an empirical correction for the temperature diffuse scattering.

[11] C. G. Shull, E. O. Wollan, G. A. Morton, and W. L. Davidson, *Phys. Rev.* **73,** 842 (1948).

The inherent difficulties of the hydrogen diffraction just described limited the accuracy of the amplitude determination to 5% in spite of the careful measurements. The coherent hydrogen amplitude obtained in this experiment was

$$a_H = -3.96 \pm 0.20 \times 10^{-13} \text{ cm},$$

a result in close agreement with the ortho-para-hydrogen value, hence one that also indicates a singlet neutron-proton range in

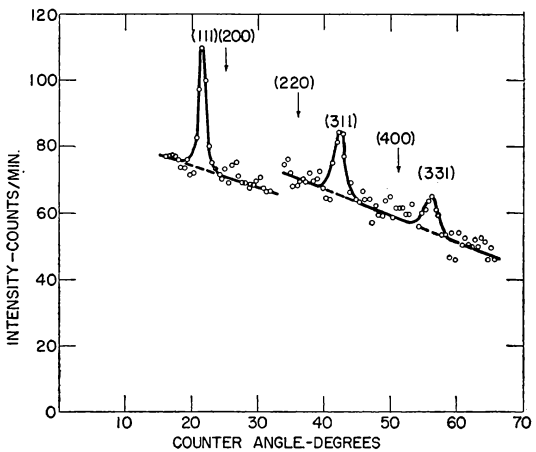

FIG. 3-2. The diffraction pattern of sodium hydride, illustrating the large amount of spin-dependent diffuse scattering.

disagreement with the accurate singlet proton-proton range. Later experiments of Shull and Wollan,[12] in which the intensity measurements were improved as well as the empirical correction method for temperature diffuse scattering, gave

$$a_H = -4.1 \pm 0.2 \times 10^{-13}.$$

This last result represents a change in the direction to increase the discrepancy in the ranges, however. It is in disagreement with the more accurate liquid mirror measurement to be de-

[12] C. G. Shull and E. O. Wollan, *Phys. Rev.* **81**, 527 (1951).

scribed by about 8%; there is no obvious explanation for this discrepancy. It must be remembered, however, that the hydrogen amplitude is a particularly difficult problem for diffraction because of the predominant incoherent scattering. It is certain that the amplitudes of other more favorable materials are measured by neutron diffraction to several per cent accuracy, and for a few individual cases one per cent has been attained.

The most recent method of measurement of the coherent hydrogen scattering utilizes liquid mirror reflection. The same fundamental principles apply as for the diffraction measurement, that is, comparison of the hydrogen amplitude to that of a standard. In fact, the standard is carbon for the mirror method just as for the diffraction measurements. The comparison of an unknown amplitude to that of a standard may be made in a very direct manner by means of mirrors if the materials involved have amenable physical properties. Thus, whereas the comparison of hydrogen to carbon scattering by diffraction is complicated by the large amount of diffuse scattering, it is much more direct and simple by means of mirror reflection. As hydrogen and carbon can be easily combined in various proportions, the comparison of scattering amplitudes can be made with a single liquid mirror in which the ratio of carbon to hydrogen content is varied. The scattering amplitudes of the components are of opposite sign, and this implies that the comparison can be made by a null method in which only small differences are measured. No corrections are necessary for temperature diffuse scattering, as the Debye-Waller factor is unity for mirror reflection. In addition, the measured critical angle is completely independent of the crystalline structure of the mirror material itself, that is, the combination of hydrogen and carbon could be liquid, solid, or gas.

In the balancing method of relative scattering amplitude measurement we are considering, the two materials are combined in a single mirror, for example as a compound, and the critical angle for the combination, given by Eq. (1-43), is then a function of the average amplitude of the mirror components. In

particular, if the carbon and hydrogen content of the mirror is adjusted to give zero average coherent amplitude, the individual amplitudes are in just the inverse ratio of the number of atoms of carbon and hydrogen present. Even though the diffuse scattering is extremely large, it will have a negligibly small effect on the critical angle, in fact its results[13] are closely similar, quantitatively as well as qualitatively, to those of absorption as given by Eq. (1-42).

The determination of the particular hydrogen-carbon ratio that has zero coherent amplitude (index of refraction unity) necessarily involves some method of extrapolation. From Eq. (1-43) we see that the limiting wavelength, λ_c, reflected at a particular angle, θ_c, becomes large as the net or unbalanced amplitude Δa decreases:

$$\lambda_c = \theta_c \sqrt{\frac{\pi}{N\Delta a}}. \tag{3-6}$$

If the entire Maxwell velocity distribution is incident on the carbon-hydrogen mirror, the intensity reflected will consist of all wavelengths longer than λ_c. As the net amplitude is decreased toward zero under these conditions, the reflected intensity will decrease as well and exact balance would be identified by zero reflected intensity (infinite λ_c). However, because of the rapid decrease in neutron intensity with increasing wavelength, λ_c cannot exceed the order of 10 A in practice and extrapolation to infinite λ_c involves considerable uncertainty.

Although there are several possible methods to extrapolate to the H-C ratio for exact balance, a careful consideration of the errors involved leads to an extrapolation method in which λ_c is held constant. In this method, used by Burgy, Ringo, and Hughes,[14] at the Argonne pile, neutrons were reflected from liquid hydrocarbon compounds and mixtures of various H-C

[13] O. Halpern, *Phys. Rev.* **88**, 1003 (1952).

[14] M. T. Burgy, G. R. Ringo, and D. J. Hughes, *Phys. Rev.* **84**, 1160 (1951); D. J. Hughes, *Pile Neutron Research* (Addison-Wesley, 1953) pp. 309–16.

ratios, and for each of these the incident angle was changed to obtain a constant reflected intensity. The constancy of reflected intensity ensures that λ_c is the same for each liquid; as a result the following relationship holds for the incident angle and the unbalanced amplitude:

$$\theta_c^2 = \lambda_c^2 \frac{N\Delta a}{\pi} = \text{constant} \times \Delta a. \tag{3-7}$$

Thus if θ^2 is plotted against any variable proportional to the net amplitude of the mirror, a straight line should result that extrapolates to zero angle at the liquid of zero scattering amplitude. Actually, θ^2 is plotted against the H-C ratio, which is proportional to the amplitude unbalance. The measured critical angles for several intensity values, shown in Fig. 3-3, vary linearly with θ^2, as expected, and intercept the axis at a single point within experimental error.

The results of Fig. 3-3 indicate that the H-C ratio of zero coherent amplitude can be determined with considerable accuracy by extrapolation. It is necessary, however, to determine the hydrogen and carbon content of the particular liquids used with equal accuracy. This latter need was met by careful purification of organic liquids and checked by chemical analysis before and after the measurements. The final result of the liquid mirror work represented a determination of the coherent amplitude *ratio* of hydrogen to that of carbon to about 0.3 %. The coherent amplitude of carbon, as we have seen, is obtained accurately from the free atom cross section for the incoherent scattering is extremely small. As the free atom cross section is known to about 1 %, the total amplitude and the coherent amplitude as well is accurate to 0.5 %. The coherent hydrogen amplitude, including both the error in the ratio and in the carbon amplitude, is finally

$$a_H = -3.78 \pm 0.02 \times 10^{-13} \text{ cm}.$$

The result of the mirror experiment is lower than the ortho-parahydrogen and the crystal diffraction values by somewhat

more than the errors involved, but is in better agreement with other results. For example, the coherent amplitude just quoted, when combined with the other low energy n-p scattering con-

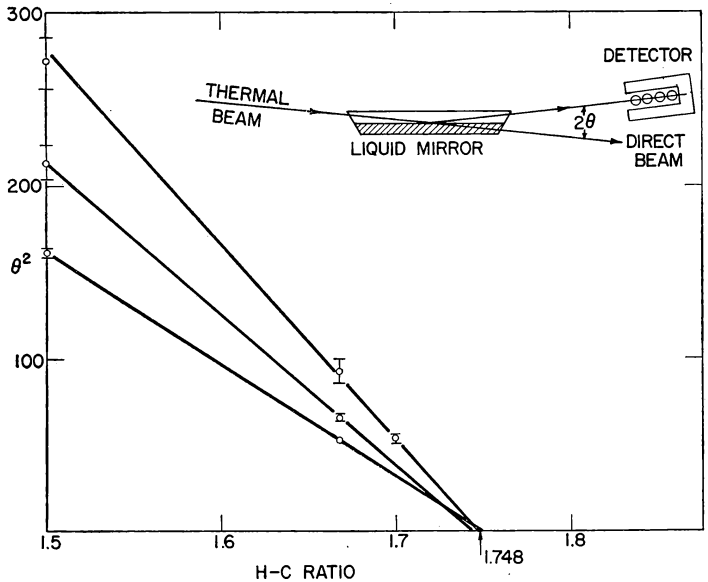

FIG. 3.3. Experimental arrangement used for measurement of coherent hydrogen scattering and the resulting critical angles for various liquid hydrocarbons. Each line represents critical angles for a particular constant intensity.

stants gives[15] a triplet n-p effective range of

$$r_t = 1.704 \pm 0.030 \times 10^{-13} \text{ cm}.$$

This range, when combined with the 1 Mev n-p scattering cross section leads to a singlet range that is in agreement with the singlet p-p range, hence consistent with charge independence of nuclear forces.[15] The coherent n-p scattering is also consistent

[15] H. A. Bethe, *Phys. Rev.* **76**, 38 (1949); J. Schwinger, *ibid.* **78**, 135 (1950); E. E. Salpeter, *ibid.* **82**, 60 (1951).

with the binding energy of the triton[16] and the mass of the π meson.[17] Some recent results of Squires[18] at the Cavendish Laboratory, Cambridge, with the ortho-para-hydrogen method result in a lower coherent amplitude than the early values and one that is in agreement with the liquid mirror value. This recent result indicates that in the earlier work the para-hydrogen contained some ortho-hydrogen.

3.4 Neutron-Electron Interaction

A constant of fundamental importance to the theory of the structure of elementary particles is the electrostatic neutron-electron interaction. As for the neutron-proton case, the electron interaction is worthy of attention not only because of its intrinsic interest but as a result of the manner in which its measurement utilizes neutron-optical properties. It also resembles the neutron-proton scattering in that it has been measured by diffraction as well as by means of a balanced-mirror arrangement. We shall consider the principles of several experimental approaches after a brief description of the significance of the neutron-electron interaction itself.

We are here not interested in the neutron-electron dipole-dipole magnetic interaction between the neutron and the magnetic moment of the atoms that will be discussed in Ch. 5. In addition to this large, well-understood magnetic electon scattering, however, there is a small spin-independent interaction arising from the meson cloud that is part of the structure of the neutron. According to meson theory, the neutron exists at times dissociated into a (point) proton and a negative meson cloud, with the latter separated from the proton a distance of the order of the range of nuclear forces. As a result of this charge distribution, a force will be exerted on a point charge when it is between the meson cloud and the proton, just as an alpha particle experiences an electrostatic force when it is within

[16] R. L. Pease and H. Feshbach, *Phys. Rev.* **81,** 142 (1951).
[17] L. Hulthen, *Phys. Rev.* **79,** 166 (1950).
[18] A. T. Stewart and G. L. Squires, *Phys. Rev.* **90,** 1125 (1953).

the electron orbits of an atom. There will be an extremely weak scattering of neutrons by electrons arising from this electrostatic potential, with an amplitude given by Eq. (1-35). The amplitude is extremely difficult to calculate from meson theory but the numerical result, expressed as a potential well with a range equal to e^2/mc^2 (the classical radius of the electron, 2.8×10^{-13} cm) has a depth of the order of a few thousand electron volts. As the properties of the meson cloud into which the neutron dissociates are basic to the explanation of nuclear force, a measurement of the electrostatic effect of this meson cloud is of obvious importance to meson theory.

Although an accurate determination of the electrostatic neutron-electron effect is highly desirable, the smallness of the interaction renders it difficult to measure. We have seen in Sec. 1.3 that the nuclear scattering is represented by a potential well depth of 20 Mev, (and a range similar to that of the neutron-electron interaction) hence, Eq. (1-35), the neutron-electron amplitude will be about 10^{-4} of the nuclear scattering. The principal experimental problem is one of separating this tiny neutron-electron interaction from that of the nucleus with any accuracy. In all the measurements of the neutron-electron scattering that have been performed, the small electron effect is detected by taking advantage of the atomic form factor that it exhibits. We are already familiar with the fact that neutron-nuclear scattering has no atomic form factor because the nuclear dimensions are small (10^{-13} cm) compared to the neutron wavelengths (10^{-8} cm). In the present case, however, the neutron-electron scattering will exhibit a typical x-ray atomic form factor, that is, the scattering from individual atoms will not be isotropic. The variation in scattering, either with angle or wavelength, contrasted to the isotropic nuclear scattering, can be used to isolate the small electron scattering. Three general methods have been used in the last few years for the neutron-electron measurement; variation of scattering with angle, with wavelength, and a balanced-mirror technique. Although the experiments differ greatly in experimental details, they all ac-

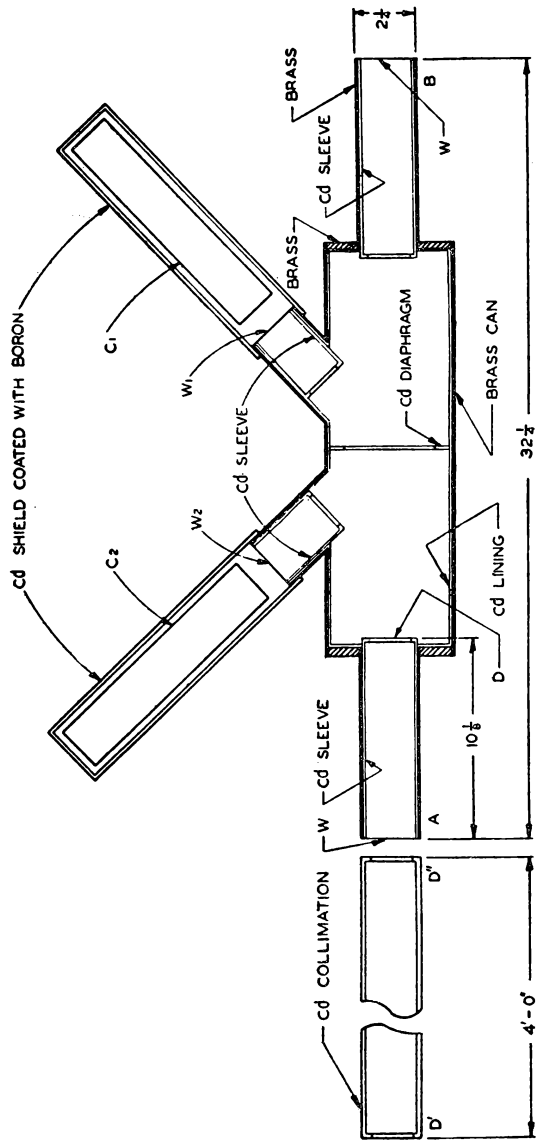

FIG. 3-4. The equipment used by Fermi and Marshall for measurement of the neutron-electron interaction by scattering of neutrons from xenon gas; counters C_1 and C_2 detect neutrons scattered at 45° and 135° from the direct beam.

tually consist of identification of the component of the cross section that has the correct atomic form factor.

The manner in which the atomic form factor variation is used to identify the neutron-electron scattering is well illustrated by the experiment performed by Fermi and Marshall[19] in 1947. Thermal neutrons from the Argonne pile were scattered from xenon gas, this gas of closed electron shells being chosen so that no magnetic scattering would be present. The scattered neutrons were detected at angles of 45° and 135° from the direct beam, with the equipment shown in Fig. 3-4. As the gas was used at a pressure of 1 atmos, the intensity of scattered neutrons was so low that it was necessary to use the entire Maxwell distribution, rather than monoenergetic neutrons. The use of the complete velocity distribution means that the observed asymmetry involves the form factor averaged over the range of wavelengths present in the incident beam, and this averaging complicates analysis of the experimental results.

The neutron-electron scattering will manifest itself in the arrangement of Fig. 3-4 as a slight difference in scattered intensity at 45° (form factor 0.78) relative to 135° (form factor 0.52), superimposed on the much larger isotropic nuclear scattering. The observed asymmetry was rather small (2.35 % excess in the forward direction) and was of the order of the experimental error (0.9 %). It was necessary to correct the asymmetry for several nonisotropic effects unrelated to the neutron-electron interaction. The geometry of the two counters was not precisely the same; a correction for this effect was determined experimentally. The differential cross section as observed in the laboratory system of coordinates is affected by the velocity of xenon atoms, and the correction for this Doppler effect varies with angle. After correction for these effects, which constituted a 2.40 % forward asymmetry, the final asymmetry was 0.05 ± 0.9 % in the *backward* direction, corresponding to a negative amplitude, that is an *attraction* between the neutron and the electron. The sign of the experimental value is mean-

[19] E. Fermi and L. Marshall, *Phys. Rev.* **72,** 1139 (1947).

ingless; the result shows only that the well depth (for e^2/mc^2 range) is less than 5 kev.

The experiment just described was repeated by Hamermesh, Ringo, and Wattenberg[20] in 1952, also at Argonne, using several improvements that decreased the experimental error. Higher neutron fluxes and longer counting periods resulted in a higher statistical accuracy than the earlier measurement, while various geometrical corrections already mentioned were checked with argon, for which the electron scattering is small. The asymmetry, of course, gives the neutron-electron interaction as a ratio to the *coherent* scattering of the gas. In the experiment of Hamermesh *et al.* xenon and krypton were used, for which the coherent scattering amplitudes are not known. Lacking this information, it was assumed that the coherent scattering cross section is 80 % of the total scattering. With this assumption, the results obtained were 2900 ev for xenon and 5000 ev for krypton. In addition to statistical error, uncertainty arises from the assumption concerning the coherent nuclear amplitudes, and from the correction for the Doppler asymmetry not associated with the neutron-electron interaction (several times the neutron-electron asymmetry). The final average value was 4100 ev with an estimated error of 1000 ev.

The form factor exhibited by the neutron-electron interaction can also be identified by the variation of the scattering cross section with wavelength. In this method, as used by Havens, Rainwater, and Rabi[21] at the Columbia cyclotron, the total cross section of liquid bismuth was measured in the wavelength range 0.3–1.3 A. For the total scattering cross section, of course, it is the *integrated* form factor that is effective. The integrated form factor does not vary from zero to unity in the wavelength range used, and only about 40 % of the full

[20] M. Hamermesh, G. Ringo, and A. Wattenberg, *Phys. Rev.* **85,** 483 (1952).

[21] W. W. Havens, Jr. L. J. Rainwater, and I. I. Rabi, *Phys. Rev.* **82,** 345 (1951).

neutron-electron scattering is observed, of the same order as is effective in the differential scattering method just described.

The form factor variation resulting from the neutron-electron effect causes a change in total cross section of the order of only 0.1 barn, and this change must be isolated from other larger variations in cross section that occur in the same wavelength region. The cross section varies by about 0.2 barn because of interatomic interference effects, which occur for liquids as for crystalline materials; this variation can be calculated[22] and its effect therefore subtracted. It is also necessary to subtract the effect of neutron capture in bismuth and in impurities that may be present. After correction for the effects just described, the residual variation of cross section with wavelength leads to a neutron-electron interaction of 5300 ± 1000 ev. The statistical accuracy of this method is reasonably good but there remains some question concerning the calculated corrections.

The most recent measurement of the neutron-electron scattering utilizes the balanced-mirror technique. Fortunately, materials exist that can be combined in a mirror arrangement and whose nuclear characteristics balance out most of the nuclear scattering, with the result that the observed critical angle is a sensitive measurement of the neutron-electron interaction. For mirror reflection, the neutron-electron interaction contributes its full amplitude to the critical angle because the form factor is unity, and the scattering is coherent with that from the nucleus. On the other hand, if the cross section of the same material is measured at an energy of several electron volts, the neutron-electron interaction will not be present because its form factor will be essentially zero. Comparison of the free atom and the coherent cross section then gives the neutron-electron effect.

The nuclear properties of liquid oxygen and bismuth match

[22] G. Placzek, B. R. A. Nijboer, and L. van Hove, *Phys. Rev.* **82**, 392 (1951).

surprisingly well so a mirror formed by the interface of these two materials increases the accuracy of the measurement greatly over that attainable with a single mirror. In this arrangement,[23] Fig. 3-5, graphite-filtered neutrons (from the Brookhaven pile) pass through the bismuth with little loss in intensity because of their long wavelength, and their critical angle is measured in the

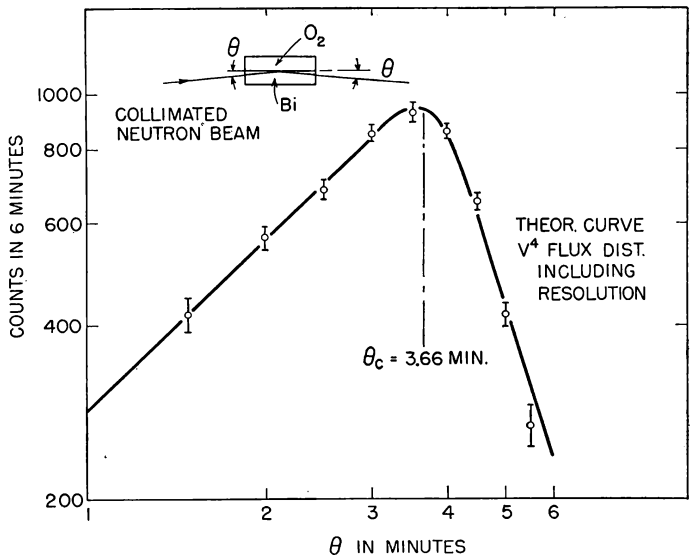

FIG. 3-5. Balanced-mirror arrangement for measurement of the neutron-electron interaction and the critical angle results for graphite-filtered neutrons.

manner described in Sec. 2.4. The nuclear scattering of oxygen is only about 2 % higher than that of bismuth, while the electron scattering in bismuth is much larger than that of oxygen because of the high Z. As a result, the observed critical angle, which is a measure of the *difference* in scattering power of the two elements, is determined approximately equally by the unbalanced nuclear amplitude and the neutron-electron effect.

[23] D. J. Hughes, J. Harvey, M. Goldberg, and M. Stafne, *ibid.* **90**, 497 (1953).

Actually, the following equation, which is somewhat more complicated than Eq. (1-43) but follows directly from it, holds exactly for the experimental arrangement of Fig. 3-5:

$$\frac{\pi}{\lambda^2}\theta_c^2 = N_{\mathrm{Bi}}a_{\mathrm{Bi}}\left(\frac{N_o a_o}{N_{\mathrm{Bi}}a_{\mathrm{Bi}}} - 1\right) + (N_{\mathrm{Bi}}Z_{\mathrm{Bi}} - N_o Z_o)a_e. \quad (3\text{-}8)$$

The equation is arranged to illustrate the manner in which the measured θ_c and the bound nuclear amplitudes of oxygen and bismuth (a_o, a_{Bi}) enter into the evaluation of the neutron-electron amplitude, a_e. As shown by Eq. (3-8), the close balance of oxygen and bismuth, while increasing the sensitivity of the measurement, necessitates an accurate knowledge of the nuclear amplitudes. Actually, only the *ratio* of these amplitudes is necessary in Eq. (3-8), and this ratio was accurately measured by means of the ratio of the free atom cross sections. Fortunately both bismuth and oxygen are essentially monoisotopic, have extremely small neutron capture and no resonances near thermal, hence the conversion from total bound, to coherent cross section can be accurately made. For this conversion, it was necessary to determine the spin-dependent scattering in bismuth by means of a separate experiment involving long wavelengths neutrons (Sec. 3.2); this scattering turned out to be only 0.02 barn.

The final result of the mirror experiment is a well depth of 3900 ± 400 ev. where the quoted error is not only experimental but includes uncertainty in such constants as the density of bismuth and liquid oxygen. The mirror measurement, while more involved experimentally than the other methods described, has an advantage that the observed effect is largely the neutron-electron interaction itself and that no involved calculated corrections are involved, the result being obtained directly from Eq. (3-8).

While some of the above experiments were still in progress, it was pointed out by Foldy[24] that part of the neutron-electron interaction could be considered a relativistic interaction between the neutron magnetic moment and the electric field,

[24] L. L. Foldy, *Phys. Rev.* **88**, 688 (1951).

with no reference to the dissociation of the neutron into a proton and a meson. The magnitude of this effect follows directly from the neutron magnetic moment and consists of a well depth (for range e^2/mc^2) of 4100 ev. At the time of Foldy's work, the most accurate result available was the cyclotron value of 5300 ± 1000 ev, hence about 1200 volts could be attributed to the meson charge cloud, assuming that it would appear as a simple addition to the Foldy effect. The more accurate results of the mirror experiment, however, now indicate that there is no dissociation effect over and above the 4100 attributed by Foldy to the magnetic moment. There is at the present time no satisfactory theoretical explanation for the nonobservance of a dissociation effect. It may be that the meson cloud exists in such a way that it produces the neutron magnetic moment and yet gives rise to no electrostatic effect, or it may be that the situation is much more complicated than the simple picture we are here considering.

CHAPTER 4

Measurement of Crystal Lattice Properties

Neutrons can be used for determination of the structure of crystal lattices, following the same principles so widely used in x-ray diffraction analysis. However, the low intensity available for neutron diffraction, together with the large size of the source (the chain-reacting pile) and of the diffraction equipment itself, indicate that neutrons should be used only for problems that are not amenable to x-ray treatment. Actually, in many applications, neutron diffraction has proved to be most useful as a supplement to x-ray investigation. The possibility of utilization of neutrons arises from the unique properties of neutrons relative to x-rays that we have already considered. An outstanding property peculiar to neutrons, of course, is the magnetic interaction, whose important applications are to be considered in the next chapter. The use of neutrons is also advantageous when the scattering amplitudes, which differ markedly from x-ray amplitudes for many elements, are of particularly favorable magnitude. We shall examine several such cases, the outstanding of which is hydrogen, in the present chapter. Still another difference between neutrons and x-rays that can be utilized at times is the small absorption of the former, as a result of which the properties inside large samples can be successfully measured. These unique properties can be applied to the study of a variety of structures; we shall see that neutron diffraction work has been performed with liquids and gases, as well as crystals.

4.1 Location of Hydrogen Atoms

A potentially important application of the neutron diffraction technique is to the study of hydrogen-containing crystals.

Here advantage is taken of the fact that the hydrogen scattering amplitude is comparable to that of other nuclei, unlike x-rays for which the scattering is so weak that hydrogen atoms are almost impossible to locate. However, in spite of the fact that the location of hydrogen atoms would be an important application of neutron diffraction, we shall see that only a very few hydrogen-containing crystals have been analyzed by means of neutrons. This paucity of results arises partly because of the extremely high spin-dependent diffuse scattering from hydrogen, Sec. 3.3, that interferes with observation of the Bragg maxima. The diffuse scattering can be reduced greatly by substituting deuterium for hydrogen, but deuterating increases the difficulty of sample preparation greatly. The crystal analysis is also made difficult by low intensity, which is a limitation on neutron diffraction not only for hydrogen but for all crystals. At the present time, the intensity limitation necessitates broad collimation, and the resulting poor resolution implies that only simple substances can be investigated. However, the constant improvement in techniques and the probable availability of higher fluxes means that more complicated crystals can be analyzed in the future.

The first use of neutron diffraction for the location of hydrogen atoms was the analysis of NaH by Shull *et al.*[1] We have already referred to the large amount of diffuse scattering present in the NaH work, the powder diffraction pattern for which was given in Fig. (3-2). As expected, the sodium deuteride pattern exhibited much higher peaks relative to the diffuse background; as a result the structure factors could be more easily determined. In this case the probable position of the hydrogen atoms had been estimated from x-ray work with LiH to be the same as that of the NaCl structure, and the neutron diffraction results justified this assumption. Lithium is sufficiently light so that the weak scattering of hydrogen was sufficient to make x-ray analysis of LiH possible; this procedure is impossible for NaH, however.

[1] C. G. Shull, E. O. Wollan, G. A. Morton, and W. L. Davidson, *Phys. Rev.* **73,** 842 (1948).

The structure of ice was investigated by Wollan *et al.*,[2] using "heavy ice," D_2O, again by the powder diffraction method of Sec. 2.5. Of the several structures that had been postulated for ice, it was possible to show from the diffraction pattern obtained that only the "Pauling model" was possible for the structure of ice. In this model, the oxygen atoms have a tetrahedral arrangement with one hydrogen on each line joining two oxygen atoms. Because of the poor resolution, all the peaks could not be identified but the intensity of the reflections was used to rule out all suggested models of the structure other than that of Pauling.

The low temperature (below $-30°$ C) form of ammonium chloride was studied by Goldschmidt and Hurst[3] at Chalk River and Levy and Peterson[4] at Oak Ridge. The basic structure of this compound had been determined by x-ray analysis but the location of the H atoms in the ammonium ion was unknown. The early results of Goldschmidt and Hurst indicated that the NH_4 ions were ordered at the low temperature but the Oak Ridge work, as well as the further results of Goldschmidt and Hurst, revealed that the NH_4 ions are orientationally disordered. The disorder of the ammonium ions contributes some diffuse scattering, the calculated angular distribution of which is in rough agreement with the experiments of Levy and Peterson, Fig. 4-1. In the powder diffraction work of both groups, the deuterated compound was used, but in single crystal measurements on the same compound Levy and Peterson found it possible to use hydrogen. The single crystal, because of its small size (a cylinder 5 mm high and 1.5 mm in diameter), had negligible extinction. The use of small (to eliminate extinction effects) single crystals, without the necessity of deuteration, will of course be of great value in the analysis of hydrogen-containing crystals.

[2] E. O. Wollan, W. L. Davidson, and C. G. Shull, *Phys. Rev.* **75,** 1348 (1949).

[3] G. H. Goldschmidt and D. G. Hurst, *Phys. Rev.* **83,** 88 (1951); **86,** 797 (1952).

[4] H. A. Levy and S. W. Peterson, *Phys. Rev.* **86,** 766 (1952).

Other examples of the location of hydrogen atoms are furnished by the work of Rundle *et al.*[5] on Th and Zr hydrides and that of Peterson and Levy[6] on potassium bifluoride. In the hydride investigation the body-centered tetragonal struc-

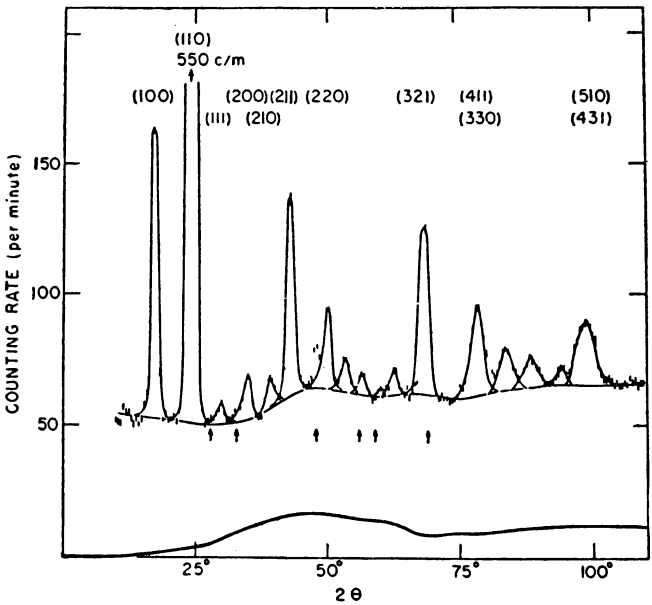

FIG. 4-1. The diffraction pattern of NH_4Cl measured by Levy and Peterson. The solid curve at the bottom of the figure is the calculated incoherent scattering arising from the orientational disorder of the ammonium ions at room temperature.

ture, indicated by x-rays, was confirmed by neutron diffraction. Here we have a good illustration of the complementary nature of x-ray and neutron techniques; the lattice constants of the metal atoms were first fixed by x-ray studies, then the H location was

[5] R. E. Rundle, C. G. Shull, and E. O. Wollan, *Acta Cryst.* **5**, 22 (1952).

[6] S. W. Peterson and H. A. Levy, *J. Chem. Phys.* **20**, 704 (1952).

performed with neutrons. For KHF_2, the position of the hydrogen atom was shown to be equidistant from the F atoms, within 0.1 A, in the linear HF_2 ion. This study, which was performed using the single crystal technique, also indicated, by the asymmetric Debye-Waller factor, that the bifluoride ion oscillates in rotatory fashion.

The single crystal technique, to which we have alluded in the present section, has also been investigated experimentally by Bacon[7] and by Lowde[8] at Harwell, and Peterson and Levy[9] at Oak Ridge. It appears as if further application of this technique to the location of hydrogen atoms will make it possible to extend the results greatly compared to the small number of materials thus far analyzed. For single crystal diffraction the coherent peaks have a very high intensity relative to diffuse background, hence normal hydrogen instead of deuterium can be used. It is necessary to avoid extinction effects (nonuniform neutron "illumination" of sample) in order to obtain correct structure factors, and this objective limits the crystal size to the order of a millimeter or smaller. Although calculations[10] had indicated that only much smaller samples could be used, the later experiments showed that in favorable cases millimeter samples were permissible.

4.2 Analysis of Crystals not Containing Hydrogen

If we consider the analysis of crystals not containing hydrogen, we realize that neutron diffraction may be superior to x-rays for several possible reasons. For light elements the situation is very similar to that of hydrogen, as the scattering power of the element may be insufficient for detection by x-rays. In some problems neutron diffraction is a powerful tool for heavy elements also; for these the x-ray scattering power is so nearly the same for different elements that they cannot be

[7] G. E. Bacon, *Proc. Roy. Soc.* (*London*) **A209**, 397 (1951).
[8] R. D. Lowde, *Nature* **167**, 243 (1951).
[9] S. W. Peterson and H. A. Levy, *J. Chem. Phys.* **19**, 1416 (1951).
[10] G. E. Bacon and R. D. Lowde, *Acta Cryst.* **1**, 303 (1948).

distinguished in a crystal. For such compounds it may well be that the neutron amplitudes differ sufficiently so that the elements can be distinguished. Still another difference between neutrons and x-rays, the isotropic nuclear, as contrasted to the atomic, form factor, may in individual cases make the former of particular value.

An example of the use of neutron diffraction for location of light atoms is furnished by the study of the intermetallic compound $M\mathrm{Be}_{13}$ (where M denotes a heavy metal) by Koehler *et al.*[11] Here again, as for H atom location, we have the case of a compound whose structure had been ascertained, but with some uncertainty, by x-rays. The difficulty in the x-ray work arose from the fact that the Be scattering power is small compared to that of the heavy metals. The neutron investigations, which were done at Oak Ridge by the standard powder method of Sec. 2.5, substantiated the structure estimated from the x-ray work, and were aided greatly by the near equality of the Be and metal amplitudes (Table 3-1). The neutron results showed that the compound is face-centered and isomorphic with NaZn_{13}, whose structure is known from x-rays (here no great difference in amplitude exists for x-rays).

For a crystalline compound composed of elements of similar atomic weight, it is difficult to identify the components contributing to individual Bragg reflections because of the similarity in x-ray scattering power. For instance, in ordered samples of FeCo, the superlattice lines, which depend on the difference in scattering power of the components, can hardly be seen with x-rays because of the near equality of scattering power. The neutron diffraction pattern of FeCo and $\mathrm{Ni}_3\mathrm{Mn}$, however, which were studied by Shull and Siegel,[12] showed the existence of superlattice lines clearly, Fig. 4-2. The difference in amplitude of the components of these two compounds fortunately differ greatly as can be seen from Table 3-1, Ni and Mn actually

[11] W. Koehler, J. Singer, and A. Coffinberry, *Acta Cryst.* **5**, 394 (1952).

[12] C. G. Shull and S. Siegel, *Phys. Rev.* **75**, 1008 (1949).

being of opposite sign. The reverse situation obtains for the superlattice lines of Cu_3Au, which are not observed with neutrons for Cu and Au have similar scattering power. Strong x-ray superlattice lines are found, however, because of the difference in atomic weight of the components. The difference in neutron scattering amplitude that often occurs for similar atomic weights was also utilized by Bacon[13] in a determination of the structure of the mineral spinel, $MgAl_2O_4$. It was possible to show that

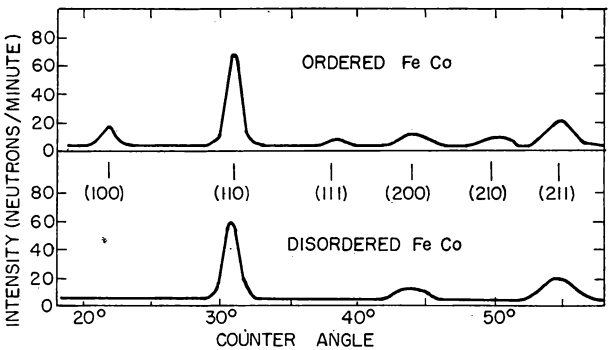

FIG. 4-2. Neutron diffraction patterns of ordered and disordered FeCo, exhibiting the superlattice lines, (100), (111), (210), etc., in the former.

the "normal" rather than the "inverse" structure held, a decision that could not be reached from x-ray evidence.

An interesting example of the use of the form factor difference between neutrons and x-rays is the work of Bacon[14] on graphite. Here advantage was taken of the fact that the x-ray scattering is determined by the distribution of the electrons in the atom, whereas the neutron scattering arises from the nucleus. An anomalous intensity pattern, observed in the x-ray diffraction pattern of graphite, had been interpreted in terms of a nonspherical distribution of the electrons around the carbon

[13] G. E. Bacon, *Acta Cryst.* **5**, 684 (1952).
[14] G. E. Bacon, *Nature* **166**, 794 (1950).

nucleus. Bacon showed that the nonspherical distribution was the correct explanation of the anomalous pattern, rather than the Debye-Waller temperature factor, to which the anomaly had also been ascribed. The distinction could be made because the temperature factor is common to x-ray and neutron scattering both, while the electron distribution would affect only the x-ray scattering. Bacon's neutron results, which showed no anomalous intensity distribution, ruled out the temperature factor explanation, and constituted strong evidence for the nonspherical electron distribution as the source of the anomaly.

In analysis of the type described in this and the preceding section it is of course necessary to have accurate values of the coherent scattering amplitudes of the elements for use in calculation of the structure factors. For some of the elements, for example oxygen and hydrogen, the amplitudes of Table 3-1 possess sufficient accuracy for the most precise diffraction analysis being performed at the present time. In some cases, the crystal diffraction analysis itself has at times revealed incorrect coherent amplitudes and as a result produced better values of the amplitudes involved. For example, a revised amplitude for H^2 resulted from the work on Th and Zr hydrides described in Sec. 4.1, and in the analysis of spinel by Bacon just discussed an inconsistency in the Mg amplitude (implying appreciable incoherent scattering) was resolved.

4.3 Further Structure Applications of Neutron Diffraction

The unique properties of neutrons relative to x-rays have been used for several applications in addition to the analysis of crystal structure already described in the present chapter. Although none of these applications have led to extensive developments, they are worthy of brief description as an indication of possible future uses of neutrons in the study of the structure of matter.

Whereas there has been extensive study of the structure of liquids by means of x-rays, there has been only a relatively small amount of effort spent on the application of neutrons to

liquid structure. There is a possible superiority of neutrons over x-rays, however, related to the isotropic nature of the neutron scattering (unit form factor) compared to the atomic form factor effect for x-rays. This difference in angular distribution implies that the coherent peaks of the neutron diffraction pattern of a liquid will be observable at larger scattering angles than they will for x-rays, for which the form factor decreases with increasing angle. Thus in principle neutrons should be useful for investigation of the details of the structure at larger interatomic spacings.

The diffraction patterns of liquid sulfur, lead, and bismuth were studied by Chamberlain[15] at Argonne, in the first application of neutron diffraction to liquids. In this work an arrangement of monochromating crystal and sample was used that had good resolution in $(\sin \theta)/\lambda$ with a wide range in λ, thus giving an increased intensity compared to the usual monochromator arrangement. The diffraction patterns obtained for the three liquids, when converted to the probability distribution of atoms in the liquid, in the manner used for x-rays analysis, showed one distinct peak in the separation of nearest neighbors for each liquid (about 2 A for S and about 4 A for Bi and Pb) and subsidiary peaks at greater distances. These results agreed with similar x-ray work but did not reveal structure in addition to that known from the x-ray analysis. The same equipment was used by Czyzak and Wattenberg[16] for study of heavy water and here again a single distinct peak was found, corresponding to a separation in agreement with that found from x-ray work.

The structure of vitreous silica was investigated by Milligan *et al.*[17] with the standard powder diffraction method, and by Ruderman,[18] using transmission of monochromatic neutrons in the manner depicted in Fig. 2-8. In contrast to the liquid

[15] O. Chamberlain, *Phys. Rev.* **77**, 305 (1950).
[16] S. Czyzak and A. Wattenberg, *Phys. Rev.* **75**, 1634 (1949).
[17] Milligan, H. A., Levy, and S. W. Peterson, *Phys. Rev.* **83**, 226 (1951).
[18] I. W. Ruderman, *Phys. Rev.* **78**, 317 (1950).

results just described, both groups of investigators found that more peaks could be resolved than was possible in previous x-ray work. The observed peaks converted to interatomic distances gave six distinct spacings between 0.7 and 2.7 A in Ruderman's work and five between 1.6 and 5.1 A in the work of Milligan *et al.*, with the spacings in agreement for the region common to both measurements. The additional structure found for neutrons compared to x-rays, for which only a single interatomic spacing was clearly evident, results from the form factor of neutron scattering, which allows extension of the measurements to large values of $(\sin \theta)/\lambda$.

The diffraction patterns obtained from molecular gases have been the subject of particular attention by Hurst and Alcock[19] at Chalk River, where patterns for deuterium, oxygen, carbon dioxide, nitrogen, carbon tetrafluoride, and methane have been obtained. For most of these gases the principal results consisted of the coherent scattering amplitudes (H^2, F, N, O) and the comparison of the observed pattern with various theoretical intensity calculations. In addition, the work with CF_4 resulted in a measurement of the C-F bond length. It was shown by Spiers[20] that the complete quantum-mechanical calculation, which could be carried out for deuterium, gave the correct results but that a semiclassical calculation, much simpler to perform, was sufficiently accurate for the experimental patterns. The accuracy with which the calculation reproduces the experimental pattern is illustrated by the results for CF_4, Fig. 4-3. In the semiclassical calculation, the energy changes resulting from changes in the rotational quantum number of the molecule are neglected, and the scattering amplitude is calculated from the spatial relationship of the molecule, with the cross section then averaged over all orientations of the molecule.

The exceedingly small absorption of neutrons in many elements opens the possibility of studying material properties

[19] D. G. Hurst and N. Z. Alcock, *Can. J. Phys.* **29,** 36 (1951); N. Z. Alcock and D. G. Hurst, *Phys. Rev.* **75,** 1609 (1949); **83,** 1100 (1951).

[20] J. A. Spiers, *Phys. Rev.* **75,** 1765 (1949).

inside samples rather than near the surface, as is done with x-rays. The small extinction of neutrons was utilized by Weiss *et al.*[21] in a study of the diffraction pattern of cold-worked brass. By examination of the Bragg discontinuities in a transmission measurement (of the type shown in Fig. 2-8), it was shown that the broadening of the peaks observed in x-ray powder diffraction resulted from distortion of the crystals. The same measurements were used as an indication that the extinction effects

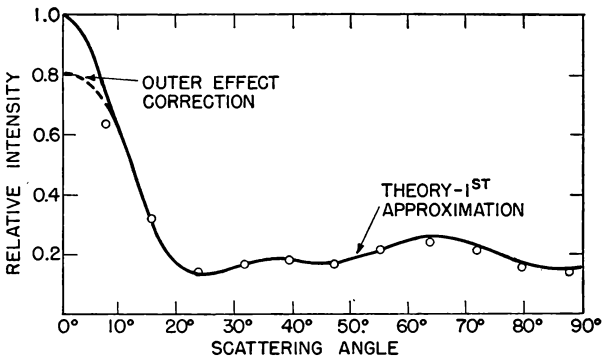

FIG. 4-3. Angular distribution of scattering from gaseous CF_4 compared to the theoretical curve. The dashed line represents the inclusion of a correction for the finite size of the molecules.

found in the x-ray work on cold-worked brass resulted from primary extinction (intensity decrease in individual mosaic blocks).

4.4 Lattice Vibrations

A field of study that may prove to be an advantageous application of slow neutrons, although still in the preliminary stages, is the measurement of properties of the thermal lattice vibrations in crystals. The advantage of neutrons compared to x-rays arises from their enhanced sensitivity to several

[21] R. Weiss, J. Clark, J. Hastings, and L. Corliss, *Phys. Rev.* **86**, 656 (1952).

properties of the lattice vibrations. Thus the exchange of energy with the lattice vibrations (absorption or emission of phonons) results in an appreciable change in the energy of the neutron, because of the similarity of neutron and atomic mass, whereas the energy change of an x-ray photon is negligible. In addition, it is possible to work with extremely slow neutrons for which the modes of energy exchange with the lattice are greatly simplified.

The theory of thermal inelastic scattering of slow neutrons is more complicated than that of x-ray thermal scattering because the energy exchanges involved are not negligible relative to the neutron energy. The x-ray scattering theory can be carried out[22] in a completely classical manner, considering the atoms as located at the lattice positions but spread over a finite volume by the temperature vibrations. This spatial spread results in a decrease of the observed coherent scattering peaks, given by the Debye-Waller factor, and in the production of the temperature diffuse background scattering. In the calculation no consideration is given to the energy change at scattering, the reduction in the intensity of the peaks resulting solely from the phase differences introduced by the variation in position of the atoms.

The correct quantum-mechanical treatment of the scattering of neutrons, in which the energy exchanges are taken into account, is very complex and has been the subject of a number of calculations.[23] The qualitative features of the scattering, Fig. 4-4, which are similar for all materials, can be described simply, however. The inelastic scattering is a minimum somewhat below thermal neutron energies, this minimum usually occurring at a wavelength near that of the crystal cutoff. At higher energies, the cross section increases as the neutron be-

[22] See, for example, W. H. Zachariasen, *X-Ray Diffraction in Crystals* (Wiley, 1947), Ch. X.

[23] References to these may be found in an article of G. Placzek, *Phys. Rev.* **86,** 377 (1952); an instructive comparison of x-ray and neutron inelastic scattering is given by M. Lax, *Rev. Mod. Phys.* **23,** 287 (1951), pp. 290–96.

comes capable of exciting more and more lattice vibrations. Finally, at energies of several volts, where the free atom cross section is attained, the atom is no longer bound at all and, with respect to the lattice, the scattering is completely inelastic. In the transition region (thermal to several electron volts), the incoherent inelastic scattering increases with energy about as rapidly as the coherent scattering decreases, with a resulting total cross section that is approximately constant.

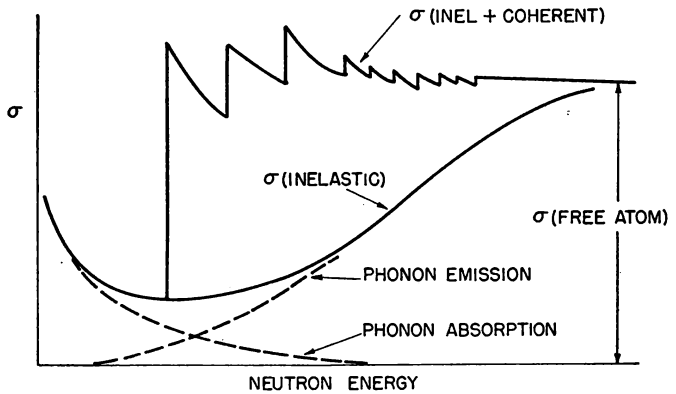

FIG. 4-4. The variation with energy of the components of the neutron scattering cross section of a polycrystal.

For neutron wavelengths beyond the cutoff, the inelastic scattering increases with wavelength because the probability of gain of energy by the neutron (phonon absorption) increases. In this "cold neutron" region, the cross section soon becomes $1/v$, or proportional to λ, because the energy of the outgoing neutron is large and independent of the energy of the incoming neutron. The inelastic scattering of cold neutrons obeying the "lambda law" consists primarily of processes in which single phonons are absorbed, and the calculations are somewhat simpler as a result. The inelastic scattering theory is also simplified for the case in which the waves scattered from individual nuclei are incoherent with those from other nuclei.

Such a case is illustrated by vanadium, which as we have seen has a scattering that is almost completely spin-dependent incoherent. Here the calculation is simplified because the interference between waves scattered by different nuclei does not need to be considered. The "incoherent approximation," when applied to the calculation of inelastic scattering for other materials with predominantly coherent scattering, still seems to give results in good agreement with experiments for several materials.

The lattice vibration scattering has not been studied extensively by the standard powder diffraction methods for the diffraction patterns are not sensitive to the details of the inelastic scattering. Actually, the diffuse scattering enters into powder diffraction work, as we have seen, as a reduction in the observed scattering, a reduction that is corrected for by the Debye-Waller factor. The Debye-Waller factor used is just the one calculated for x-rays by a strictly classical approach. The reduction in coherent scattering is given correctly by this approach, however, as shown by the consistency of coherent amplitudes obtained in neutron diffraction using the x-ray Debye-Waller factor. An example is given by Fig. 4-5, which shows the experimental results of Shull and Wollan[24] for lead compared with the theoretical Debye-Waller factor. The Debye-Waller factor, Eq. (1-47), involves only the Debye temperature as a parameter and its value for lead gives good agreement with the observed result shown in Fig. 4-5.

Although the results obtained with powder diffraction relative to the Debye-Waller factor justify its use with neutrons, they do not give information on the details of the scattering, such as the frequency spectrum of lattice vibrations and the energy changes involved. This information can be obtained more directly from the inelastic scattering itself. Several investigations of this nature have been made, consisting of measurement of the total inelastic cross section as a function of wavelength or of the energy of the inelastically scattered neu-

[24] C. G. Shull and E. O. Wollan, *Phys. Rev.* **81,** 527 (1951).

trons. The total cross sections can be measured rather accurately and are useful for comparison with the rather complicated theoretical calculations, while the energy measurements can be compared with the specific features of the theory involving energy exchange.

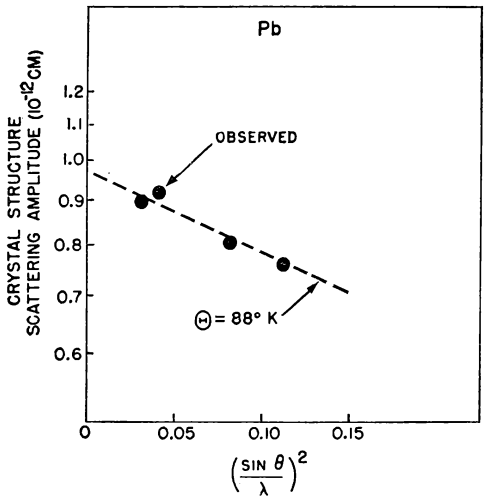

FIG. 4-5. The variation of the measured scattering amplitude of lead with angle, illustrating the decrease given by the Debye-Waller factor for thermal diffuse scattering. The slope of the dashed line, which is calculated from a Debye temperature of 88° K, is in agreement with the experimental values.

The inelastic cross section can be studied very effectively by measurement of the sample transmission for wavelengths beyond the crystal cutoff if the material chosen does not have high neutron capture. For long wavelengths, at which the coherent scattering disappears, the total cross section is made up of capture, incoherent scattering (spin-dependent and isotopic), and inelastic scattering. For some materials, of which graphite is a good example, the first two are negligible and the inelastic scattering comprises the entire observed cross section.

For others, the noninelastic effects, while present, are not large, and they can be identified by the variation of the observed scattering with wavelength and temperature. The identification is possible because spin-dependent and isotopic incoherence do not vary with wavelength, whereas capture does not vary with temperature.

The total inelastic scattering is observed to be accurately $1/v$ at long wavelengths (the lambda law), and its change with temperature agrees very well with the theoretical calculations. Carbon is one of the few exceptions; its inelastic scattering, while $1/v$, increases much less rapidly with temperature than is expected theoretically. This behavior is explained in terms of the layer structure of graphite and in fact is similar to the anomalous temperature variation of the graphite specific heat,[25] a property that depends on the Debye-Waller frequency spectrum in a manner similar to the inelastic scattering. The inelastic scattering of long wavelength neutrons as a function of temperature has been studied for graphite, beryllium, bismuth, copper, and iron at Brookhaven[26] and for magnesium, aluminum, nickel, iron at Cambridge.[27]

The results for iron are of particular interest because they reveal an inelastic scattering slightly above the theoretical value at room temperature. The discrepancy increases with temperature up to the Curie point, where it levels off and even decreases slightly at higher temperature, Fig. 4-6. When plotted against wavelength, the behavior is accurately lambda law, hence the scattering is inelastic, with the energy change large compared to the neutron energy. The transition at the Curie point, Fig. 4-6, is a strong indication that the scattering is magnetic in nature, a view supported by the normal inelastic

[25] R. W. Gurney, *Phys. Rev.* **88,** 465 (1952).

[26] G. W. Johnson, H. Palevsky, and D. J. Hughes, *Phys. Rev.* **82,** 345 (1951); H. Palevsky and R. R. Smith, *ibid,* **86,** 604 (1952); H. Palevsky and D. J. Hughes, *ibid* (in press).

[27] J. M. Cassels, *Proc. Roy. Soc. (London)* **208A,** 527 (1951); G. L. Squires, *ibid,* **212A,** 192 (1952); R. Latham and J. M. Cassels, *Proc. Phys. Soc. (London)* **65A,** 241 (1952).

scattering of copper, of similar atomic weight. The conclusion is that the excess inelastic scattering in iron is almost certainly magnetic inelastic scattering associated with the "flipping" of spins, that is, the excitation and absorption of magnetic spin waves. The fact that the lambda law holds several hundred degrees above the Curie point proves that the spins are not free but that energy is imparted to the neutrons when the spins

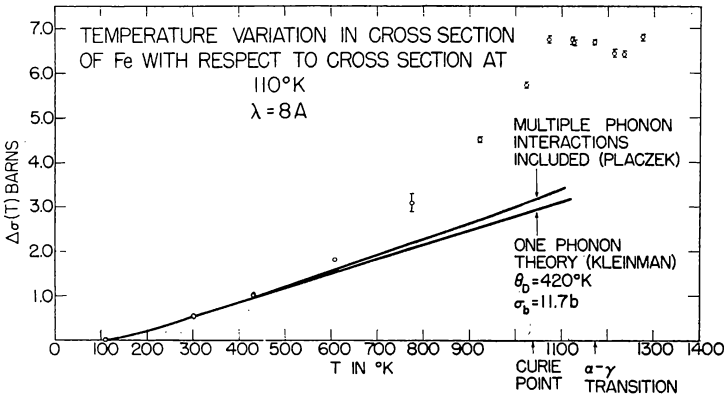

FIG. 4-6. The inelastic scattering of slow neutrons in iron as a function of temperature; the scattering in excess of the theoretical value is interpreted as magnetic inelastic scattering.

flip. Apparently the spins are coupled in such a way that ferromagnetism does not result.

Although measurement of the energy change in inelastic scattering is exceedingly difficult, some progress has been made at Chalk River and at Harwell. In some recent experiments at Chalk River, Brockhouse and Hurst[28] have observed the change in energy at inelastic scattering by observing the transmission of the scattered neutrons in cadmium. The incident neutrons, of energy 0.35 ev. were obtained from a NaCl crystal, and the small changes in the transmission of cadmium cal-

[28] B. N. Brockhouse and D. G. Hurst, *Phys. Rev.* **88**, 542 (1952).

culated from the expected inelastic scattering were verified experimentally. The cadmium transmission curves for neutrons scattered from several materials, Fig. 4-7, show a lower transmission for 0.35-ev neutrons, indicating a loss of energy on the average. While this work shows that the change in energy is about the magnitude expected, it does not give any detailed

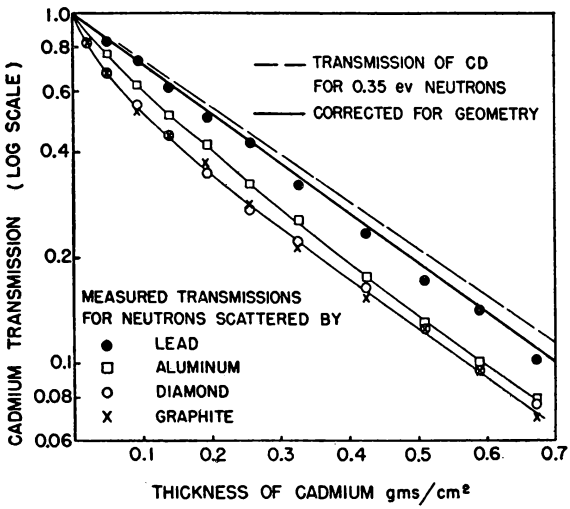

FIG. 4-7. Transmission curves in cadmium of the neutrons inelastically scattered in various materials. The change of neutron energy is shown by the difference in transmission.

information on the energy changes involved. The energy change was also studied by Egelstaff[29] at Harwell with slower neutrons (Pb filtered) than the Chalk River work, but using the same general method. The filtered neutrons were scattered from several materials and the energy after scattering was measured by transmission in lithium. The increase in energy that is the predominant change for cold neutrons was detected, but the accuracy was insufficient for detailed results.

[29] P. A. Egelstaff, *Nature* **168**, 290 (1951).

Increased intensity and improvements in technique will probably make detailed measurements of the energy transfers possible, and these measurements will certainly be useful for the information on the spectrum of lattice vibrations that will result. For the case of magnetic inelastic scattering, the information that would be obtained on the spectrum of spin waves would be of great value to the theory of ferromagnetism. Lowde[30] has recently studied the diffuse streaks near Bragg peaks in the neutron diffraction pattern of a single crystal of iron that result from inelastic scattering. Although the diffuse streaks have intensities only one thousandth of the Bragg peaks, it is possible that their study, in single crystal diffraction, may lead to useful results.

[30] R. D. Lowde, *Proc. Phys. Soc.* (*London*) **65A**, 857 (1952).

CHAPTER 5

Magnetic Scattering

In our discussions thus far, we have seen that there are actually only a few examples of crystal analysis by neutron diffraction that could not also be accomplished with x-rays. The most advantageous use of the new technique for nonmagnetic crystals, at least at the present stage of development, seems to be as an adjunct to x-ray analysis. For magnetic scattering, however, the situation is fundamentally different because the magnetic structure of crystals, invisible to x-rays, is open to direct investigation with neutrons. The interaction of neutrons with magnetic materials has been studied by all the methods of neutron optics; small angle scattering, reflection, transmission, and diffraction. After a consideration of the basic principles of magnetic scattering, we shall turn to a consideration of the experimental results and the information they have given concerning the magnetic structure of crystals.

5.1 Principles of Magnetic Scattering

In the interest of simplicity, magnetic scattering, which does not occur for electromagnetic waves but is extremely important for neutrons, was neglected in the discussion of neutron-optical principles in Ch. 1. This magnetic scattering, the principles of which we now consider, has led to some of the most valuable applications of neutron diffraction. The interaction between the atomic magnetic moments and the neutron moment affects all the phenomena of diffraction and refraction when paramagnetic or ferromagnetic materials are under consideration, in some cases complicating them greatly. In the present section we shall consider the basic form of the magnetic

scattering amplitude and the manner in which it affects neutron refraction and diffraction.

The interaction between a neutron and the spin magnetic moment of an atom was formulated in detail by Halpern and Johnson,[1] who considered the magnetic scattering from isolated atoms, as well as ferromagnetic and paramagnetic crystals, for both polarized and unpolarized neutron beams. The applications of this interaction to refraction, diffraction, polarization, and depolarization of neutrons were then carried out in a series of papers by Halpern and his co-workers.[2] These papers, written a few years after the discovery of the neutron and before intense sources were available, are still the primary references for the effects of magnetic scattering on all the phenomena of neutron optics. The basic results that we shall discuss briefly are developed in detail in the paper of Halpern and Johnson.[1]

In order to consider the magnetic interaction in the most uncomplicated form we shall first examine the scattering amplitude of an atom in a ferromagnetic material, assuming no incoherent scattering. The case of paramagnetism will be examined later, for which the random orientation of the atomic moments causes the magnetic scattering to be incoherent. The amplitude can be divided into that arising from the nucleus alone and that from the magnetic moment of the atom,

$$a = a_n \pm a_m. \tag{5-1}$$

Because the interaction between the neutron and the magnetic moment of the atom changes sign with the orientation of the neutron moment, the magnetic amplitude will be either plus or minus, corresponding to the two possible orientations of the neutron with respect to the spin of the atom.

In the case of nuclear scattering alone, for which there is no variation of intensity with angle of scattering, the cross

[1] O. Halpern and M. H. Johnson, *Phys. Rev.* **55**, 898 (1939).

[2] O. Halpern and T. Holstein, *Phys. Rev.* **59**, 960 (1941); O. Halpern, M. Hamermesh, and M. H. Johnson, *ibid.* **59**, 981 (1941); M. Hamermesh, *ibid.* **61**, 17 (1942).

section is given simply as $4\pi a_n^2$. The magnetic scattering is not isotropic and its cross section is given by a considerably more complicated result. Because of this variation of magnetic scattering amplitude with angle, it is necessary to evaluate the differential cross section, which is the cross section per unit solid angle, $d\sigma/d\omega$,

$$\begin{aligned} d\sigma/d\omega &= (a_n \pm a_m)^2 \\ &= a_n^2 \pm 2a_n a_m + a_m^2. \end{aligned} \tag{5-2}$$

For a single neutron incident on the nucleus, either the positive or negative sign will apply, depending on the orientation of the neutron. The same situation will obtain for an incident beam in which all the neutrons are aligned, i.e., a beam of polarized neutrons.

If the incident neutron beam is unpolarized then the cross term in the expansion of the differential cross section will average to zero with the result,

$$d\sigma/d\omega = a_n^2 + a_m^2, \tag{5-3}$$

hence the intensities (not amplitudes) are added in net scattering for this case. This equation, in spite of its simple appearance, still represents an involved angular distribution because the magnetic amplitude is a function of angle and, as we shall see, of direction of magnetization also.

The magnetic amplitude can be expressed[3] in terms of the spin of the atom S (in units of $h/2\pi$) and the magnetic moment of the neutron γ (in nuclear magnetons) as

$$\begin{gathered} a_m = \pm \frac{2e^2\gamma S}{mc^2} f(\boldsymbol{q}\cdot\boldsymbol{s}) \\ (e^2/mc^2 = 2.8 \times 10^{-13} \text{ cm}). \end{gathered} \tag{5-4}$$

The quantity f is an *atomic form factor* that expresses the decrease in the scattered amplitude resulting from the finite extension of the magnetically active electrons (the $3d$ electrons

[3] O. Halpern and M. H. Johnson, *loc. cit.*, p. 910.

in iron, for example). The phase differences arising from this spread cause some destructive interference, the amount depending on the neutron wavelength, the scattering angle, and the electron distribution. While closely similar to the atomic form factor familiar[4] in x-ray work, the magnetic factor differs quantitatively because only a small number of electrons contribute to the scattering.[5] In general the form factor is small for short wavelength and large scattering angle (actually, it is a function of the parameter $\sin \theta/\lambda$) and becomes unity in the limit of long wavelength or small scattering angle.

The dependence of the amplitude on orientation of magnetization and angle of scattering, θ, is expressed by the scalar product of the vectors $\boldsymbol{q}$ and $\boldsymbol{s}$. Whereas $\boldsymbol{s}$ is just the neutron spin, $\boldsymbol{q}$ is a function of scattering angle and magnetization direction,

$$\boldsymbol{q} = \boldsymbol{e}(\boldsymbol{e}\cdot\boldsymbol{\kappa}) - \boldsymbol{\kappa}\,, \tag{5-5}$$

where $\boldsymbol{\kappa}$ is a unit vector in the magnetization direction and $\boldsymbol{e}$ a unit vector in the direction of the momentum transfer in the collision (i.e., perpendicular to the lattice planes in a Bragg reflection). The geometrical relations involved are shown in Fig. 5-1, from which it is clear that $\boldsymbol{q}$ is perpendicular to $\boldsymbol{e}$, its magnitude is $\sin \beta$, where β is the angle between $\boldsymbol{\kappa}$ and $\boldsymbol{e}$, and that its projection on $\boldsymbol{\kappa}$ is $q^2 = \sin^2 \beta$.

We thus see that the magnetic amplitude in the case of aligned (polarized) neutrons and magnetized scatterers has an extremely complicated variation with angle, depending on the distribution of electrons in the atom, the direction of the magnetizing field, and the direction of neutron polarization. For the usual applications of the scattering formula, however, experimental conditions are such that simplifications can be made in the equations. In diffraction work, for example, the incident

[4] A. H. Compton and S. K. Allison, *X-rays in Theory and Experiment* (Van Nostrand, 1935).

[5] The magnetic form factor for iron is treated by J. Steinberger and G. C. Wick, *Phys. Rev.* **76,** 994 (1949).

neutrons are unpolarized and in that case the amplitude of Eq. (5-4) can easily be evaluated and substituted into the appropriate expression for the differential cross section, Eq. (5-3). Making use of the simplification,

$$(\boldsymbol{q}\cdot\boldsymbol{s})(\boldsymbol{q}\cdot\boldsymbol{s}) = \tfrac{1}{4}\, q^2. \tag{5-6}$$

we obtain

$$d\sigma/d\omega = a_n^2 + \left(\frac{e^2\gamma S}{mc^2}\right)^2 f^2 q^2, \tag{5-7}$$

and the net scattering (averaged over the neutron spin states) has an angular variation given by f^2 and q^2.

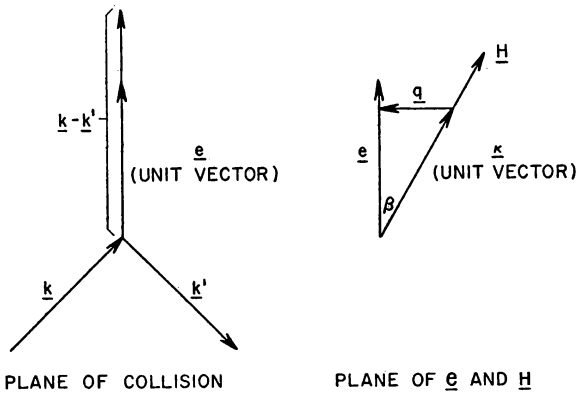

FIG. 5-1. Geometrical factors involved in the scattering of neutrons from an atomic magnetic moment. The momentum transfer in the collision is proportional to $\boldsymbol{k} - \boldsymbol{k}'$, where $\boldsymbol{k}$ and $\boldsymbol{k}'$ are the initial and final wave vectors.

Still further simplification results if the scattering material is unmagnetized for in that case q^2 is averaged over all directions of magnetization. The differential cross section in this case becomes

$$d\sigma/d\omega = a_n^2 + \frac{2}{3}\left(\frac{e^2\gamma S}{mc^2}\right)^2 f^2, \tag{5-8}$$

for the average value of q^2 (that is, of $\sin^2\beta$) is $\frac{2}{3}$. Com-

parison of Eqs. (5-8) and (5-7) shows that the cross section of magnetized iron, for example, will be larger or smaller than that of unmagnetized iron, depending on the particular angle of scattering involved (which determines the value of q^2 relative to its average value $\frac{2}{3}$).

When the scattering from more than one atom is calculated, the interference of nuclear and magnetic amplitudes from the various atoms must be considered; that is, the angular variation of scattering intensity resulting from diffraction effects must be combined with the magnetic variation of Eq. (5-8). When the various kinds of incoherent scattering are also taken into account, the resulting equations become very complicated. Actually the magnetic scattering itself can also give rise to an incoherent scattering in which the spins of the atom are changed with simultaneous spin reversal of the neutrons. This type of scattering occurs when the magnetic moments of the atoms are not ordered, that is in a paramagnetic material, and the scattering is closely analogous to nuclear spin-dependent scattering.

Because of the random orientation of the atomic moments in a paramagnet, the scattering is completely incoherent, hence no Bragg maxima are observed. The differential cross section for this case, of course, retains an angular variation arising from the atomic form factor f, and in fact is just

$$d\sigma/d\omega = a_n^2 + \frac{2}{3} S(S+1) \left(\frac{e^2\gamma}{mc^2}\right)^2 f^2. \tag{5-9}$$

For long wavelength f becomes unity and the scattering cross section is given by $4\pi a^2$ or

$$\sigma_S = 4\pi a_n^2 + \frac{8\pi}{3} S(S+1) \left(\frac{e^2\gamma}{mc^2}\right)^2, \tag{5-10}$$

that is, the paramagnetic and nuclear scattering are both isotropic and their intensities are additive. We shall examine the experimental verification of these results for paramagnetic scattering in Sec. 5.4.

The effect of magnetic scattering on neutron diffraction

from crystals is taken into account by substituting the formulas we have discussed for the nuclear and magnetic amplitudes in the crystal structure factors. The crystal structure factors are then used in analysis in just the way that they are for non-magnetic neutron diffraction, with the additional fact that information on the magnetic amplitude, hence on the magnetic structure of the crystal is also obtained from the measured structure factors. We shall discuss several specific examples of this important technique in later sections of the present chapter.

The inclusion of magnetic scattering in neutron refraction turns out to be extremely simple for, as we have seen, the index is given very directly by the potential in the scattering medium. For a neutron in a ferromagnetic material, this potential is just μB where μ is the magnetic moment of the neutron (in units such that μB will be in the same units as the neutron energy, E) and B the saturated magnetic induction. The index of refraction for a ferromagnetic material is thus given by a simple modification of Eq. (1-38):

$$n^2 = 1 - \lambda^2 Na/\pi \pm \mu B/E. \tag{5-11}$$

This equation refers to a ferromagnetic material only, the two signs referring to the two neutron spin states relative to the magnetization. In a paramagnetic medium, the average amplitude, which is effective for refraction, is zero and the magnetic scattering has no effect on the refractive index. The doubly refracting nature of iron has important consequences for the production of highly polarized neutron beams, Sec. 5.5.

At the time the early experiments on neutron reflection and diffraction from magnetic materials were being performed, there was considerable uncertainty concerning the correctness of the fundamental form of the neutron-electron magnetic interaction. The uncertainty concerned the angular variation of the magnetic scattering amplitude as well as the index of refraction in a ferromagnet. The uncertainty that existed can also be expressed simply as an uncertainty concerning the

correct field, that is H or B, that is effective for the neutron in a ferromagnet. The answer to this question was first given in a definite manner by neutron reflection experiments, which showed that the correct field is certainly B. This finding was later substantiated by diffraction experiments, which also showed in detail that the angular variation as expressed by Eq. (5-7) is correct. Both the reflection and diffraction experiments will be described in the next section. A review of the derivations that led to the contradictory results is given by Lax,[6] Ekstein,[7] and Halpern;[8] references to the earlier theoretical work may be found in these papers.

5.2 Verification of Magnetic Scattering Theory

Even if the only interest in magnetic scattering of neutrons were the investigation of the structure of magnetic crystals, it would be necessary to measure the fundamental interactions in order to understand the magnetic form factors involved in the crystal analysis. However, because of the intrinsic interest in the magnetic interaction of neutrons with atoms, it has been studied even more as an end in itself than for its practical applications. In fact, there had been considerable uncertainty concerning the exact form of the forces acting on a neutron in a ferromagnet, and it was not until intense neutron fluxes were available that these uncertainties could be resolved.

Before the availability of high neutron fluxes, some magnetic scattering of neutrons had been performed, but the low intensities meant that very little in the way of significant results could be obtained. With high pile fluxes it was possible to study a number of effects that were direct tests of the theoretical magnetic interaction. Some verification of the theory was obtained, for example, in connection with work on the production of polarized neutrons by transmission in magnetized iron, experiments similar to those performed with cyclo-

[6] M. Lax, *Phys. Rev.* **80,** 299 (1950); *Rev. Mod. Phys.* **23,** 287 (1951).
[7] H. Ekstein, *Phys. Rev.* **76,** 1328 (1949); **78,** 731 (1950).
[8] O. Halpern, *Phys. Rev.* **88,** 1003 (1952).

tron neutrons but with higher statistical accuracy. It was clear from the polarization experiments of Hughes, Wallace, and Holtzman (Sec. 5.5) that the general form of the interaction as expressed by Halpern *et al.*[9] was correct, in particular that the neutron behaved as a current element rather than a point dipole. These experiments, however, involving the entire Maxwell distribution and total rather than differential cross sections, depended on rather complicated integrals of the interaction. While they indicated strongly the correctness of the equations, they were not capable of giving the detailed verification that was required. During these experiments magnetic small angle scattering, which we have briefly described in Sec. 2.3, was discovered and the doubly refracting nature of a ferromagnet for neutrons was made evident. The double refraction in iron was then studied with mirrors, and the reflection work was able to give a definite check on several uncertain aspects of the theory.

The two values of the index of refraction for neutrons in a ferromagnet given by Eq. (5-11) should result in the appearance of two definite critical angles for mirror reflection, with a separation given by the induction B. Experiments performed by Hughes and Burgy[10] with magnetized iron mirrors exhibited these two critical angles, and the quantitative results were used to verify the correct form for the magnetic interaction. The possible interaction forms that were considered were those in which the neutron is considered a point dipole or a current element (an "Amperian" or "Dirac" current). This difference can also be described in terms of the effective field for the neutron in iron, the dipole assumption corresponding to H, and the other, underlying Eq. (5-11), to B, as the effective field. These assumptions lead to greatly different results for the critical angles because H is extremely small compared to B. The predicted curves are compared with the experimental results, obtained by the methods of Sec. 2.4, in Fig. 5-2. The

[9] See references at beginning of Sec. 5.1.

[10] D. J. Hughes and M. T. Burgy, *Phys. Rev.* **81**, 498 (1951).

close correspondence between the results and the curve based on the Dirac current hypothesis (effective field B) justifies its correctness. A few points were also obtained with the magnetization in the mirror at right angles to the neutron beam direction ($\phi = 90°$) to investigate a possible dependence of the

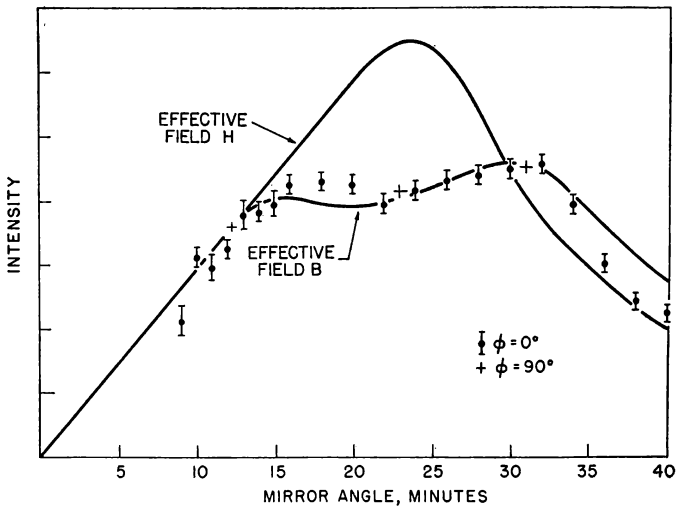

FIG. 5-2. Demonstration that the effective field for a neutron in a ferromagnetic material is B by means of mirror reflection. The agreement between the results for ϕ (angle between B and neutron motion) = 0° and 90° shows that the index of refraction is independent of magnetization direction, and the presence of two peaks in the curve is a proof that the neutron spin is one-half.

critical angle on the direction of magnetization. The results show no variation with the magnetization direction, and hence are in accord with the simple form[11] of Eq. (5-11). The appear-

[11] We shall not describe the alternative forms; a discussion of them, with literature references, may be found in a recent article of O. Halpern, *Phys. Rev.* **88,** 1003 (1952). Actually, the average B should appear in Eq. (5-11) for the work of Hughes and Burgy showed that the separation of the two critical angles decreased for unsaturated iron, approaching coincidence for complete de-

ance of two critical angles in Fig. 5-2 is a direct demonstration that the spin of the neutron is $\frac{1}{2}$, for the number of critical angles is just $2i + 1$.

The same conclusion regarding the correct interaction form was reached by neutron powder diffraction measurements of Shull, Wollan, and Koehler.[12] In this work the intensity of

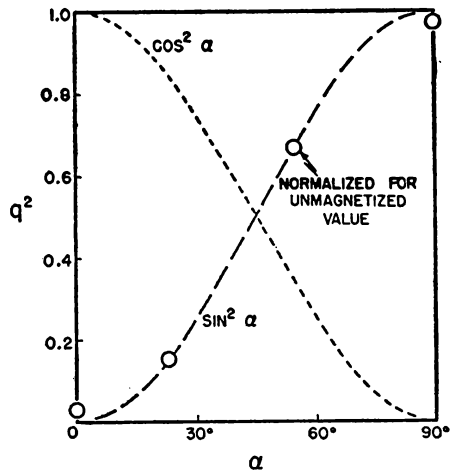

FIG. 5-3. Variation of scattering intensity from magnetite with direction of magnetization (Shull *et al.*). The angle α in the figure is the same as β of Fig. 5-1. The agreement with the curve $\sin^2 \alpha$ demonstrates that the effective field is B rather than H.

the (111) reflection of Fe_3O_4 was measured with the sample magnetized in various directions. The variation of the scattered intensity with magnetization could then be interpreted in terms of the variation of q in Eq. (5-7). The value of q thus obtained is plotted in Fig. 5-3 as a function of the angle β of Fig. 5-1 (labeled α in Fig. 5-3). The dotted curve is that expected from

magnetization. These results show that for reflection the amplitude is averaged over regions larger than the domains (about 10^{-3} cm times the neutron wavelength).

[12] C. G. Shull, E. O. Wollan, and W. C. Koehler, *Phys. Rev.* **84**, 912 (1951).

the dipole interaction and the dashed curve, with which the experimental points agree, is that for the Dirac current case (effective field B). This verification of theory, as well as the mirror results, justifies the assumptions underlying the equations of Sec. 5.1, all of which are based on the Dirac current assumption.

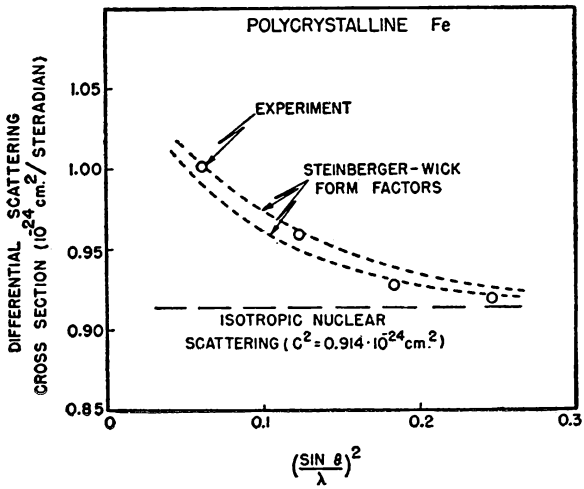

FIG. 5-4. Differential scattering cross section of iron compared with that calculated from the form factors of Steinberger and Wick.

In predicting the results to be obtained for diffraction from a magnetic crystal, or in interpreting the results of magnetic crystal analysis, it is necessary to take into account the magnetic atomic form factor, f. This form factor of course does not enter the mirror work because the scattering is in the forward direction in that case and a unit form factor obtains. The form factor for magnetic diffraction work is similar to that familiar from x-ray diffraction, arising as it does from the distribution of the electrons in the atom, but some difference exists because only a few of the electrons in the atom are responsible for the magnetic scattering.

The form factor for the iron atom as calculated by Stein-

berger and Wick[13] had given good quantitative agreement for the neutron polarization experiments of Hughes *et al.*, but, as already stated, these experiments involve the entire Maxwell distribution and are not a good test of the detailed theory. The form factor was measured in a more direct manner by Shull *et al.* in the work just quoted, using standard neutron diffraction techniques. The differential scattering cross section obtained is shown as a function of scattering angle in Fig. 5-4, compared with two form factors obtained by Steinberger and Wick on slightly different assumptions. The agreement shows that the theoretical form factor of iron gives correctly the observed scattering variation with angle, and this verification of theory, together with the results concerning the form of the fundamental interaction, amply justifies the use of the theoretical results in the analysis of magnetic materials.

5.3 Analysis of Ferromagnetic and Antiferromagnetic Crystals

Because of the directness of the information supplied, the magnetic scattering of neutrons has proved to be of great value in the study of magnetic crystals. The magnetic structure of ferromagnets and antiferromagnets, in spite of extensive theoretical work over many years, is still in an unsatisfactory, somewhat controversial state. Although space does not permit us to deal with the complications of ferromagnetic theory and its present day uncertainties, we can illustrate the manner in which neutron optics is used as a test of the fundamental aspects of the theory. Neutrons furnish such a direct check because the magnetic scattering gives a detailed description of the microscopic distribution of the electronic magnetic moments in the crystal, revealing their orientation as well as their spatial distribution.

The investigation of magnetic structure by means of neutron diffraction is carried out essentially by the methods described in Sec. 2.5 and applied to nonmagnetic crystals in Ch. 4. The measured magnetic structure factors are somewhat more

[13] J. Steinberger and G. C. Wick, *Phys. Rev.* **76**, 994 (1949).

difficult to interpret because they depend not only on the distribution of magnetic moments in the crystals, but on the orientation of these moments. Further complications compared to the nonmagnetic neutron diffraction also arise because the magnetic scattering may be coherent or incoherent, depending on the orientation of the moments with respect to neighboring atoms. Thus if the moments have a definite orientation pattern, ferromagnetic or antiferromagnetic, coherent peaks analogous to the nonmagnetic diffraction result, whereas the case of nonaligned neighboring moments, or paramagnetism, leads to incoherent scattering. Reserving the incoherent paramagnetic scattering for the next section, we shall consider at present only the coherent scattering that produces Bragg maxima in the diffraction pattern.

In one respect the magnetic diffraction is simpler than the nonmagnetic, because the coherent amplitude, which cannot be predicted theoretically for nuclear scattering, can easily be calculated. The magnetic amplitude, as we have seen, is a simple function of the magnetic moment per atom and of the orientation of the magnetization and the scattering vector $\boldsymbol{q}$, Eq. (5-5). As the moment per atom is usually known, the amplitudes for the scattering atoms do not require measurement as in the case of nuclear amplitudes. As a result, the expected intensities in a diffraction pattern for a certain assumed magnetic structure can be calculated with confidence from the atomic moment and the magnetic atomic form factor.

Some of the early diffraction measurements with magnetic materials were useful mainly in the elucidation of the theoretical interaction and as an aid in understanding the connection between the observed diffraction pattern and the scattering amplitudes. Thus the work of Shull, Wollan, and Koehler[12] with polycrystalline iron (Sec. 5.2) showed that the diffraction pattern observed was correctly given by the formulas we have considered in Sec. 5.1, for a magnetic moment per iron atom of 2.2 Bohr magnetons or an S value of 1.1. In this work it was not necessary to magnetize the iron as q^2 could be assigned the average value $\frac{2}{3}$, Eq. (5-8).

Magnetic diffraction was used by Shull *et al.* in the same series of experiments as an aid in determining the magnetic structure of magnetite, Fe_3O_4. The results of the powder diffraction study showed that the *ferrimagnetic* structure proposed by Néel[14] was in accord with the diffraction pattern rather than several other possible structures. The degree of ferromagnetism (magnetic moment per iron atom) exhibited by magnetite is less than that of iron, and according to the theory of Néel the decreased moment is the result of a structure in which some of the moments are directed oppositely to the majority, with a resultant partial cancellation of the net moments. This ferrimagnetic structure leads to definite predictions for the diffraction pattern, hence to a direct experimental test.

The magnetic pattern of magnetite is complicated by the fact that it contains one Fe^{++} ion and two Fe^{+++} ions with different magnetic scattering amplitudes (corresonding to $S = 2$ and $\frac{5}{2}$). As some of the observed peaks are sensitive mainly to the nuclear scattering and others to the magnetic scattering of the two kinds of ions, it is possible to rule out various structures in which different types of magnetic orientation are postulated. By a comparison of observed and calculated intensities it was shown that the Néel model, in which the octahedral and tetrahedral iron ions are coupled antiferromagnetically, is in accord with the observed intensities. Although magnetite shows discontinuities at 80° K in magnetic properties, no significant differences in the diffraction pattern were observed in cooling the sample, thus indicating that the orientation of the magnetic moments is the same at high and low temperatures. The *ferrites*, of which magnetite is an example, are now undergoing study by neutron diffraction at several laboratories although few results have been published.[15]

[14] L. Néel, *Ann. Phys.* **3,** 137 (1948).

[15] The diffraction pattern of magnesium ferrite, Fig. 2-9, obtained by Corliss and Hastings at Brookhaven, is an illustration of this work; see also J. M. Hastings and L. M. Corliss, *Rev. Mod. Phys.* **25,** 114 (1953); G. E. Bacon and T. T. Roberts, *Acta Cryst.* **6,** 57 (1953).

The antiferromagnetic coupling, which lowers the net magnetic moment of magnetite, is complete in MnO, which has no net ferromagnetic moment at all. The investigation of this *antiferromagnetic* material was actually one of the first applications of neutron diffraction to magnetic structure analysis. The powder diffraction results of Shull *et al.*[16] showed very directly that the antiferromagnetic arrangement of magnetic moments in MnO at low temperature was correct. This arrangement, in which alternate Mn ions have moments antiparallel to each other obviously produces a magnetic unit cell with twice the dimensions of the chemical unit cell, that is, the distance between ions of equal scattering amplitude is double the distance between Mn ions. Because of this double spacing, maxima in the diffraction pattern will occur at values of $(\sin \theta)/\lambda$ half those for nuclear scattering alone. The demonstration of these extra lines, which do not occur at all in the x-ray pattern of MnO, constituted definite proof of the antiferromagnetic behavior.

The magnetic reflections in MnO not only verified the antiferromagnetic structure but in addition made possible a study of the manner in which this orientation, which obtains at temperatures below its Curie temperature of 120° K, disappears as the temperature is raised. This disappearance of the magnetic order is shown as a gradual disappearance of the magnetic peak as the temperature is raised, Fig. 5-5. Should the material become paramagnetic above the Curie point (spins completely uncoupled), then incoherent paramagnetic scattering, Sec. 5.4, would be observed. Actually at temperatures somewhat above the Curie point a weak, broadened reflection is observed. This behavior is probably related to a slight degree of spin ordering that persists somewhat above the Curie temperature. The coupling between spins is related to the magnetic inelastic scattering that has been observed above the Curie point in iron, Sec. 4.4 and 5.4.

Although the intensity of the antiferromagnetic peaks

[16] C. G. Shull and J. S. Smart, *Phys. Rev.* **76,** 1256 (1949); C. G. Shull, W. A. Strauser, and E. O. Wollan, *ibid.* **83,** 333 (1951).

measured by Shull, Strauser, and Wollan for MnO was in good agreement with $S = \frac{5}{2}$ for the Mn ion, some excess magnetic scattering (about 30% in amplitude) was observed for CoO. The intensity of the magnetic peaks, as we have seen, follows simply from the magnetic moment per ion, usually taken as the spin magnetic moment, under the assumption that the orbital moment is quenched and does not contribute to the

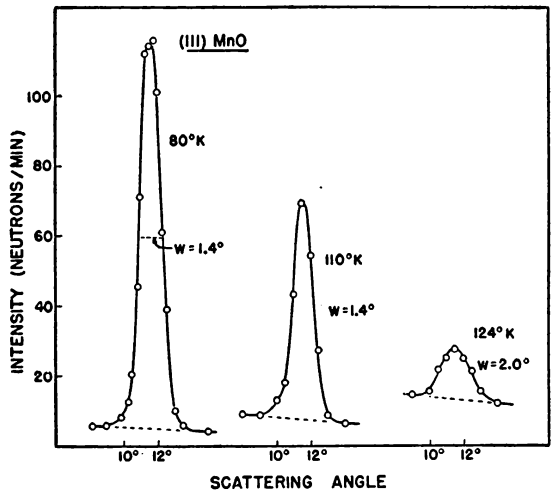

FIG. 5-5. The variation of the antiferromagnetic peak in MnO with sample temperature. The antiferromagnetic Curie point is 120° K.

magnetic scattering. However, in the case of the cobalt ion, which is in an F state with orbital angular momentum 3, there should be some orbital contribution to the magnetic scattering, and the calculated value is in reasonable agreement with the observations of Shull *et al.*

In our discussions of the ferromagnetic structure factors, we have assumed that the magnetic moment to be associated with each lattice site is the value observed in bulk measurements, for example, 2.2 magnetons per iron atom in the case of ferromagnetic iron. This assumption, which implies that there is a nonintegral number of spins at each lattice site, actually

corresponds closely with the observed patterns. Were integral spins to exist at each site for iron, yet average 2.2 in the bulk, the variation of magnetic amplitude from point to point would produce definite intensity differences among the reflections. As this latter behavior is not observed the conclusion can apparently be drawn that the nonintegral spin number is definitely associated with each individual lattice site. This conclusion is at variance with one theoretical view,[17] according to which integral spins are associated with each site in partially antiferromagnetic arrangement. However, the conclusion cannot be reached with complete definiteness because of the possibility that integral spins might be associated with lattice points at any given instant, in a pattern that shifts rapidly relative to the time of the neutron interaction, with a resulting nonintegral effective spin. This question of nonintegral spins is intimately related to the collective electron theory of magnetism, and while we cannot go into its details, it is clear that magnetic scattering will be extremely useful in testing theoretical treatments of ferromagnetic structure.

5.4 Paramagnetism

The neutron scattering from an ideal paramagnetic material, in which the spins are completely uncoupled, is given by Eq. (5-9) and is relatively uncomplicated, following directly from the spin magnetic moment of the ion and the form factor. The study of paramagnetic scattering is important, however, because the assumption of uncoupled spins can be tested for actual materials as a function of temperature, and the form factor that enters into Eq. (5-9) can be experimentally determined. Experiments on paramagnetic scattering had actually been performed several years before pile neutrons were available. These experiments, which were designed to measure the magnetic moment of the neutrons, were handicapped greatly by low intensity, however, and detailed information about paramagnetic scattering could not be obtained.

With pile neutrons it has been possible to measure para-

[17] C. Zener, *Phys. Rev.* **81,** 440 (1951); **85,** 324 (1952).

magnetic scattering by transmission, in which the integral form factor is effective, for a wide range of wavelength, and also by diffraction in which the differential form factor is directly measured. The pile work enabled detailed measurements of the magnetic form factor to be made although the expected form factor behavior had already been shown in some measurements of Ruderman's[18] using cyclotron neutrons. The cyclotron work gave the integrated form factor to a wavelength of 6 A, corresponding to an integrated form factor extending to about 0.7. The paramagnetic form factor was investigated in some detail by Shull, Strauser, and Wollan,[16] in connection with the powder diffraction studies of Sec. 5.3, for several paramagnetic salts containing Mn. In the powder diffraction measurements, the differential scattering cross section gives the form factor as a function of angle by use of Eq. (5-9). The form factor variation with angle can be converted to the actual distribution of the magnetically active neutrons in the atom (the 5 electrons in the 3*d* shell for Mn), by use of a Fourier inversion integral, the standard method used for x-rays.[19] The electron distribution obtained in this way for Mn^{++} (from MnF_2) is shown in Fig. 5-6 together with a theoretical curve calculated by Dancoff. The agreement between the calculated and observed distribution is satisfactory and implies that little uncertainty in interpretation of experiments should arise from the form factor behavior of the magnetic scattering.

The integrated form factor as a function of wavelength has recently been investigated over a wide wavelength region by Smith *et al.*[20] using the Brookhaven slow chopper. In this work the incoherent scattering beyond the crystal cutoff (for wavelengths extending to 15 A) was studied for several paramagnetic salts. In this wavelength region, the residual cross section after subtraction of capture and lattice vibration scatter-

[18] I. W. Ruderman, *Phys. Rev.* **76,** 1572 (1949).

[19] As discussed, for example, in A. H. Compton and S. K. Alison, *X-Rays in Theory and Practice* (Van Nostrand, 1940).

[20] R. Smith, T. Taylor, and W. Havens, *Phys. Rev.* **88,** 163 (1952).

ing is mainly paramagnetic diffuse scattering. As an example, in the results given in Fig. 5-7 the experimental magnetic scattering for MnF_2 is compared with the calculated integral form factor. As the wavelength becomes large compared to the size of the electron distribution, the form factor becomes unity and the magnetic scattering reaches the value 21 barns, which follows directly from Eq. (5-10) and an S of $\frac{5}{2}$. These

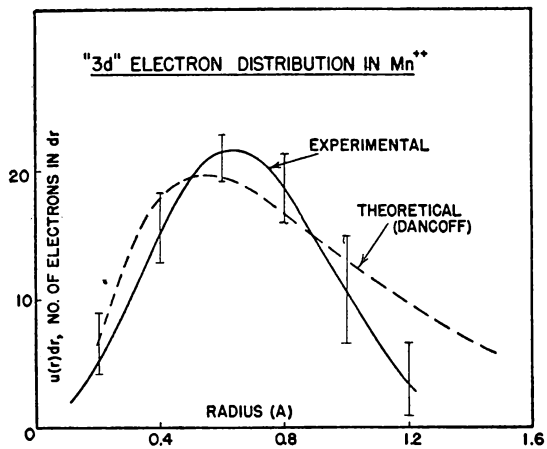

FIG. 5-6. The magnetic electron distribution of Mn^{++} obtained from the experimental form factor compared with a theoretical curve calculated by Dancoff.

results again show, in a somewhat different manner than those of Shull *et al.*, that the form factor variation of the paramagnetic scattering for an ideal paramagnetic material is well understood.

The paramagnetic scattering, well understood for materials of completely uncoupled spins, can hence be studied for materials near their Curie points, and the transition from the uncoupled state to the ferromagnetic or antiferromagnetic coupling thus followed by means of neutron scattering. We have already seen, Sec. 5.3, that for MnO the observed diffraction

scattering was not diffuse for temperatures above the Curie point but was concentrated near the positions where antiferromagnetic Bragg reflections occurred for low temperature. The concentration of scattered neutrons is apparent even at room temperature, well above the antiferromagnetic Curie point (120° K).[16] This behavior implies some ordering of spins at temperatures well above the Curie point for MnO, hence a departure from the assumption of uncoupled spins in a paramagnet. The

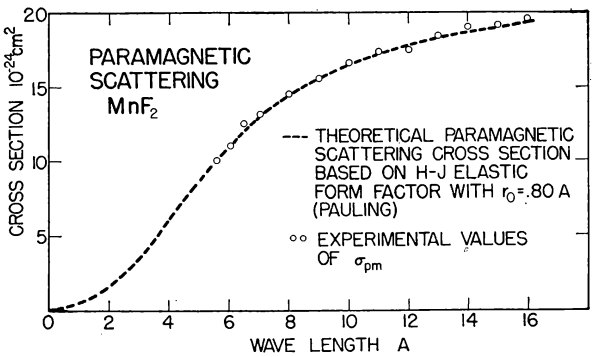

FIG. 5-7. The scattering cross section of MnF_2 for long wavelength neutrons, illustrating the approach of the paramagnetic scattering to the constant value corresponding to unit form factor.

occurrence of short-range antiferromagnetic order has also been detected[21] by the slow rise in radiofrequency resonance absorption above the Curie point for MnO relative to MnF_2, for which the absorption reaches its full value sharply above the Curie point.

Evidence for spin coupling is also obtained, in a somewhat different way, by the observation of magnetic inelastic scattering that we have mentioned in Sec. 4.4. The magnetic inelastic scattering has been studied by several workers in iron below the Curie point, but it was found by Palevsky, Carter, and

[21] R. K. Wangsness, *Phys. Rev.* **89**, 142 (1953).

Hughes[22] that the same type of scattering also occurred above the Curie point, implying that the spins were coupled. The energy exchanges associated with the coupling were shown to be large compared to the neutron energy by the proportionality of the observed cross section to λ. A similar behavior has been observed recently by Smith *et al.*[23] in connection with work on paramagnetic scattering for very slow neutrons. It was found that the theoretical form factor was correct for several paramagnetic materials (FeF_3, $ZnFe_2O_4$, and MnF_2) but for MnO the paramagnetic scattering, instead of leveling off for long wavelength at the expected 21 barns, had a rather large component proportional to λ. Here again the λ proportionality indicates that the neutrons gain energy in increments large compared to their own energy in the scattering process.

The study of the ordering above the Curie points gives information of a somewhat different type when studied by neutron diffraction as contrasted to transmission for long wavelength neutrons. The former approach reveals the size of the regions over which ordering obtains whereas the latter study is a measure of the energy exchanges involved in flipping the spins in their partially ordered arrangement. Measurement of the energy gained by slow neutrons in the scattering by the methods discussed in Sec. 4.4 would be of great value for it would yield directly the coupling energy of the spins in various spatial arrangements.

5.5 Polarized Neutrons

The polarization of a neutron beam, that is, the net alignment of the neutron spins along a particular direction, while superficially analogous to the polarization of light, differs greatly in its fundamental nature and in many respects is simpler in its manifestations. Polarized neutrons have not been exten-

[22] H. Palevsky, R. Carter, and D. J. Hughes, *Phys. Rev.* **89**, 910 (1953); H. Palevsky, and D. J. Hughes, *ibid* (in press).

[23] R. Smith, T. Taylor, and W. Havens, *loc. cit.*

sively used for the study of nuclear interactions for the simple reason that polarization of the nuclei is also necessary to attain significant results, and the latter is as yet hardly an established research technique. The main application of highly polarized neutron beams thus far has been to the study of bulk magnetization properties, such as the size and orientation of ferromagnetic domains. A consideration of the production and properties of polarized neutrons, however, furnishes a very instructive illustration of neutron-optical principles.

The results of Sec. 5.1 reveal the possibility of several methods of separating the two neutron spin states present in an unpolarized beam. For example, as the cross section for magnetized iron, Eq. (5-2) differs for the two spin states, transmission of neutrons through magnetized iron will result in a difference in transmission of the states, hence production of partial polarization. Likewise, the results for the index of refraction for a ferromagnetic material, Eq. (5-11), indicates that the difference in critical angle for the spin states could be used for production of polarized neutrons. The difference in amplitude that is a function of magnetization direction also implies that neutrons will be polarized when diffracted from crystals, to a degree dependent on the particular reflection. We shall see that all of these methods have been used for production of polarized neutron beams, each with its characteristic properties.

The method of polarizing neutrons by transmission in magnetized iron was studied with cyclotron-produced neutrons even before the advent of chain-reacting piles. The depolarization of such beams by radio frequency fields resulted in an accurate determination of the magnetic moment of the neutron.[24] The polarization obtained by transmission through a given thickness of magnetized iron could be calculated very simply from the difference in cross section for the two spin states,

[24] Bloch, Nicodemus, and Staub, *Phys. Rev.* **74**, 1025 (1948); the magnetic moment determination was also carried out with pile neutrons by W. R. Arnold and A. Roberts, *ibid.* **71**, 878 (1947).

Eq. (5-2), were it not for the finite lack of saturation of the iron that in practice lessens the polarization greatly. The existence of only a few domains out of line with the applied field gives rise to a precession of the neutron moment that results in a serious decrease in the polarization. Actually a departure from saturation as small as 0.1 % results in a sizable decrease in polarization from the value expected from a direct application of Eq. (5-2) assuming no depolarization. The degree of polarization of the beam is measured by its transmission through a second block of iron, the analyzer, as a function of magnetization direction.[25]

The highest polarization that has been produced[26] by transmission is of the order of 0.5, with the polarization P defined as

$$P = \frac{n_+ - n_-}{n_+ + n_-}, \tag{5-12}$$

where n_+ and n_- are the neutron intensities with spins in the $+$ and $-$ direction. Even this limited degree of polarization required a transmission through 6 cm of highly magnetized iron with a magnetizing field of 13,000 oersteds, and under these conditions the depolarization reduced the polarization by a factor of about 1.2. The use of such thick samples in transmission of course causes a serious loss in intensity (a factor of about e^6).

For production of polarization by mirror reflection it is fairly obvious that complete polarization would result only for monochromatic neutrons. If the entire Maxwell distribution is incident on a magnetized iron mirror there will always be *some* long wavelength neutrons reflected for the spin state of smaller scattering amplitude, corresponding to the index closer

[25] The calculation of the single and double transmission effects, which is highly complex, has been carried out by Halpern and co-workers in the references quoted at the beginning of Section 5.1.

[26] D. J. Hughes, J. R. Wallace, and R. H. Holtzman, *Phys. Rev.* **73**, 1277 (1948).

to unity in Eq. (5-11), regardless of the critical angle. At any given incident angle, the scattering amplitude determines the shortest wavelength that reflects, hence, while shorter wavelengths reflect for the spin state of larger amplitude, some intensity will always result for the other spin state. If monochromatic neutrons were reflected from iron at a critical angle intermediate to that of the two spin states, complete polarization would result but the monochromatization represents a serious loss in intensity.

Fortunately, the use of cobalt mirrors results in complete polarization and at the same time permits use of the entire Maxwell distribution. For cobalt, the magnetic scattering amplitude in the forward direction is larger than the nuclear amplitude and the net amplitude is positive for one spin state, for which total reflection occurs, and negative for the other, for which there is no reflection. The Maxwell distribution, when reflected from a cobalt mirror will thus be completely polarized regardless of incident angle. The minimum or limited reflected wavelength, however, will increase with increasing incident angle, as given by Eq. (1-43). Cobalt mirrors have been used[27] to produce extremely long wavelength polarized neutrons, an application that is impossible for the transmission method, which of course is effective only for neutrons of wavelengths shorter than the cutoff wavelength in iron. In the cobalt mirror work of Hughes and Burgy, the polarization was shown to be complete by the change in reflection at a second cobalt mirror (the "analyzer") with reversal of its magnetization.

Because of the magnetic form factor, the net amplitude (nuclear plus magnetic) in diffraction work will exhibit large changes with angle for ferromagnets, and in principle it is possible to pick a reflection for which the magnetic amplitude is equal to the nuclear amplitude. For this reflection the amplitude of one spin state will thus be twice the nuclear amplitude, whereas it will be zero for the other. As only one spin state will reflect, the reflected neutrons, which are nearly

[27] D. J. Hughes and M. T. Burgy, *Phys. Rev.* **81,** 498 (1951).

monochromatic, will at the same time be completely polarized. The separation of spin states resulting from the cancellation of magnetic and nuclear amplitudes, originally tried by Fermi, was demonstrated by Shull, Wollan, and Koehler[28] for the (220) reflection of magnetite, Fe_3O_4, for which the cancellation is almost exact. A single crystal was used in this work in order to increase the intensity over that attainable with powders, and the polarization, measured by transmission in magnetized iron, was complete within the experimental error of 5%. The intensity produced by this method is high, considering the fact that monochromatization is also obtained, but the wavelength of course is limited to that appropriate for the particular reflection.

As already mentioned, polarized neutron beams are not of much use in the investigation of spin-dependent nuclear interactions because of the difficulty of polarization of the nuclei. Without the latter, polarization of the incident beam does not give more information in general than does an unpolarized beam. Spin-dependent scattering does produce depolarization of the beam and this depolarization can be used as a measure of spin-dependent scattering. In practice,[29] however, this application has not proved to be valuable, for the method is not sensitive and the spin-dependent cross section can usually be determined by other means, Sec. 3.2. It is of interest also that production of oriented nuclei by capture of polarized neutrons, at first thought a promising application, is of practically no value. It might be expected that nuclei capturing polarized neutrons would be oriented hence would give a typical angular asymmetry in the emission of capture gamma-rays. Such an asymmetry would be observed for aligned nuclei but nuclei formed by capture of polarized neutrons are not aligned in the same manner. This result is actually an example of the uncertainty principle in relation to angular orientation, which

[28] C. G. Shull, E. O. Wollan, and W. C. Koehler, *Phys. Rev.* **84,** 912 (1951).

[29] W. E. Meyerhoff and D. B. Nicodemus, *Phys. Rev.* **82,** 5 (1951).

shows, for example, that capture of spin $\frac{1}{2}$ polarized neutrons by protons of spin $\frac{1}{2}$ results in deuterons of spin 1, $\frac{2}{3}$ of which are oriented along the direction of the neutron polarization and $\frac{1}{3}$ at right angles to it. This type of asymmetric population distribution in magnetic substates can be shown[30] to produce the same angular distribution of the capture radiation as unaligned nuclei.

While the uses thus far of polarized neutrons in nuclear phenomena have been extremely limited the possibility of useful application to study of bulk magnetic material seems more likely. For example, the great sensitivity of polarized neutrons to unaligned magnetic domains already mentioned furnishes a very sensitive means of measuring small departures from saturation. This method has been used[31] to follow the approach of magnetization to saturation in high fields, a phenomenon that exhibits features not explicable by current theory. As the depolarization is also a sensitive function of the domain size and orientation, a polarized beam when transmitted through thin samples of unmagnetized material can be used to study the properties of the domains. Experiments of this type, which have been carried out by Burgy *et al.*,[32] have resulted in determinations of domain sizes that were in good agreement with those expected from various types of metallurgical treatment. For example, extreme cold rolling, which reduced the grain size of the material, was shown to reduce the size of the magnetic domains correspondingly, thus evidencing the association of domain and grain size. While these experiments have not been carried very far it seems extremely likely that similar measurements will give very useful information on the properties of magnetic materials, expecially with regard to domain structure.

[30] O. Halpern, *Phys. Rev.* **82,** 752 (1951); **85,** 747 (1952); G. B. Arfken, L. C. Biedenharn, and M. E. Rose, *ibid.* **84,** 89 (1951).

[31] D. J. Hughes, J. R. Wallace, and R. H. Holtzman, *loc. cit.*

[32] M. T. Burgy, D. J. Hughes, J. R. Wallace, R. B. Heller, and W. E. Woolf, *Phys. Rev.* **80,** 953 (1950).

INDEX

INTERSCIENCE TRACTS ON PHYSICS AND ASTRONOMY

Editor:
R. E. MARSHAK, *Harris Professor of Physics in the University of Rochester*

Interscience Tracts on Physics and Astronomy are being published in order to provide non-specialists with authoritative and relatively brief and inexpensive accounts of recent advances in the many specialized branches of physics and astronomy.

The following tracts are in active preparation and many others are in the planning stage:

R. Smoluchowski, *Carnegie Institute of Technology*
IMPERFECTIONS IN CRYSTALS

W. Baade, *Mt. Wilson & Palomar Observatories*
GALAXIES and Their STELLAR POPULATIONS

M. S. Livingston, *Massachusetts Institute of Technology*
BILLION-VOLT ACCELERATORS

L. Goldberg, *University of Michigan*
SOLAR PHYSICS

H. W. Liepmann and J. Laufer, *California Institute of Technology*
TURBULENCE PHENOMENA

M. Deutsch, *Massachusetts Institute of Technology*
POSITRONIUM

J. L. Greenstein, *California Institute of Technology*
RADIO ASTRONOMY

E. H. Land, *Polaroid Corporation*
POLARIZED LIGHT

INTERSCIENCE PUBLISHERS, INC.
250 Fifth Avenue, New York 1, N. Y.